UNIVERSITEIT VAN PRETORIA
UNIVERSITY OF PRETORIA
YUNIBESITHI YA PRETORIA

Sediment yield modelling in the upper Tsitsa Catchment, Eastern Cape, South Africa.

By

Simone Norah Pretorius

Submitted in partial fulfilment of the requirements for the degree Master of Science in Environmental Management in the Faculty of Natural and Agricultural Sciences. University of Pretoria
Pretoria

Supervisor: Professor Paul D. Sumner

Co-supervisors: Mr Harold L. Weepener

Dr Jacobus J. Le Roux

Department of Geography, Geoinformatics and Meteorology

August 2016

Declaration

By submitting this assignment/thesis/dissertation electronically, I, Simone Norah Pretorius declare that the thesis/dissertation, which I hereby submit for the degree Master of Science in Environmental Management at the University of Pretoria, is my own work and has not previously been submitted by me for a degree at this or any other tertiary institution.

Signature: ..... Date: 14/12/2016

Simone Norah Pretorius

Abstract

The Mzimvubu River is the largest river in South Africa without a dam. The Department of Water and Sanitation has identified the Tsitsa River Catchment on the Mzimvubu River as a potential site for a water resource development. The soils in the Tsitsa Catchment are prone to extreme soil erosion, in particular gullying. The sediment generated from these gullies and other forms of erosion will have a detrimental effect on any water resource development. Changing climate and land use will also affect soil erosion dynamics and thus need to be considered before any development is planned in the catchment. Previous studies have mapped the gully systems in the catchment as well as used hydrological models to determine erosion from sheet and rill processes. However, these studies did not account for the effects of change in land use or climate. The mapping of the gullies was also done manually, which is extremely time-consuming and is susceptible to human error.

This study aims to determine the sediment yield in the catchment under current and future climate and land use scenarios as well as develop a methodology to identify and map the gullies automatically in order to determine the rate of gully growth from a time series of images. The study had two main components, the first was to study gully erosion in the catchment. In the second section the sheet and rill aspects of erosion under various climate and land use changes were modelled. Using object-based image analysis (OBIA) on SPOT 5 images a methodology was created to automate the task of gully mapping. This was applied to two SPOT 5 data sets one from 2007 and the other from 2012 in order to determine the rate of gully growth over the five-year period. Various accuracy assessments were also conducted to assess the accuracy of the methodology. It was determined that the methodology had an overall accuracy of 98% for the 2012 image and 99% for the 2007 image. There was an overall increase in gully erosion in the catchment by 28% in the five-year period. The estimated sediment yield generated from the gullies ranged between 7 and 14 t/ha/yr. It was concluded that OBIA resulted in faster processing times and more objective classification results.

The second part of the study used the Soil and Water Assessment Tool (SWAT) to determine the sediment yield from sheet and rill erosion. SWAT only considers sheet and rill aspects of erosion and disregards gully erosion thus

both methods needs to be incorporated into the study in order to understand the complete dynamics of soil erosion in the catchment. SWAT was used to model the current land use and climate scenario using land cover data and observed weather data for the 2007-2012 period. On average 0.18 t/ha/yr of sediment is generated in the catchment from sheet and rill erosion.

Using climate data from 1969 and projected to 2100, future sediment yield from sheet and rill erosion was estimated. The effects of possible land use change on sheet and rill erosion was also estimated by changing the land use component in SWAT into various crops that may be cultivated in the catchment over the next century. The results of the land use change showed that the current land use is optimal for minimal sheet and rill erosion and converting to maize crops will have the greatest impact on sediment yield

This study aimed to understand the dynamics of soil erosion under current and changing land use and climate scenarios. It was concluded that the majority of the sediment is derived from gully erosion, which accounts for up to 70 times more sediment yield annually than sheet and rill erosion. Gully formation and propagation in the catchment is of critical concern to any land or water developments proposed for the Tsitsa Catchment.

Acknowledgements

I would like to take the opportunity to thank the various people who helped me both professionally and personally throughout the years working on my MSc thesis. An MSc thesis is a huge undertaking and it would not have been possible to complete without the help of the following people.

First and foremost, I would like to extend my sincere gratitude to my supervisors who gave me guidance throughout the project. In particular, my supervisor at the ARC-ISCW, Mr Harold Weepener, who not only gave me technical support and recommendations but who also patiently, taught me so much in the fields of GIS and remote sensing. In addition, his weekly reviews of my thesis gave me the motivation to continually write throughout my project. I would also like to thank Dr Jay Le Roux who structured my project from the beginning, as it was a wonderfully intriguing topic where I was able to study so many aspects of the environment, from remote sensing and GIS modelling to climate change and water resources. Lastly, Professor Sumner who was always supportive and who edited my thesis.

I would also like to thank the many staff at the ARC-ISCW and the University of Pretoria for their continuous advice and guidance. I was fortunate enough to receive recommendations and knowledge from Ms E. van den Berg on my SPOT 5 images and analysis. As well as from Dr Mohamed Ahmed who guided me in the photographic analysis of soil erosion.

I am very grateful to Christien Engelbrecht who formatted the climate data from the six GCM models, which I was then able to use. Dr Franscois Engelbrecht and the CSIR for the use of their climate change data and for Dr Engelbrecht's advice on analysing the results. I would also like to thank Louw Potgieter who took the time to peruse my soil information. Dr Danie Beukes, Dr Gary Patterson and Mr Piet Nell who all advised on soil sampling.

I would also like to thank the wonderful support I received from the technical staff at the ARC-ISCW who always helped me fix technical errors on my PC and the various software issues that frequently arose throughout my project. In particular, Mr Philip Beukes whom I bothered many times with small problems and queries and who was always ready to help.

The staff at the University of Pretoria also gave their advice throughout my studies. Mr Barend van der Merwe who was always there to assist and give advice on any topic and Mr Fritz van der Merwe who gave his assistance and worldly knowledge of GIS whenever I needed it.

I would also like to thank the ARC and their PDP program who gave me the opportunity to pursue my MSc. Through the program, I received not only the financial support to conduct my research, the wonderful facilities and use of their software but also amazing experiences. I was able to attend conferences both in South Africa and abroad, which opened horizons and allowed my work to be reviewed numerous times helping me to see the many angles this project has. The ARC and the staff have been wonderful mentors throughout the project I am extremely grateful for everything they offered.

I would also like to thank the Water Research Commission who funded this project and whose advice in the early stages helped me to develop a wonderful and hopefully valuable thesis.

Last but certainly not least, I would like to thank the people who are closest to me and who provided support throughout the thesis. My loving parents who were my biggest believers throughout my undergraduate and post-graduate studies and who supported me wholeheartedly every step of this long journey. I will be forever grateful. My sister who was always there giving me the boost I needed to keep going and who listened to my endless moaning about software failures. Finally, my loving boyfriend Andre. Who believed in me every day even when I did not, and whose constant support I could always rely on. He gave me the strength and advice to push through the tough times and I am so grateful to him.

Table of Contents

List of Figures

List of Tables

List of Abbreviations

ACRU	Agricultural Catchments Research Unit
ARC-ISCW	Agricultural Research Council- Institute for Soil, Climate and Water
Asl	above sea level
ASTER	Advanced Spaceborne Thermal Emission and Reflection Radiometer
B	Blue
CCAM	Conformal Cubic Atmospheric Model
CGCM	Coupled Global Climate Model
CN	Curve Number
CREAMS	Chemicals, Runoff and Erosion from Agricultural Management Systems
CSIR	Council for Scientific and Industrial Research
CSIRO	Commonwealth Scientific and Industrial Research Organisation
DAFF	Department of Agriculture, Forestry and Fisheries
DEM	Digital Elevation Model
EPIC	Erosion Productivity Impact Calculator
G	Green
GCM	General Circulation Model
GCP	Ground Control Points
GFDL	Geophysical Fluids Dynamics Laboratories
GIS	Geographic Information Systems
GLCM	Grey Level Co-ordinance Matrix
GLEAMS	Groundwater Loading Effect on Agricultural Management Systems
GLASOD	Global Assessment of Human-induced Soil Degradation
HRU	Hydrologic Response Unit
IPCC	Intergovernmental Panel on Climate Change
JERS-1-SAR	Japan Earth Resources Satellite- Synthetic Aperture Radar.
LiDAR	Light Detection and Ranging
MIROC	Model for Interdisciplinary Research on Climate
MLC	Maximum Likelihood Classifier
MNDWI	Modified Normalized Difference Water Index
MPI	Max Planck Institute
MUID	Multiple Unit Identity
MUSLE	Modified Universal Soil Loss Equation
NDVI	Normalised Difference Vegetation Index
NDWI	Normalised Difference Water Index
NIR	Near Infrared
NOAA	National Oceanic and Atmospheric Administration
OBIA	Object-based Image Analysis
OFE	Overland Flow Elements
PESERA	Pan-European Soil Erosion Risk Assessment Model
R	Red
RUSLE	Revised Universal Soil Loss Equation
SA	South Africa
SCS	Soil Conservation Services

SCS-CN	Soil Conservation Services- Curve Number
SDR	Sediment Delivery Ratio
SLEMSA	Soil Loss Estimation Method for Southern Africa
SPAD	Spatially Distributed Scoring Model
SPOT	Satellite Pour I' Observation de la Terre
SRES	Special Report on Emissions Scenario
SRTM	Shuttle Radar Topography Mission
SVM	Support Vector Machines
SWAT	Soil and Water Assessment Tool
SWERB	Simulator for Water Resources in Rural Basins
SWIR	Short Wave Infrared
TM	Thematic Mapper
UKMO	United Kingdom Met Office
USA	United States of America
USDA	United States Department of Agriculture
USLE	Universal Soil Loss Equation
VHR	Very High Resolution
WATEM/SEDEM	Water and Tillage Erosion Model/ Sediment Delivery Model
WEPP	Water Erosion Prediction Project

1. Introduction

1.1 Introduction to the study

Soil erosion is one of the largest environmental problems facing Sub-Saharan Africa (Symeonakis & Drake, 2010). The problems related to soil erosion such as decreasing water quality and soil productivity as well as land degradation, are a major concern to both rural and urban communities (Sidorchuk *et al.*, 2003). In water-scarce countries such as South Africa water bodies are increasingly threatened by pollution and sedimentation due to high concentrations of suspended sediment in streams, which adversely affects water use and ecosystem health (Le Roux *et al.*, 2013). Growing population sizes, densities and changes in global climate are worsening the problem of soil erosion (Flugel *et al.*, 2003). A recent study conducted by the Council for Scientific and Industrial Research (CSIR) created a climate model of South Africa at an 8 km resolution Engelbrecht *et al.* (2011). The model predicted an increase in rainfall through high-intensity rainfall events over the eastern parts of South Africa while the western parts of the country will experience drier conditions (Engelbrecht & van Garderen, 2013). These predicted changes to the climate of South Africa will influence sediment generation and runoff as well as water distribution over the country. An increased population growth along with growing industry and urban population puts further demands on South Africa's limited water resources (Abalu & Hassan, 1998).

It is imperative to devise the means through which soil erosion and its associated problems can be controlled such as reservoir sedimentation. Prevention and remediation measures rely largely on the understanding of factors controlling the sediment dynamics in a catchment, including sediment generation, transport and deposition (Le Roux *et al.*, 2013). Thus it is important to model sediment yield in a catchment under various scenarios in order to determine how changing climate and land use will affect, for example, the water quality and dam lifespan.

The Mzimvubu catchment is the only major river catchment in South Africa without a dam (Le Roux & van den Berg, 2014). The river sources in the Drakensberg range and flows from the escarpment through the Eastern Cape and into the Indian Ocean at Port St Johns. The catchment area of the

Mzimvubu River is roughly 19 000 km^2 and spans across both KwaZulu-Natal and the Eastern Cape. One of the tributary rivers to the Mzimvubu is the Tsitsa river which sources in the Drakensberg and has a catchment area of 4 924 km^2. It flows into the Mzimvubu River after a length of approximately 200 km from northwest to southeast (see Figure 3.1). The area surrounding the river is used for larger commercial farms and plantations as well as rural farming and housing and once formed part of the Transkei. The people living in the area are still facing financial and social difficulty due to the legacy of the homeland policy set in the 1970's. Overgrazing, over cultivation and social and political issues, have all led to the degradation of the land in the area.

Geology in the area is dominated by mudstones, shales and sandstone of the Karoo Supergroup (Le Roux *et al.*, 2015). This geology gives rise to highly erodible soils that are prone to gullying and sheet and rill erosion (Le Roux & Sumner, 2012) and the area is also considered one of the highest sediment yield areas in the country (Msadala *et al.*, 2010). Gully erosion in the area is widespread and common with over 18 000 gullies been mapped in a study conducted by Mararakanye and Le Roux (2012).

The Department of Water and Sanitation are considering the Mzimvubu River for a potential water resource development project (Le Roux *et al.*, 2015). Five possible sites have been identified throughout the catchment, with the Tsitsa River at Ntabalenga the most promising site for a dam project (Le Roux *et al.*, 2015). The upper Tsitsa catchment falls in one of the poorest and least developed areas of South Africa. Thus it is hoped that the dam will spark economic activity through agricultural irrigation and tourism (Department of Water and Sanitation, 2014). Another important role of the dam will be to help secure water resources to alleviate vulnerability to droughts such as the ones experienced in 1992 and more recently 2015. The Department of Water and Sanitation stated that 98% of South Africa's water resources have already been allocated and water availability is crucial to industrial and economic activity. Water storage is the most important way of securing water resources (Mokonyane, 2015). The construction of a dam can help this region cope better with droughts in the future.

Studies on the dam site and catchment area need to be conducted in order to determine sediment transport and delivery. This will help to establish the

predicted lifespan of the dam and other dam management measures (Le Roux *et al.*, 2015). Measurement of sediment production is necessary in order to determine areas which are most susceptible to erosion or acting as sediment conduits. Hydrological models such as the soil and water assessment tool (SWAT) are able to use various factors such as land use, vegetation, climate and soils to predict soil loss, sediment production and deposition to model catchment processes (Nietsch *et al.*, 2005).

The SWAT model is a physically based, basin-scale, continuous-time model that functions on a daily time step and aims to predict the impact of management on water, sediment and agricultural chemical yields in ungauged watersheds (Gassman *et al.*, 2007). SWAT allows for multiple scenario analyses of a catchment at different scales using different variables, sources, and sinks for erosion (Le Roux *et al.*, 2013). Such an approach helps predict the sediment generated in a catchment and can be used to determine potential dam sites, dam construction designs and dam management strategies. SWAT has gained international acceptance as a robust watershed modelling tool (Gassman *et al.*, 2007) and has been applied to support various large catchment modelling studies across the world with minimal or no calibration effort (Le Roux *et al.*, 2013). The foundational strength of SWAT is that it considers most connectivity aspects into one simulation process, including factors controlling upland sediment generation, channel transport and deposition into sinks. SWAT can also be run in a GIS, which gives it flexibility in the representation and organization of spatial data. (Le Roux *et al.*, 2013)

Over the last decades, most research dealing with soil erosion by water has concentrated on sheet and rill erosion processes operating at the plot scale. Relatively few studies have been conducted on gully erosion operating at larger spatial scales (Mararakanye & Le Roux, 2012). A major disadvantage of not only the SWAT model but other hydrological models is that they lack the ability to model gully erosion processes (Sidorchuk *et al.*, 2003). The absence of gully erosion in models is due to two main reasons. First, the development of erosion models has focused on areas of intense agriculture, which are common in developed countries. The second reason is due to the spatial and temporal heterogeneity of gully erosion processes, which make the modelling of gully erosion difficult (Sidorchuk *et al.*, 2003). Field-based evidence suggests that modelling only sheet and rill erosion will not provide realistic representations

of the total catchment erosion especially as many models also do not account for redistribution of eroded soil within a field. Gully erosion acts as a conduit channelling a large amount of eroded soil within a catchment and delivering it to the water channels (Poesen *et al.*, 2003). Thus gully erosion is an important factor controlling the connectivity in a catchment (Poesen *et al.*, 2003). It is very important to consider gully erosion processes in erosion studies (Sidorchuk *et al.*, 2003) conducted in many areas of South Africa, especially in the former homelands such as Transkei in the Eastern Cape Province (Kakembo & Rowntree, 2003). This can be achieved through accurate gully location mapping (Mararakanye & Le Roux, 2012).

Numerous mapping approaches have been carried out which emphasize the continuously growing need and the importance of mapping gullies. Mapping gully systems and quantifying their changes over time are essential for catchment rehabilitation and implementing soil conservation measures (Shruthi *et al.*, 2015). Perspectives on sediment yield contribution from gully erosion have typically been obtained from field scale ($<10^{-1}$ km^2) and are confined to local conditions (Grellier *et al.*, 2012; Manjoro *et al.*, 2012; Slimane *et al.*, 2015). Few studies model the sediment yield contribution from gully erosion at a regional scale.

In the past, field-based methods were used until aerial photos and later satellite imagery became more readily available. Early assessment of gully erosion was based on the manual interpretation of aerial photographs (d'Oleire-Oltmanns *et al.*, 2014). Manual interpretation, however, is laborious, time-consuming and has the potential for human error and bias. As computer software improved, automated methods such as pixel-based and object-based image analysis (OBIA) became the preferred methods of image classification as they are faster and more objective.

Object-based image analysis is the most practical approach for mapping gully features over large areas, due to the variation in gully size, shape and occurrence (Knight *et al.*, 2007; Shruthi *et al.*, 2012). OBIA, which takes into account auxiliary information, such as geometric properties and the spatial relationship with surrounding features, allows for an approach similar to the cognitive approach of the human operator. Through OBIA, it is possible to analyse erosion features as spatial objects so they can be categorised based on

their geometric properties as well as their spatial relationship with neighbouring features. Recent work has shown OBIA to be superior to pixel-based methods for the identification and classification of gullies due to their spectral heterogeneity (Shruthi *et al.*, 2015). OBIA is better able to replicate human interpretation than pixel based or manual methods and thus reduces the subjectivity of digitising and makes the results more repeatable (Dezso *et al.*, 2012). However, the potential of OBIA to identify and map gully erosion features from high spatial resolution satellite imagery has only been tested in a number of studies (Shruthi *et al.*, 2012). Although manual digitising produces more accurate results, the process remains time-consuming and may contain bias or simple errors in gully interpretations. Monitoring large catchments or countrywide gully development through manual interpretation will be expensive and difficult to replicate. It is, therefore, necessary to develop new OBIA based methodologies which will be less expensive and easier to repeat (Mararakanye & Nethengwe, 2012).

Building a dam is a large financial investment and the communities which benefit from dam projects can be greatly uplifted. Thus it is important that the planned dam remains functional for a long period of time. The Welbedacht dam in the Free State lost up to 80% of its capacity in the first 50 years of use (Le Roux *et al.*, 2015). This was due to extreme siltation which reduced the water holding capacity of the dam from 115 million m^3 to 16 million m^3 within the first 20 years after completion (Department of Water and Sanitation, 2015). The Welbedacht Dam example shows how important it is to assess the sediment yield in a catchment prior to dam construction. Results from erosion studies on a proposed catchment can aid dam location selection, dam design and management strategies. Considering the effects of changing climate and land use can further aid managers of the dam project to identify negative consequences which may be brought about in the future. It is thus imperative that sediment yield studies are conducted on dam catchments in order to optimise the dam lifespan.

Due to the increasing risk associated with climate change, it is important not only to understand current climate/sediment models but also how projected climate change will alter the sediment yield in a catchment as dams are built with expected lifespans of 70-100 years. The Department of Water and

Sanitation have commissioned a project to create framework strategies that will allow for better management of South Africa's dams currently and going into the future. An advantage of the SWAT model is that it can assist in modelling sediment yield in a catchment based on projected climate change. Engelbrecht *et al.* (2011) created six 50 km resolution climate change prediction models for South Africa. The study relied on the detailed projections of a regional climate model, which were obtained through the dynamic downscaling of six different Coupled Global Climate Models (CGCM) projections of future climate change to high resolution over southern Africa (Engelbrecht *et al.,* 2011). The regional model used is the Conformal-Cubic Atmospheric Model (CCAM) which is a variable resolution global atmospheric model of the Commonwealth Scientific and Industrial Research Organization (CSIRO) in Australia. This model was applied in stretched-grid mode over southern and tropical Africa to obtain simulations at a resolution of approximately 0.5° in longitude and latitude (Engelbrecht *et al.* 2011). A detailed description of the downscaling procedure is provided by Engelbrecht *et al.* (2011). All the CGCM simulations used were for the A2 Special Report on Emissions Scenarios (SRES) scenario and were downscaled for the period 1961-2100. The CGCMs downscaled by Engelbrecht *et al.* (2011) are listed as follows:

- GFDL-CM2.0 from the National Oceanic and Atmospheric Administration (NOAA)
- GFDL-CM2.1 of NOAA
- ECHAM5/MPI-Ocean Model from Germany
- UKMO-HadCM3 from the United Kingdom
- MIROC3.2-medres from the Japanese Agency for Marine-Earth Science and Technology (JAMSTEC)
- CSIRO Mark3.5 from Australia

1.1.1. Problem statement

Recent soil erosion mapping and modelling studies indicate that large parts of the Tsitsa River Catchment consist of highly erodible soils and widespread soil erosion (Le Roux *et al.*, 2007; Mararakanye & Le Roux, 2012; Le Roux & Sumner, 2012; van Tol *et al.*, 2014; Le Roux *et al.*, 2015). The gully location

map created by Mararakanye and Le Roux (2012) provides only location and the spatial extent of the gullies. Furthermore, the Universal Soil Loss Equation (USLE) assessment models used by Le Roux *et al.* (2007) only considers sheet and rill erosion and disregards erosion contribution by gullies.

More recently, a study by Le Roux *et al.* (2015) in the larger Mzimvubu Catchment determined the sediment contribution from both sheet and rill erosion as well as gully erosion, however, this study did not focus on the upper Tsitsa catchment in specific detail. All these studies lacked temporal variability in the catchment and gave no indication of varying sediment production under projected land use and climate change. A methodology to produce a detailed gully location map of the upper Tsitsa River Catchment needs to be created, which will allow for faster mapping and results that are more objective. It is also important to model sediment yield under projected climate and land use change to understand how soil erosion will change temporally throughout the dam lifespan. Through the study of Le Roux *et al.* (2015) certain research needs were identified such as the use of automated gully identification techniques and the need for more scenario analysis. The results of this study will refine and fill in the gaps which were out of the scope of the report produced by Le Roux *et al.* (2015).

1.1.2. General aims and objectives

The main aim of the study is to determine the sediment yield at the proposed dam site at Ntabalenga under various climate and land use scenarios.

The aim of the study is met through the following objectives:

- To create a model of the sediment yield from sheet and rill erosion for the upper Tsitsa Catchment using SWAT.
- To use eCognition software and object-based classification to identify and map gullies in the catchment for two separate years: 2007 and 2012.
- To use the resultant gully location maps from 2007 and 2012 to estimate the sediment yield contribution from gullies over the 5-year period.
- To determine the impacts of projected climate change on sediment yield in the catchment.

- To determine the impacts of proposed land use change under till and no till scenarios on sediment yield in the catchment.

The use of SWAT and OBIA are very different in terms of their theoretical basis. The SWAT model has a GIS basis whereas OBIA is a tool used for the automatic classification of remote sensing imagery. The SWAT model is based on a pre-defined, programmed model where the user can alter the inputs in order to obtain results for their specific case study. In contrast, when using OBIA software the users have to create their own methodology to allow for the identification of soil erosion in the images. Although the two techniques are very different, in this study the applications of both these approaches are identical: which is to estimate soil erosion and the resulting sediment yield. Combining these two techniques gives the project a stronger relevance in the field as integrating both techniques in a single study allows for the complete analysis of soil erosion in the catchment and the results will, therefore, be a more accurate representation of reality. SWAT's strength lies in modelling sheet and rill erosion yet it does not account for gully erosion. With the use of OBIA, gully erosion can be mapped and the sediment yield from the gullies can then be estimated. Thus through the combination of both techniques, a more detailed and accurate estimation of sediment yield from both gully and sheet and rill erosion for the catchment can be calculated.

1.2. Rationale

1.2.1. Modelling sheet and rill erosion

The SWAT model was selected because it is a spatially semi-distributed model, which has gained international acceptance and it has been applied to many large catchments across the world with minimal calibration needed. SWAT is also easily downloaded free of charge and has an ArcMap extension, ArcSWAT, which allows it to be run in the ArcMap interface. This gives the user flexibility in the representation and organisation of spatial data. SWAT also considers many aspects of connectivity such as upland sediment generation, channel transport and sink deposition (Le Roux *et al.*, 2013). Another strength of SWAT is that it allows for scenario analysis with minimal effort in changing the input

data. Since this study was based on the effects of various scenarios on sediment output in the catchment, it was important to run a model in which the input data can be changed easily. SWAT was tested in a previous study in the Mkabela catchment and it was shown to accurately, although slightly overestimate, most of the peak flow events during the simulation period (Le Roux *et al.*, 2013). Le Roux (2009) assessed various catchment models of international standing and concluded the SWAT model was the most suitable for large-scale catchment modelling in South Africa.

1.2.2. Modelling gully erosion

The SWAT model only accounts for sheet and rill erosion and disregards sediment produced from gully erosion (Le Roux *et al.*, 2015). Methods are thus needed to predict the extent and patterns of gully erosion across large areas as well as determine their contribution to the overall sediment yield in the catchment (Hughes & Prosser, 2012).

In a catchment such as the upper Tsitsa, where the soils are prone to gullying and there is widespread gully erosion it is important to determine the sediment produced from the gullies (van Tol *et al.*, 2014; Le Roux *et al.*, 2015). The most widely used method to access gully erosion is to manually digitise gullies from aerial or satellite imagery. However, this process is time-consuming and contains human error and bias thus it is preferable to automate the task of gully detection.

Object-based image analysis software has developed into a powerful tool as it allows the user to develop custom rulesets for automatic classification, without the need for human digitising. For this study, the software package, eCognition, was used to conduct image analysis of SPOT 5 images to extract the gully objects for further analysis. eCognition Developer is distributed by Trimble Navigation Limited and is a powerful development tool for OBIA. eCognition has been widely used in earth sciences to develop rule sets for the automatic analysis and classification of remote sensing data. eCognition Developer can be used for feature extraction, change detection and object recognition. The object-based approach can facilitate analysis of a variety of data sources, such as medium to high-resolution satellite data, high to very

high-resolution aerial photography, light detection and ranging (LiDAR), radar and even hyperspectral data (Trimble Navigation Limited, 2014).

The methodology developed and tested in this study along with the derived gully location maps will be a valuable tool for the improved assessment of gully-derived sediment yield and gully mapping. The results will be particularly useful in modelling gully derived sediment yield under changing climate scenarios. If the gully location or gully expansion maps are not accurate and objective, the sediment yield results derived therefrom will also not be accurate.

1.2.3. Catchment selection

The study area chosen was the upper Tsitsa River Catchment upstream of the Ntabalenga village in the Eastern Cape Province, South Africa. The area falls in the former Transkei homeland and is one of the poorest and least developed areas in South Africa. The primary reason for this area been chosen was because it is a site for a potential dam construction. The Tsitsa River feeds the larger Mzimvubu River, which is on record the only large river in South Africa without a dam (Le Roux *et al.*, 2015). The construction of a dam in the upper Tsitsa Catchment is envisioned to spark economic and agricultural activity in the poor rural area surrounding it (Duncan *et al.*, 2015).

The Tsitsa catchment is also an area of agricultural concern and there are discussions by the Department of Agriculture, Forestry and Fisheries (DAFF) about potential commercial farming in the catchment. Parts of the Eastern Cape are predicted to become suitable for avocado, sugarcane, maize and pasture cultivation with predicted climate change (Weepener *et al.*, 2015). Third, the Tsitsa catchment has been an area of interest for many years and there is a considerable amount of literature available produced through numerous soil and hydrological studies (Esprey, 1997; van Huyssteen *et al.,* 2005; Freese *et al.*, 2010; van Tol *et al.*, 2010; Le Roux *et al.*, 2015). DAFF selected the Tsitsa Catchment as one of three priority tertiary catchments in South Africa. The other two are in KwaZulu-Natal and Limpopo (Lindemann & Pretorius, 2005). There is also a substantial amount of data such as soil,

land use, climate, geology, vegetation and topography available for the study area.

Finally, a R450 million project initiative has been funded by the government to prevent and rehabilitate soil erosion in the catchment over a period of 10 years. The project's main aim is to restore eroded land and therefore reduce the sediment generated in the catchment, which will be achieved through the restoration of wetlands and cultivated agricultural land (Duncan *et al.*, 2015). The benefits of such an initiative are many, ranging from returning the land to productive agriculture to improving water quality and preventing dam siltation (Duncan *et al.*, 2015). It is hoped that this study can shed some light on the effects of soil erosion on the dam as well as the effects of potential land use and climate change on sediment generation in the catchment.

Through this study the gullies in the catchment will be identified and mapped. Gully growth rates will also be determined through time series analysis. This can help identify gullies which are more active and where resources can be distributed in order to gain the most out of the rehabilitation project (Shruthi *et al.*, 2015).

1.3. Specific objectives

1.3.1. Modelling sheet and rill erosion under current conditions

SWAT will be used to model sheet and rill erosion in the upper Tsitsa Catchment under the current land use and climate conditions. Measured rainfall and temperature data from a weather station located in the Tsitsa Catchment for the period 2007-2012 (Agro meteorology Staff, 1984-2008) along with soil and land use data provided by the land types map (Land Type Survey Staff, 1972-2006) and the national land cover map (Le Roux *et al.,* 2015)) will be used to set up the model.

1.3.2. Modelling gully erosion

Gully erosion in the catchment will be modelled using SPOT 5 images and eCognition software. eCognition software facilitates OBIA and allows for a user-defined ruleset to be created. A ruleset which will be applicable to other

SPOT 5 images, will be created and run on both the 2007 and 2012 SPOT 5 images. The lateral growth of the gullies will be calculated by subtracting the 2007 results from the 2012 results. This will give an indication of gully activity over the 5-year period. Using the U and V shape gully model (Poesen *et al.*, 2003) along with a constant sediment delivery ratio the sediment yield contribution from the gullies in the catchment will be estimated and presented as a range.

1.3.3. Modelling effects of climate change on erosion

Climate data acquired from six CGCM simulations from the A2 Special Report on Emissions Scenarios (SRES) for the period 1961-2100 (listed below) will be used.

- GFDL-CM2.0
- GFDL-CM2.1
- ECHAM5/MPI
- UKMO
- MIROC3.2
- CSIRO

It is important to use multiple GCMs in a study involving the effects of climate change (Crosbie *et al.*, 2011). The use of multiple models helps account for the large potential uncertainties in future estimates of soil erosion and sediment yield. By choosing only the best performing GCMs the range of projections may be narrowed. Similarly, by choosing the extremes of the GCMs for rainfall may not produce the extremes of the sediment yield as different parametres within the model may outweigh the effects of rainfall. Thus it is best to use as many as possible, which has the added benefit of providing a range sediment yield forecasts (Crosbie *et al.*, 2011).

Temperature and rainfall data will be calibrated for SWAT using the WGN Maker, Macro, which formats the climate data and calculates the statistics needed for SWAT to run. The new data will be put into the SWAT model and the sediment yield from sheet and rill erosion will be calculated for three

separate 19-year periods 2015-2034, 2046-2065 and 2081-2100 to derive short, medium and long-term estimates.

1.3.4. Modelling effects of land use change

There is potential for commercial crop agriculture.in the Tsitsa River Catchment. Some of the crops considered for cultivation in the catchment include sweet potato, sugarcane, cabbage, avocado orchards and corn. These crop types will be simulated into the SWAT model and run under till and no-till scenarios in order to determine how they will affect the sheet and rill aspects of erosion.

Tillage operations redistribute plant residue, nutrients, pesticides and bacteria through the soil profile. Tillage operations were first introduced to remove the plant residue from the soil so that there would be no food sources for pests, thus reducing the number of pests and the negative effects associated with them (Nietsch *et al.*, 2005). However, it was noticed that tillage operations made the soils more prone to erosion due to the destruction of the soil structure and the removal of organic matter, which helps consolidate the soil and give it structure. The removal of mechanical pest control, unfortunately, forced farmers to use more chemical pest control methods, which lead to environmental contamination (Nietsch *et al.*, 2005).

No-till agriculture limits the amount of soil disturbance to only necessary activities such as the application of nutrients, the conditioning of crop residue and planting crops. By not tilling the fields there is an improvement in soil organic matter content, which contributes to enhanced soil structure and resilience to erosion. It also reduces the CO_2 and particulate losses in the soil. No-till activities have proven to reduce sheet and rill erosion from water as well as wind erosion (Waidler *et al.*, 2011).

Various studies have shown the benefits of conservation tillage and no-till agricultural practices on water and material fluxes at the local field scale. It is important, however, to determine the effects of these practices at the watershed scale in order to guide management practices (Ullrich & Volk, 2009). The Eastern Cape province is one of the areas in South Africa where a lot of

investment is being made into conservation agriculture, which makes studying the effects of tillage on soil erosion in this area important.

1.4. Project outline

The primary aim of the project is to determine the sediment yield in the upper Tsitsa River Catchment. The first step of the project is to write a ruleset in eCognition to identify gullies over the gullies in 2012 and 2007. The rate of gully growth will be calculated and the gully activity will be established. The second phase of the study is to setup the SWAT model for the catchment using current land use and climate data to calculate the sediment yield from sheet and rill erosion. This will be used as a baseline. Once the current soil erosion phenomena have been mapped and modelled, the models will be extended to predict soil erosion under future scenarios. The land use input will be changed to account for large-scale agriculture. This will be done by converting all agricultural land in the catchment to the various crops simulated overall six different land type scenarios will be run and compared.

The next phase will be to model sediment generated in the catchment under projected climate change data. The results from the six simulated GCM will be put into SWAT and run under current land use scenarios using the generic agriculture simulation in SWAT. Using the gully activity and growth rate the sediment generated from gully erosion in the catchment will be calculated for the period 2015-2100. This will be combined with the results of the climate change model and the land use model to get the overall sediment production in the catchment. The study hopes to clarify the effects of land use change and climate change on an economically important catchment in South Africa in order to aid dam management practices.

2. Literature Review

2.1. Erosion phenomena

Soil erosion is defined as the loosening of the land surface by physical processes such as rain, flowing water, wind, ice, temperature change, gravity or other natural or anthropogenic agents that abrade, detach and remove soil or geological material from one point on the earth's surface to be deposited elsewhere (Jones & Thompson, 2007). In a catchment, there are numerous rills and channels which can channel erosion and particles. During a rainstorm event, rain droplets can detach unprotected soil particles and transport them to the rills and channels. From here the sediment is transported to larger rills and ephemeral channels and finally into the main channel. The deposition of sediment can happen throughout the catchment so not all the sediment generated in the catchment will reach the catchment outlet (Nietsch *et al.*, 2011).

2.1.1. Sheet erosion

Sheet erosion also known as rain splash or sheet wash is defined as the uniform detachment of soil particles by rain splash and the subsequent removal of the soil particles downslope by overland flow as a sheet rather than in a defined channel such as with gully erosion or rill erosion. Sheet erosion results in the loss of fertile top soil and occurs most commonly in ploughed fields or areas with sparse vegetation (Nearing *et al.,* 1994).

2.1.2. Rill erosion

Rill erosion is one of the most common forms of erosion and is defined as the detachment of soil particles and the subsequent concentrated removal of particles along streamlets, or head cuts. Rill erosion is not often deep being less than 30 cm and can be removed by tillage (USDA-ARS National Soil Erosion Research Laboratory, 2015).

2.1.3. Gully erosion

Gullies are three-dimensional erosion forms that may appear in various shapes, sizes and complexities. They range from simple longitudinal linear incisions to deeply incised dendritic networks with V-shaped, U-shaped and even overhanging cross-profiles. Their length may vary from a few meters to hundreds of meters and their width and depths from several decimetres to tens of meters (d'Oleire-Oltmanns *et al.*, 2014). Gullies occur when runoff water is channelled into grooves and deepen over time forming a distinct head with steep sides that may collapse by water seepage or undermined by water flow within the gully (Mararakanye & Nethengwe, 2012). Gullies mainly occur in drainage ways at lower slope positions and are the most obvious erosion features in the landscape ranging from 30 cm to 30 m deep (Poesen *et al.,* 2003; Mararakanye & Nethengwe, 2012). Gullies may be classified as continuous or discrete, with the former having many branches whilst the latter are independent with no distinct connection with the main gully or stream channel (Mararakanye & Nethengwe, 2012).

2.2. Monitoring of erosion

2.2.1. Field-based methods

Traditional field-based methods of monitoring soil erosion are conducted in the field and make use of plots, pins or points (Gillan *et al.*, 2016). These methods are often labour intensive and limited in spatial and temporal extent (Gillan *et al.*, 2016) they are also vulnerable to theft and vandalism (Hudson, 1993). Today, many erosion studies rely on aerial or satellite images and hydrological models to determine soil erosion rates. Although these methods are less labour intensive and remove the potential for human disturbance and vandalism, many still require field observations and ground truth data for validation and calibration (Nearing, 2000).

2.2.1.1. Plot-based methods

Traditionally soil erosion has been measured by collecting data from small plots called runoff plots. The gathered data are then extrapolated to the larger catchment (Evans, 2002). The plots are available in various sizes and types depending on the geomorphology of the landscape and the processes involved in erosion (Boix-Fayos *et al.*, 2006). There are numerous disadvantages and limitations to plot based methods. One of the biggest drawbacks is that the simulated runoff is either caught by directing the flow of water over the lower edge of the plot which causes an abrupt drop in height into the containers, or it is discarded. With such a rapid increase in gradient, a potent 'driver' of erosion is created which would not usually have been there in the field (Evans, 2002). Field assessments of soil erosion are based on two main assumptions. First, the effects of rain splash and sheet wash are insignificant, in the short term, in the redistribution of soil within a field other than over distances of a few metres. Second, rills and gullies are the main channels of soil redistribution in a catchment (Evans, 2002).

Another limitation to plot-based models is the lack of a temporal scale. Most research projects using plot based methods are limited to a few years therefore, they are not indicative of long-term erosion processes and variations (Boix-Fayos *et al.*, 2006). In closed plots, a common problem when conducting temporal experiments is the depletion of material. Numerous studies have shown that the erosion rates of closed plots were reduced over a 6-year period. This was caused by the system changing from a transport-limited to a detachment-limited environment. One explanation for this observation could be due to the formation of a harder surface layer which can inhibit detachment. Another problem with closed plot experiments is the lack of input material from outside the plot. There is, however, an advantage to the use of closed plots in that they allow for the comparison of different responses at the same spatial scale with the same size drainage area (Boix-Fayos *et al.*, 2006).

Plot based erosion-measuring methods also lack a spatial component. Hydrological and geomorphological processes which regulate the delivery, transport and storage of sediment in the catchment are highly scale dependent. Processes which dominate at the hillslope scale may be overridden at the catchment scale. Plot based methods are unable to account for the change in

processes when extrapolating to the larger catchment (Boix-Fayos *et al.*, 2006). Errors in the experimental design can lead to the creation of artificial boundaries and human disturbance of the natural processes (Boix-Fayos *et al.*, 2006).

Finally, plot-scale measurements are unable to account for the natural heterogeneity in the catchment as well as the complexities of connectivity, continuity and the system interactions. Due to the short temporal scale of plot measurements they often do not include extreme rainfall events where most of the detachment and downslope movement of particles occur (Hudson, 1993).

2.2.1.2. Point-based methods

There are various field-based measurements which are measured by changes at a single point. If these methods are simple enough and inexpensive a large number of points can be sampled, which can give a good estimation of soil loss over an area (Hudson, 1993). Examples of point measurements include:

- Erosion pins which are a widely used method whereby a pin is placed carefully in the ground where the top of the pin gives the date that pin was placed. Pins can be placed at random points across the study area. The pins usually form a 'T' shape at the top and the soil loss can be measured by measuring the distance from the top of the pin to the ground surface after a certain period of time (Hudson, 1993; Stroosnijder, 2005).
- Paint collars involve painting a line at ground height on suitable, longstanding features such as boulders or trees. The soil loss can then be determined after a period of time by measuring the distance from the painted line and the new ground height (Hudson, 1993).
- The bottle cap or pedestal method uses a bottle cap or other protective surface placed into the ground. This will shield the area from rain and create a pedestal. The height of the pedestal can then be measured to determine the amount of soil loss (Hudson, 1993; Shakesby *et al.*, 2006).

Point-based methods can be extremely time-consuming especially when working over a large area. Another problem with point-based methods is the disturbance of the placements by animals or people. They are also susceptible to theft and vandalism (Hudson, 1993).

2.2.1.3. Radiometric dating techniques

The Ceasium-137 isotope and radiometric dating technique is another field-based method. Using Cs-137 for erosion studies has proven reliable and been successfully used in a variety of environments for the last 30 years (Soto & Navas, 2008). This technique is able to give longer-term estimations than plot measurements, up to 35 years. It is also able to give estimations over large areas on a single site visit. Thus Cs-137 dating has become an important tool for measuring soil erosion and can be used in a wide range of environments (Walling & Quine, 1992).

It is based on the fact that Cs-137 was released into the environment as a result of thermonuclear bomb tests during the 1950's-1970s. The isotope went into the stratosphere and was then distributed globally. The method derived from this phenomenon is based on the assumption that a consistent relationship can be established between the degree of increase and depletion of the Cs-137 inventory in the soil and the total depth of soil loss or accretion. (Walling & Quine, 1992).

2.2.2. Computer-based methods

2.2.2.1. Geographic information systems

Geographic Information Systems (GIS) have proven to be useful in mapping and modelling soil erosion at various spatial and temporal scales in complex watersheds (Huang *et al.*, 2003). With the advancement of computers and software GIS, many of the more recent studies on soil erosion have been conducted using GIS. GIS mainly uses models to simulate catchment processes and model soil losses. The simplest and widely used model is the universal soil loss equation (USLE) model (Zivotic *et al.*, 2012). Many other models are based on the USLE and its derivatives such as the modified universal soil loss

equation (MUSLE) and the revised universal soil loss equation (RUSLE). The main advantage of using GIS to calculate soil erosion is the ease at which data can be interpreted.

Many models use various inputs such as soil properties, climate data, digital elevation models (DEM) and land use, which are widely available especially in developed nations such as the United States of America where it was created. Using a grid approach, along with the spatial data sets mentioned above GIS models are able to capture the complexity and heterogeneity of catchments (Jain *et al.*, 2005). GIS models are also able to run over various temporal scales from a few months to decades as well as model sediment yield at various spatial scales which plot measurements fail to achieve. These models have also evolved over time and many are now able to simulate surface and subsurface processes (Jain *et al.*, 2005). This can all be done at the desktop and various scenarios can be simulated with slight changes to the inputs. GIS models are also more reliable and produce more reproducible results than field data.

Many GIS models are able to simulate complexity and heterogeneity in the environment more successfully than plot-extrapolated data. The use of Hydrological Response units (HRU) in GIS allows the models to group areas with similar properties. This gives more heterogeneity to the model and the simulations are closer to reality. Models run in GIS are also not susceptible to disturbance by animals or people. This makes GIS a more attractive method to determine soil losses than other traditional methods. It is important to note that GIS models have numerous drawbacks. Most important for this study is that they fail to model gully erosion. Further disadvantages of hydrological models include lack of user friendliness, large data requirements, absence of clear statements of their limitations and over-simplification of catchment processes (Devia *et al.*, 2015).

2.2.2.2. Soil loss equations (USLE, MUSLE, RUSLE)

2.2.2.2.1. USLE

The universal soil loss equation (USLE) (Equation 2.1) was developed by Wischmeier and Smith (1978) and has become the most widely used and supported soil conservation tool (Tombus *et al.*, 2012). It takes into account rainfall erosivity, soil erodibility, slope, vegetation and land management practices to predict long-term average annual soil loss on uniformly cultivated fields (Cardei, 2010). The equation is empirical and is based on measurements rather than theoretical principles. The model is constructed on the theory that erosion is a multiplier of rainfall erosivity which also multiplies the resistance of the environment (i.e. topography, land cover and land management) (Bruland, 2015).

Equation 2.1. $A = R * K * LS * C * P$

Where A = Annual soil loss (in tonnes per acre per year or tonnes per hectare per year)

R = rainfall erosivity

K = soil erodibility

SL = slope length and gradient

C = crop management factor (cover)

P = crop management factor (support factor)

The main limitation to the USLE model is that it only models sheet and rill erosion and disregards sediment produced from gully erosion. However, there are also a number of other limitations such as it never applies to linear or mass erosion, as the source of energy in the equation is rainfall. Another limitation is that the rainfall simulation energy only applies to the Great Plains of the United States of America (USA). The model has also only been verified in countryside environments with slopes of 1-20% and so it excludes mountainous

areas with slopes greater than 40%. Another major limitation of the model is that neglects certain interactions between the factors. Finally, the model applies to long-term data and it cannot be used to model the effects of a single storm (Cardei, 2010).

USLE was first used on catchments in South Africa by Crosby *et al.*, (1983) and McPhee & Smithen (1984), however, the USLE was never widely implemented in South Africa (Smith, 1999).

2.2.2.2.2. MUSLE

The modified universal soil loss equation (MUSLE) replaced the rainfall erosivity factor in USLE with a runoff factor, which is effectively the product of rainfall amount and runoff amount (Equation 2.2). This improves the prediction capabilities of the model as the runoff factor becomes a precursor of moisture as well as rainfall energy and it eliminates the need for delivery ratios (Zhang *et al.*, 2009). The main advantage of the MUSLE is that it is able to predict sediment losses for a single storm event (Zhang *et al.*, 2009).

The MUSLE applies to the points in the watershed where overland flow enters the streams. All the points are then summed to give the total sediment entering the stream from the watershed (Zhang *et al.*, 2009).

Equation 2.2. $S = 95(Qp_p)^{0.56} * K * L * S * C * P$

Where S = sediment yield for a single event (in tonnes)

Q = total event runoff

The rest of the factors are the same as for the USLE equation described earlier.

The MUSLE model, however, was shown to overestimate soil erosion in a catchment in the Drakensberg by over 1000% (Laker, 2004). It is believed that the USLE model and its derivatives are designed for slopes in America where

slope is the dominant factor whereas in South Africa soil erodibility is a more dominant factor controlling soil erosion (Laker, 2004). This is especially true in catchments is the Eastern Cape where the soils are known to be highly erosive and dispersive (Le Roux *et al.*, 2015).

2.2.2.2.3. RUSLE

The revised universal soil loss equation (RUSLE) is based on USLE but the factors for slope length and angle as well as the conservation and land management practices have been modified. However, this modification has shown to have little effect on the efficiency of the model (Tiwari *et al.*, 2000). The RUSLE model does not account for the complex processes of deposition in the catchment and simply assumes that all sediment will end up in the river. Newer developments of the model are trying to simulate the catchment processes to more accurately model sediment yield (Tiwari *et al.*, 2000).

RULSE has been more widely used in catchment studies in South Africa than USLE. Smith *et al.* (2000) applied RUSLE to catchments within the Lesotho Highlands Water Project to determine soil losses and depict the distribution and extent of soil erosion in the catchments. The study also used the model to screen different land use practices in order to determine the ones causing the highest erosion rates. Le Roux *et al.* (2008) applied RULSE to determine actual and potential erosion risk areas at a national scale in South Africa. Mhangara *et al.* (2012) used RUSLE within the Sediment Assessment Tool for Effective Erosion Control model to assess the soil erosion risk in the Keiskamma catchment.

2.2.2.3. SWAT

The soil and water assessment tool (SWAT) is a physically based, catchment-scale, continuous-time model developed by the United States Department of Agriculture (USDA). It functions on a daily time step and aims to predict the impact of management on water, sediment, and agricultural chemical yields in ungauged watersheds (Gassman *et al.*, 2007). The SWAT model allows for multiple scenario analyses of the catchment area at various scales. Thus the

effect of certain variables such as source and sink zones on erosion and deposition can be tested (Le Roux *et al.*, 2013). The use of the SWAT model can help predict the sediment generated in the catchment and can thus provide useful information for the selection process of potential dam sites, dam construction designs and dam management strategies by testing various scenarios and their effects. Due to the continuous design of the SWAT model, it cannot be used as a field-scale, event-based model. The emphasis is on annual average results on sediment migration as represented by the SWAT model's spatial elements including sub-catchments and catchments (Le Roux *et al.*, 2013).

SWAT is based mainly on the Simulator for Water Resources in Rural Basins Model (SWERB). Nevertheless, other models such as CREAMS, GLEAMS and EPIC have also been incorporated into the SWAT modelling equations (Nietsch *et al.*, 2011). The land management inputs can be in high resolution due to the models structure and its basis on the EPIC (Erosion Productivity Impact Calculator) model (Ullrich & Volk, 2009). SWAT has been extensively used for soil erosion monitoring in various catchments in North America (Kannan *et al.*, 2007), Europe (Ullrich & Volk, 2009), Asia (Zhou *et al.*, 2013) and Africa (Asres & Awulachew, 2010) . There are numerous benefits of using the SWAT model, which are listed below (Nietsch *et al.*, 2011):

- SWAT is able to model watersheds without monitoring data.
- The relative impact of varying practices such as land use management on the catchment can be quantified.
- SWAT uses commonly available input data.
- Running SWAT is computationally efficient; the simulation of large or complex watersheds does not take long to run.
- The SWAT model also enables the study of long-term impacts on a catchment by allowing for decades of data to be used as an input.

The most important equation in the SWAT model is the water balance equation (Equation 2.3). In SWAT, the simulation of the hydrologic cycle happens in two divisions. The first division is the land phase of the cycle this controls the water, sediment, nutrients and pesticide loadings washing into the main basin. The second phase is the water routing division, this phase controls the

movement of water, sediment and nutrients through the channel network to the outlet (Nietsch *et al.*, 2011).

SWAT uses the MUSLE equation (Equation 2.4) to calculate sediment yield. The MUSLE equation is based on the USLE equation but it uses the runoff to simulate erosion rather than using rainfall as an indicator of erosive energy. This brings a number of benefits to the model (Nietsch *et al.*, 2011):

- It increases the prediction accuracy of the model.
- Eliminates the need for a delivery ratio.
- It allows for single storm estimates of erosion to be calculated.

Equation 2.3 $$SW_t = SW + S(R_{day}-Q_i-E_a-P_i-QR_i)$$

Where SW = soil water content

t = time

R_{day} = precipitation

Q_i = surface runoff

E_a = evapotranspiration

P_i = percolation

QR_i = return flow

Equation 2.4 Sediment Yield = $11.8 (Q_{SURF} * q_{PEAK} * Area)^{0.56} K*C*P*LS*CFRG$

Where

Sediment yield = daily sediment yield

Q_{SURF} = daily runoff volume

q_{PEAK} = 30 min peak runoff rate

Area = sub-catchment area

K = soil erodibility factor

C = crop management factor (cover)

P = crop management factor (support practice)

LS = topographic factor

CFRG = Coarse fragment factor

SWAT has an inbuilt climate change modelling simulation where the user can adjust factors such as precipitation, solar radiation, temperature and carbon dioxide levels. It is also able to simulate climate change by using weather information generated by other models as the climate inputs. This study will make use of climate data generated by Engelbrecht *et al.* (2011) to model sediment yield under various climate scenarios. SWAT uses a number of variables and factors in its simulation equations and these are described below.

2.2.2.3.1. Soil erodibility factor

The soil erodibility factor is based on the susceptibility of a soil to erode. This is determined by the properties of the soil itself (Nietsch *et al.*, 2011). It was noted by Wischmeier and Smith (1978) that soils become less erodible with a decrease in the silt content even if there is a subsequent increase in the sand or clay fractions of the soil. Other factors which influence soil erodibility are organic matter content, particle size, soil structure and soil permeability (Wischmeier & Smith, 1978). The soil erodibility factor is defined as the soil loss rate per erosion index unit for a specified soil as measured on a unit plot (Nietsch *et al.*, 2011).

2.2.2.3.2. Land cover and management factor

The land use and management in the catchment has a profound effect on the soil properties. Crop management such as tilling and type of crop planted affects the soils ability to withstand erosion. The crop management factor is defined as the ratio of soil loss from land cropped under specific conditions to the corresponding loss from cleaned tilled, continuous fallow (Wischmeier & Smith, 1978). Plant cover helps negate the effects of rain splash erosion as it reduces the speed at which the rain droplets hit the soil and thus their potential to dislodge soil particles. Plants also reduce runoff by reducing its transport capacity and velocity (Nietsch *et al.*, 2011).

2.2.2.3.3. Support practice factor

Support practices are crop management operations such as contour tillage, strip cropping on the contour and terracing. The support practice factor is defined as the ratio of soil loss with a specific support practice to the corresponding loss with up and down slope culture (Wischmeier & Smith, 1978). Contour tillage works best on slopes of 3-8% and provides good protection of the soil from erosion during low to moderate storms, however, they provide no protection during severe storm events (Nietsch *et al.*, 2011).

2.2.2.3.4. Topographic factor

The topography plays an important role in soil loss in the catchment. Steep slopes are more prone to erosion whereas valley bottoms and depressions can act as sinks for sediment. The topographic factor is defined as the expected ratio of soil loss per unit area from a field slope to that from a unit length of uniform 9% slope under identical conditions (Wischmeier & Smith, 1978). Slope, gradient and angle are all considered in the topographic factor (Wischmeier & Smith, 1978).

2.2.2.3.5. The coarse fragment factor

The coarse fragment factor is defined as the percentage by mass of rock fragments in the first soil layer.

2.2.2.3.6. The use of SWAT for erosion studies

There have been numerous studies conducted on the use of SWAT for sediment yield modelling both in Africa and abroad. Chen and Mackay (2004) studied how the structure of the SWAT model and the input data affected the results produced by SWAT by looking specifically at how the two factors influenced sediment production in a catchment. Focussing on the use of the MUSLE equation in SWAT and the delineation of hydrologic response units (HRU) the study showed that HRUs did not conserve sediment loads across the different levels of the portioned watershed in fact, the HRUs introduced roughly half of the variability in sediment generation. Previously this variability had been attributed completely to the aggregation of the input data. The reason for the observations were explained by the use of the MUSLE equation which defines a non-linear relationship between sediment generation, and the area of a specific HRU. However, there is a linear relationship in sediment load from the HRU level to the sub-watershed level. The second reason the study found was that HRUs aggregate surface land areas without regard to connectivity aspects, these are implicit in the MUSLE equation. This causes conflict between the two components of the SWAT model and makes it difficult to use the model for determining land use change effects on soil erosion (Chen & Mackay, 2004).

De Vente *et al.* (2008) studied and compared three different soil erosion models. The main reason for testing three separate models was that some erosion models, such as SWAT, do not account for gully erosion or channel erosion and transport methods through the catchment. By testing three models, a comparison of the significance of gully erosion on the sediment yield results can be made. WATEM-SEDEM model, which is based on the RUSLE equation, the Pan-European Soil Erosion Risk Assessment model (PESERA) based on the sediment transport equation and the Pan-European Soil Erosion Risk Assessment model (PESERA) were compared. After testing the three models

on 61 catchments in Spain, it was concluded that SPADS and WATEM-SEDEM provided best results. PESERA was suggested as a good alternative model for catchment scale studies in diverse environments, yet he warns that the PESERA model calculates soil erosion rates and not sediment yield in the catchment.

De Vente *et al.* (2013) further analysed 14 soil erosion models, of which SWAT was one. All the models tested only accounted for sheet and rill aspects of erosion and disregarded gully erosion. After analysing the 14 models it was found that they only provide reliable results where the considered processes of the model are indeed dominant in reality. The study concluded that of the 14 models, the most accurate predictions using the least data requirements were provided by SPADS and WATEM–SEDEM. Furthermore, they noted that no single model fulfils all modelling objectives and additional integration of field observations for validation and calibration as well as different model concepts are needed to obtain better predictions of current and future of soil erosion.

Yang *et al.* (2009) used SWAT to determine the efficiency of flow diversion terraces in counter-acting soil erosion and maintaining the quality of surface water in a catchment in Canada. They used three years for model calibration. The results showed that SWAT was effectively able to model the seasonal water yield. Asres and Awulachew (2010) also used SWAT to model areas which are prone to erosion in Ethiopian Highlands at the catchment scale. In the study, they also looked at how the use of vegetation strips can further prevent soil erosion. The study ran for 5 years and using 3 years for validation. Results showed that SWAT performed well at determining soil erosion and sediment yield at the catchment scale and that vegetation strips significantly reduced soil erosion. It was recommended by the authors that more models need to be run in the area using more accurate data sets. (Asres & Awulachew, 2010).

Qiu *et al.* (2012) studied the use of the SWAT and the calibration techniques to model sediment yield in hilly catchments in China. The study showed that SWAT underestimated sediment production during high flow events such as thunderstorms. SWAT also underestimated the sediment yield during both the calibration and validation periods. It was suggested that the main reason for SWAT's under-estimation was due to the limitations presented by the SCS-curve number and the MUSLE equation which SWAT is based on. The main

limits presented by the SCS-CN are that it does not account for time and was developed for the estimation of single storms. The SCS-CN works best for agricultural land and its accuracy diminishes when applied to rangelands and grasslands. Finally, the SCS-CN is an average value of flow. However, despite this, the authors concluded that the results from the SWAT model were acceptable. SWAT has also been used to as a scenario analysis tool to model connectivity aspects in soil erosion at the catchment scale by Le Roux *et al.* (2013).

Dechmi *et al.* (2012) determined that the various versions of SWAT did not all model the water flow appropriately and they developed a method to modify SWAT 2005 to correctly simulate the main hydrological processes. Bossa *et al.* (2012) studied the effects of soil data resolution on the results of the SWAT model and showed that with coarser data SWAT underestimated water yield in the catchment. The study also showed that the combined effects of the coarser data mapping in contrast with less coarse data had a measurable influence on lateral flow and sediment yield within the study area. Baker and Miller (2013) studied the use of SWAT to model the impacts of land use on a watershed in Kenya, East Africa. For their model, they used land use data from a 17-year period and the SWAT model to determine the effect of land use on the recharge rates of both surface and ground water. Results showed that over the 17-year period the rate of recharge was lower for both surface and ground water. They concluded that SWAT was able to assess adequately the effects of land use on catchments in Africa but also admitted that finer detail data sets would have resulted in results that are more accurate.

Yesuf *et al.* (2015) used SWAT in the north-eastern highlands of Ethiopia in order to identify soil erosion processes and estimate sediment runoff. Using the results to advise best management practices and monitor and evaluate different management scenarios. After model evaluation using multi-objective function statistics such as P and R factors, root mean square error and the coefficient of determination it was found that SWAT underestimated peak sediment loads. However, they stated that according to the model evaluation guidelines and performance, the derived sediment yield could be rated as satisfactory. Data related difficulties and limitations in the study resulted from inadequate and inconsistent measured sediment yields for some of time periods.

2.2.2.3.7. Description of SWAT inputs

The SWAT model developed by Arnold *et al.* (1998) for the USDA was implemented in the GIS environment as an extension of ArcMap called ArcSWAT and it is currently distributed by Spatial Science Laboratories. ArcSWAT is a graphical user interface for SWAT and was used for this study. A digital elevation model, land use, land management, soil characteristics, daily rainfall and temperature are all required as input data for the SWAT model (de Vente *et al.*, 2013). Most of the required input parameters (up to 25) are estimated through calibration. In SWAT, all relevant eco-hydrological processes such as water flow, nutrient transport, vegetation growth, land use and water management are integrated at the sub-basin scale and regression equations are used to determine the relationship between the input and output data (Ullrich & Volk, 2009). SWAT divides the catchment into multiple sub-catchments based on the number of tributaries. The size and number of the sub-basins can vary and depends on the stream network and size of the watershed (Ullrich & Volk, 2009). These sub-basins can be further divided into hydrological response units (HRUs) consisting of homogeneous soil and land use characteristics (Le Roux, 2009; Ullrich & Volk, 2009; Le Roux *et al.*, 2013). HRU are the spatial unit where the vertical flows of water and nutrients are calculated through a water balance equation, which is represented by four storages: snow, soil, shallow and deep aquifers (Ullrich & Volk, 2009). The HRU's in SWAT are spatially intrinsic, their exact position in the landscape is unknown, and it might be that the same HRU covers different locations in a sub-basin (Ullrich & Volk, 2009).

2.2.2.3.8. The SCS- curve number

The hydrologic component of sediment transfer is based on the water balance equation, which integrates various processes. Surface runoff volume is calculated using the USDA Soil Conservation Service curve number (SCS-CN) method (Le Roux, 2009; Le Roux *et al.*, 2013). The SCS-CN method was developed by the United States Department of Agriculture- Natural Resources Conservation Service to predict runoff in agricultural fields (Nietsch *et al.*, 2011). The curve number (CN) is a lumped factor used for the estimation of

flood volumes and peak discharge, it accounts for the effects of land use and surface conditions, along with other characteristics such as the effects of the soil hydraulic properties and ground cover (Mottes *et al.*, 2014). Equation 2.4 is used to calculate SCS-CN (Nietsch *et al.*, 2011).

Equation 2.4 $$Q(surf) = \frac{(R(day)-I(a))^2}{(R(day)-I(a)+S}$$

Where $Q\ (surf)$ = accumulated runoff

$R\ (day)$ = Rainfall depth for the day

$I\ (a)$ = initial abstractions

S = retention parameter

The CN represents a combination of land use types and the specific hydrological soil group based on the soil's potential to generate runoff. The values are given as A, B, C or D or a combination (Schulze, 2012). The SCS-CN has been widely adopted in models because the equations are simple, the inputs are related to physical properties of the catchment such as soils and land cover, the method provides uniform answers and finally the SCS-CN also uses daily rainfall amounts (Schulze, 2012). Although the SCS-CN incorporates the effects of canopy storage on surface runoff it cannot directly model infiltration rates (Nietsch *et al.*, 2011).

Soil hydrologic groups were developed by the United States Natural Resource Conservation Service, which classified soils into classes based on their infiltration characteristics (Nietsch *et al.*, 2011). The soils are grouped according to their runoff potential under certain storm conditions. This is determined by certain properties of the soil, which include depth to water table, saturated hydrologic conductivity, depth to slowly permeable layer. There are four soil hydrologic groups namely A, B, C, D and dual classes such as A/D, B/D, C/D. The description for each are given in Table 1.1 (Schulze, 2012).

Table 1.1: The hydrologic groups and their descriptions used by the SWAT model (Schulze, 2012).

Hydrologic Group	Description
A	Low stormflow potential. Infiltration is high and permeability is rapid in this group. Overall drainage is excessive to well-drained (Final infiltration rate ~ 25 mm/h. Permeability rate > 7.6 mm/h).
B	Moderately low stormflow potential. The soils of this group are characterized by moderate infiltration rates, effective depth and drainage. Permeability is slightly restricted (Final infiltration rate ~ 13 mm/h. Permeability rate 3.8 to 7.6 mm/h).
C	Moderately high stormflow potential. The rate of infiltration is slow or deteriorates rapidly in this group. Permeability is restricted. Soil depth tends to be shallow (Final infiltration rate ~ 6 mm/h. Permeability rate 1.3 to 3.8 mm/h).
D	High stormflow potential. Soils in this group are characterized by very low infiltration rates and severely restricted permeability. Very shallow soils and those of high shrink-swell potential are included in this group (Final infiltration rate ~ 3 mm/h. Permeability rate < 1.3 mm/h).

The most detailed and easily available map covering South Africa to which SCS soil groups can be linked is the Land Type map, produced by the Agricultural Research Council's Institute for Soil, Climate and Water (ARC-ISCW) (Land Type Survey Staff, 1972 – 2006).

2.2.2.3.9. Model theoretical foundations

Sediment yield caused by rainfall and runoff is calculated using the MUSLE, which incorporates surface runoff and peak flow rate along with the variables used in the USLE equation: soil erodibility, slope length and steepness, crop cover management and erosion control practice (Le Roux *et al.*, 2013). Evaporation, surface runoff, infiltration, plant uptake, lateral flow and percolation to lower layers are the soil water processes which are incorporated into SWAT (Ullrich & Volk, 2009). After SWAT has calculated the loadings of water and sediment, they are summed at the sub-catchment level which is then channelled through the stream network where it may encounter ponds,

wetlands, depression zones, or reservoirs. SWAT uses a mass balance equation to model the sediment transported in and out of the water bodies. Settling is calculated as a function of concentration and transportation out of a farm dam. Water flow is then channelled through the stream network using variations of the kinematic wave model. Sediment is routed by means of a simplified stream power theory where the maximum amount of sediment that can be transported, deposited or re-entrained from a channel segment is a function of the peak channel velocity (Le Roux *et al.*, 2013). One of the main limitations of SWAT is that the model often underestimates the role of the soil as a prime regulator in absorbing, retaining and releasing water after a rainfall event (Schulze, 2012).

SWAT uses the EPIC model to simulate crop growth and land management practices in the catchment. The EPIC model is a comprehensive, field-scale agricultural management model able to simulate non-point source loadings. It was originally developed to model the impact of soil erosion on crop productivity. EPIC incorporates management practices by taking into account the specific management operations such as the beginning and end of growing season, timing of tilling and fertilizer, pesticide, and irrigation applications for each HRU (Ullrich & Volk, 2009).

2.2.2.4. WEPP

The water erosion prediction project (WEPP) commissioned by the USDA is a computer based, continuous, process driven model designed for soil and water conservation planning. WEPP takes into account the natural processes in hydrology, soil sciences, botany and erosion to simulate the interactions between them. WEPP also accounts for both the spatial and temporal variability in topography, soil properties and land cover across a catchment. As sediment detachment and deposition is taken into account, WEPP is an improvement on USLE based models (Tiwari *et al.*, 2000). The model is based on the steady state continuous equation, the Green–Ampt Mein Larson equation (GAML) (Shen *et al.*, 2009). GAML considers rainfall duration as a time-step when solving the infiltration equation, when the infiltration rate is greater than the rainfall intensity no excess rainfall is calculated (Shen *et al.*, 2009). In the WEPP model, the catchment is divided into areas of homogenous soil, topography and land management properties known as overland flow

elements (OFE) (Shen *et al.*, 2009). Runoff, detachment and sediment deposition are calculated for each hillslope for the entire simulation period. These are then added for all the hillslopes in the catchment and then the runoff and sediment is routed through all the channels and impoundments (Shen *et al.*, 2009). WEPP has been successfully used in a range of environments including agricultural fields, rangelands, forests and construction sites (Flanagan *et al.*, 2001). There are a number of advantages of using WEPP over other sediment prediction models: (1) it can predict spatial and temporal variability of soil losses at the hillslope scale for any period of time. (2) It has a wide range of applicability and it considers various interactions between the input factors (Tiwari *et al.*, 2000). (3) It can also model the sediment yield from ephemeral gullies and channels (Laflen *et al.*, 1997). The biggest limitation of the WEPP model is that it was designed for small watersheds of less than 2.6 km^2 (Shen *et al.*, 2009). Another limitation of the model is that it less efficient to run than the USLE model (Tiwari *et al.*, 2000). WEPP also, like other erosion models, tends to underestimate high erosion losses and overestimate low erosion losses (Tiwari *et al.*, 2000).

van Zyl & Lorentz (2003) applied the WEPP model to three catchments in South Africa, two in Kwa Zulu-Natal and one in the Eastern Cape, in order to determine the impact of farming on sediment yield after integrated catchment management strategies had been implemented. The study found that the WEPP model was able to accurately measure soil water content yet was unable to accurately predict the frequency of saturated or near saturated soil conditions for the hydromorphic soil profiles.

2.2.2.5. ACRU

The agricultural catchments and research unit (ACRU) model was created at the university of KwaZulu-Natal as an agro-hydrological model. The aim of the model was to simulate the effects of stream flow; evaporation and land cover management on water resources in catchments (Jewitt & Schulze, 1999). ACRU is a multi-layer and multi-purpose integrated, physical conceptual model that operates at a daily time step interval (Jewitt & Schulze, 1999). It can operate on either a lumped or a distributed basis and works on a multi-layer soil/water budget. Runoff is dependent on the magnitude of daily rainfall

in relation to the daily soil/water budget. The ACRU model is able to simulate many aspects of the catchment such as irrigation, sediment and crop yield and water supply (Jewitt & Schulze, 1999). It is also a dynamic model so it can simulate changes in climate or land use. In the model, the catchment is divided into relatively homogeneous areas or sub-catchments with unique hydrological responses. Ideally, the model should not be used to model catchment hydrology on areas less than 1-2 km^2 because of the type of stormflow and base flow equations used and it should also not be used on spatial units exceeding 50 km^2.

The flow routing in the ACRU model is designed on the Muskingum method, which is based on the storage routing equation (Equation 2.5) (Smithers *et al.*, 1997). Two main parameters K and x are used in the equation along with the storage characteristics of the reach, which can be derived from historical flood data. K, the first parameter, is a storage constant also known as the lag or travel time through the reach. This value is assumed to remain constant at all flows and expresses the ratio between storage and discharge, usually expressed in hours. The second parameter, x, expresses the relative importance of inflow and outflow to the storage in the reach (National Oceanic and Atmospheric Administration, 2004).

Equation 2.5 $$S = K[xI + (1 - x)O]$$

Where S = Storage

I = Inflow rate

O = Outflow rate

K = Storage Constant

x = represents relative importance of inflow and outflow to storage.

The ACRU model is unlike SWAT in that the parameters do not need to be calibrated in order to produce a good fit but rather the model estimates the input values based on the physical characteristics of the catchment using available information. Thus to verify the models outputs a field study needs to be conducted (Warburton *et al.*, 2010).

ACRU was used in the study by van Zyl & Lorentz (2003) in the Weatherly Catchment, Eastern Cape. It was found that ACRU was able to model run off well yet slightly under-estimated daily flows.

2.2.2.6. SLEMSA

The original Soil Loss Estimation Method for Southern Africa (SLEMSA) is a field scale mathematical modelling approach designed for annual soil erosion estimations in agricultural land in southern Africa (Rademacher, 1991). It was developed as an alternative to the USLE model for more tropical regions such as Southern Africa (Igue, 2002). When compared with the USLE model SLEMSA produces lower erosion values (Igue, 2002). The SLEMSA model only considers soil loss from sheet erosion and can only be applied at scales 1: 50 000 or less (Rademacher, 1991). There are five main variables which are considered in the SLEMSA model, these are seasonal rainfall energy, amounted of rainfall intercepted by the crop, soil erodibility, slope length and slope percentage. In the SLEMSA model, these variables make up three sub-models. These sub-models account for soil loss from bare soil, cropping practices and topography (Rademacher, 1991). These sub-models calculate erosion using the formula in equation 2.6 below.

Equation 2.6 $$Z = K * X * C$$

Where

Z = estimated annual soil loss in t/h/yr.

K = average annual soil loss (in t/ha/yr) from a standard plot under conventional tillage (30 m x 10 m at a 4,5% slope) for a soil with a known erodibility factor of F, under a weed-free bare fallow.

X = the ratio of soil loss from a field with a slope length of L in metres and a slope percent of S to the loss from the standard plot.

C = the ratio of soil loss from a cropped plot to that of a fallow plot.

Stocking *et al.* (1988) created an improved SLEMSA model where it predicts soil loss over large catchment areas and not just at the field scale. Stocking *et al.*'s (1988) model makes use of a factorial scoring approach and the parameters: annual rainfall and rainfall energy, crop cover, average slope and the soil erodibility factor to estimate soil erosion (Manyatsi & Ntshangase, 2008). The results of the enhanced SLEMSA model is not in t/ha/yr as SWAT but rather in Erosion Hazard Units (Rademacher, 1991).

There are limitations to the SLEMSA model (1) the model can only accurately predict soil loss on slopes less than 20%. Above the 20% slope gradient, a small increase in gradient results in a disproportionally large increase in erosion. (2) All slope lengths in SLEMSA are assumed to have a maximum length of 100 m and the model's erosion predictions have not yet been verified on slope lengths which exceed 100 m.

SLEMSA was first applied to South African catchments in studies by Schulze (1979) and Hudson (1987) who found that the model over-estimates of soil losses in mountainous regions. More recently, SLEMSA has been applied to a catchment in Kwa Zulu Natal, South Africa by Breetzke *et al.,* (2013). The study aimed to estimate soil loss rates per land use type in a quaternary catchment. It was found that SLEMSA is sensitive to variations in slope

steepness and over-estimates soil loss in mountainous catchments. Gilau & James (2015) used SLEMSA on the Boksburg Lake in the Ekurhuleni Metropolitan Municipality in order to quantify what impact soil erosion, resulting from changes in land-use, had on the urban impoundment. It was concluded that SLEMSA can be applied to urban catchments in South Africa with high levels of accuracy.

2.2.3. Remote sensing

2.2.3.1. Remote sensing

Optical remote sensing is defined as the study of the earth surface using images collected by either drones, aeroplanes or satellites. It measures the spectral properties of the landscape but cannot directly measure the type, severity or extent of soil erosion. This needs to be done either using GIS or image analysis techniques. Optical remote sensing has been used quite extensively in studies on soil erosion (Manyatsi & Ntshangase, 2008). These sensors sense wavelengths in the visible and near infrared spectrum (0.4 - 1.3 µm) and the short wave infrared spectrum (1.3 – 3 µm) and in the thermal infrared spectrum (3 – 15 µm). One of the most widely used satellites for mapping soil erosion is the Landsat satellite this is due to its long-time of service and consequently, the data has been used since the 1970's (Vrieling, 2005). Landsat data are also freely available which, makes it easily accessible to researchers. The benefits of using optical remote sensing techniques to study catchments include the ability to see what is happening in difficult to reach areas or areas, which are possibly unsafe to visit. Remote sensing also allows for good temporal analysis of areas as many of the satellites have been in orbit and functional for number of years or decades (Vrieling, 2005). The data are also in the same format for each specific satellite mission, which makes it easy to compare various years or seasons.

2.2.3.1. Pixel based techniques

Pixel-based image classification is based on the spectral properties of the individual pixels and each pixel can only belong to one class (Yan, 2003). Pixel based classification can be divided into two main method types, supervised and unsupervised classification (Yan, 2003)

2.2.3.1.1. Unsupervised classification

Unsupervised classification is based on the principle that spectral values of a certain land cover type will be similar and their values will be comparatively very different to other classes (Yan, 2003). Unsupervised classification does not use training pixels instead, it analyses the unknown pixels in an image and clusters them into various classes based on the natural groupings in the image values. Essentially creating spectrally homogenous groupings or clusters (Duda & Canty, 2002). This method is generally used when there is little external information about the land cover types in the image. The image can then be divided into spectral classes which the analyst can associate a certain land cover to (Yan, 2003).

There are various algorithms which can be used in unsupervised classification. One of the most popular algorithms is the 'k-means' (Duda & Canty, 2002). The analyst will assign a number of classes to which the image is divided. The algorithm then randomly allocates that number of cluster centres across the image and the surrounding pixels are then assigned to the cluster whose centre is closest to it. Once all the pixels have been assigned to a cluster, the revised mean vector for each cluster is computed and these are then used as the basis to reclassify the image. This procedure will be repeated iteratively until there are no significant changes to the classification. The analyst will then determine the land cover class for each spectral cluster (Yan, 2003).

Another unsupervised classification algorithm is the agglomerative hierarchal clustering. This method assigns each pixel to a certain class or cluster. The clusters are then analysed for similarities and sizes and similar classes are combined to form larger ones. Smaller classes are also absorbed into larger classes with similar spectral properties. This method runs iteratively until the

desired number of classes has been reached or a single class has been formed (Duda & Canty, 2002).

2.2.3.1.2. Supervised classification

In supervised classification, the analyst supervises the classification process by selecting a number of training pixels. The training pixels are a set of pixels that describe the spectral properties of certain land cover types found in the image and they facilitate the classification process (Yan, 2003). The selection of suitable training pixels has a significant influence on the results of the classification and it is important to choose the best training pixels in order to get an accurate classification (Duda & Canty, 2002). The training pixels need to be representative of all the pixels in that class. During the training stage of supervised classification, the analyst chooses a number of suitable training pixels to train the classifier. The location, size, shape and orientation of the point clouds for each land cover type are determined through a set of statistics which describe the response pattern for each specific land cover (Yan, 2003). The more pixels selected during the training phase the more accurate the classification will likely be (Chen & Stow, 2002).

The next phase of supervised classification is the classification stage; here the classification is performed based on the selected training pixels and a specified algorithm (Yan, 2003). There are many algorithms used in supervised classification and they assign each pixel a value of either 0 (not belonging to the class) or 1 (belonging to the class) depending on whether that pixel belongs to a certain class or not. These types of classifiers, where a pixel either belongs to a class or not, are known are hard classifiers. Soft classifiers allow pixels to be assigned to one or more classes based on their similarity to that class. Fuzzy classifiers, on the other hand, allow pixels to belong to different classes based on various levels of similarity (Yan, 2003).

One of the most common and powerful algorithms used in supervised classification is the maximum likelihood classifier. This algorithm assumes that the distribution of point clouds forming the training pixel categories is normally distributed (Lu *et al.*, 2012). The algorithm is then based on the Gaussian estimate of the probability density function of each class. This

classifier evaluates both the variance and co-variance of the category's spectral response patterns when classifying an unknown pixel (Yan, 2003). The distribution of a category can be entirely described by the mean vector and the covariance matrix and with this, the statistical probability that a pixel belongs to a particular class can be computed (Yan, 2003). Once this has been done for all pixels for all classes, the pixel is assigned to the class which it has the highest probability of belonging to. The major drawback to the maximum likelihood classifier is it requires a large amount of computational power, which can be time-consuming when working with large images (Yan, 2003).

Kernel based methods such as Support Vector Machines (SVM) is a complex method of supervised classification (Ivanciuc, 2005). In SVM classification, different classes are separated by the construction of hyperplanes in a multi-dimensional space (Statsoft Incorporated, 2015). SVM is based on the statistical learning theory and the concept of decision planes which support decision boundaries (Ivanciuc, 2005). Decision planes separate areas of different classes and is produced through an iterative process which finds the minimum amount of error (Statsoft Incorporated, 2015).

The minimum distance to mean classifier requires that the mean spectral value for each spectral band in each training pixel cluster be calculated (Yan, 2003). This comprises the mean vector for each class. The unknown pixels are then classified based on the distance between the value of the unknown pixel and each of the class means. The analyst sets a maximum distance threshold for the pixels, in order to be classified into a certain class (Yan, 2003). This method is simple and does not require intense computational power to run. However, it is insensitive to varying variance in the spectral response signals and so the method cannot be used in data sets where the spectral response data are close together and have high variance (Yan, 2003).

Parallelepiped Classifier or multi-level slicing takes into account the variance of the spectral response data by considering the range of spectral values in each training pixel category (Japanese Association of Remote Sensing, 2012). This range is defined as the highest and lowest digital number value in each band. Unknown pixels are classified according to the category range or decision region in which they lie. It is important in the parallelepiped method to select accurate training pixels which cover the entire spectral range of each

representative class (Japanese Association of Remote Sensing, 2012). Multi-level slicing is computationally efficient yet it encounters errors when the category ranges overlap and pixels fall within that overlap. The overlap is caused when there is high covariance in the category distributions which the rectangular decision region is not able to adequate, describe (Yan, 2003).

Once all the pixels have been assigned a class the final phase of supervised classification, which is an accuracy assessment, needs to be conducted. An accuracy assessment compares the closeness of results between the classification and reality measured through ground control points (GCP's) (Yale's Centre for Earth Observation, 2003). This is done to evaluate the quality of the maps produced through image classification. Accuracy assessments use statistically sound sampling designs to compare the reference data to the results of the classification (Stehman, 1996). One method of conducting an accuracy assessment is to select unbiased random samples throughout the image and put them in an error matrix along with the GCP results. From the error matrix, a number of equations can be drawn that determine the user's, producer's and overall accuracies (Yale's Centre for Earth Observation, 2003).

A second method of carrying out an accuracy assessment is by conducting Kappa statistics. Kappa statistics are a discrete, multivariate technique which determines if one error matrix is statistically significantly different to another (Yan, 2003). The kappa coefficient returns the difference between the actual agreement and the agreement expected by chance (Yan, 2003). Data used in the error matrix or kappa statistics should not be from the training data as this will only show how well the training data performed and not how well the classification worked over the entire image (Yan, 2003).

2.2.3.2. Object-based image analysis

In recent years, OBIA has become a successful new methodology that goes beyond the pixel-based classification approach. With OBIA, an image is classified based on image objects or segments rather than the individual pixels (Yan, 2003). OBIA still uses individual pixel information, but through the clustering of pixels to form segments, additional properties can be utilised such

as homogeneity of a region, within-region variation or relationships to neighbouring objects (Dezso *et al.*, 2012; d'Oleire-Oltmanns *et al.*, 2014). OBIA has been built on older concepts of image segmentation, edge detection and feature extraction that have been in use for decades (Blaschke, 2010). However, it was the advent of high-resolution imagery and off the shelf specialised software that has made OBIA so popular in recent years (Blaschke, 2010). The OBIA classifiers are not hard classifiers like pixel-based analysis but instead they allow for fuzzy logic classification, also known as soft classification (Yan, 2003). This type of classifier has the advantage over hard classifiers as it allows for the possibility of uncertainties about the class descriptions (Yan, 2003).

OBIA relies on segmentation of the image into homogeneous objects and this is the first step when conducting OBIA and provides the building blocks for the rest of the analysis (Blaschke, 2010). There are four main types of segmentation namely point-based, edge-based, region-based or a combination of two or more (Blaschke, 2010). The regions created during the segmentation process are based on one or more criteria of homogeneity in one or more dimensions. In addition, and sometimes of an even greater advantage than the diversification of spectral value descriptions of objects, is the supplementary spatial information for objects such as spatial topology, geometric descriptions, etc. (d'Oleire-Oltmanns *et al.*, 2014).

2.2.3.2.1. Use of eCognition and OBIA for erosion studies

Gully and erosion mapping techniques have remained largely unchanged since the 1940's (Shruthi *et al.*, 2011). These techniques used visual interpretation of aerial photographs to identify and manually map gullies and erosion features usually for small areas. However, after the introduction of pixel-based classification methods, it was highlighted that the use of surface reflectance values and various other pixel-based classification methods could be applied in the identification of erosion features in aerial imagery (Lilliesand *et al.*, 2004). Metternicht and Zinck (1998) have conducted such a study where Landsat TM and JERS-1-SAR data were used to create an erosion map of the Sacaba Valley in Bolivia.

Casanovas and Zaragova (1996) applied supervised classification on Landsat 5 TM images to determine areas of high gully activity in the Anioa-Penedes Region, north-east Spain. NDVI created from the satellite image was used to estimate the percentage of vegetation cover on gully sidewalls and consequently the activity of the gullies.

Flanders *et al.* (2003) conducted a study which looked at eCognition software for feature extraction. They concluded that object-based analysis using eCognition software allowed for greater accuracy than manual or pixel-based classification techniques and that these techniques can be used for an array of projects. Although the same results can be obtained through series of masks and rules within a per-pixel classification software, eCognition was found to be easier to use and more versatile. Knight *et al.* (2007) used eCognition to segment ASTER images and then created an object-based approach to map gully erosion in Australia's tropical regions.

Vrieling *et al.* (2007) also used ASTER imagery in the Brazilian Cerrados to create a supervised, automatic classification of gullies based on the maximum likelihood approach. However, the conventional supervised and unsupervised classification techniques such as Maximum Likelihood Classification have been proven less effective than that of object-based gully extraction techniques due to their spectral similarities with other non-erosion features. Martha *et al.* (2010) showed that OBIA can be used with multi-type auxiliary information in the detection of landslide features in the Indian Himalayas. The study was able to quantify large-scale topographic changes caused by landslides and found that higher resolution imagery such as SPOT 5 can detect smaller scale features.

Anders *et al.* (2011) created a method to semi-automatically map alpine geomorphology in Austria. A stratified OBIA approach was used as they argued that if segmentation parameters are optimized for each geomorphological feature it will allow for each feature to be extracted separately. The accuracy of their method varied between 47% and 88% depending on the land type classified. In all, eroded bedrock produced the best accuracy while ablation until produced the lowest accuracy. d'Oleire-Oltmanns *et al.* (2014) highlighted the advantages of using object-oriented classification over conventional methods as it uses both spectral and spatial patterns when classifying the

image. The study was able to extract gullies using eCognition and QuickBird imagery with an overall classification accuracy of 62%. Wang *et al.* (2014) used OBIA to delineate the boundaries of gullies from high spatial resolution aerial photographs in the Beiyanzikou catchment of Qixia, China. The results showed good accuracy in delineating gully boundaries.

Other forms of remote sensing data such as LiDAR has been proposed to facilitate accurate mapping of gullies, as LiDAR accounts for changes in depth. Eustace *et al.* (2009) developed a semi-automated method to map the extent and locations of gullies with high-resolution LiDAR data in the Fitzroy Catchment, Australia. The study concluded that through applying OBIA on LiDAR data, it is possible to delineate gullies with good accuracy. Chen *et al.* (2009) compared a hierarchal classification system using LiDAR and QuickBird Imagery to improve the results of a traditional pixel-based classification approach. It was concluded that a hierarchal method improved the results by 20%. Johansen *et al.* (2010) used LiDAR to detect riparian features in Australia, the study highlighted the accuracy of LiDAR in distinguishing various geomorphological features. Johansen *et al.* (2012) used LiDAR to determine the extent and volume of gully erosion in Northern Australia, the results had an overall accuracy of 92%. Höfle *et al.* (2013) applied terrestrial LiDAR along with GIS techniques to detect gullies in a Peruvian peatland. The study provided a 93% accuracy when compared with manually digitised gullies for the same area.

The application of OBIA to identify gullies in Africa has been limited to studies in Morocco and South Africa. Shruthi *et al.* (2011) conducted a study on the use of eCognition for gully identification in Morocco. The study employed a method based on very high resolution (VHR) satellite data from IKONOS and GEOEYE-1. Using this data, they were able to derive a digital surface model (DSM) that was developed for the extraction of gully features. The results showed that object-based analysis was quicker and more objective than manual interpretation and that it was more accurate at finer scale analysis. Jetten *et al.* (2011) applied object-based analysis in eCognition software to delineate gullies in Morocco, using slope, catchment area and NDVI. The accuracy assessment indicated negligible overestimation and an overall good accuracy of eCognition to extract gullies was concluded. Shruthi *et al.* (2015) extended the study in 2015 and used OBIA to analyse changes to gully systems in Sehoul

region of Morocco over an eight-year period. They used the panchromatic and multispectral blue, green, red and near-infrared (Multispectral Scanner) bands from Ikonos-2 and GeoEye-1 along with a 1 m digital surface model and a DEM. From this, they were able to use texture and slope to identify gullies in three sub-watersheds.

An extensive study conducted by Taruvinga (2008) reviewed the use of satellite imagery for gully identification in Kwa- Zulu Natal, South Africa. The study looked at various techniques using either Landsat or SPOT 5 images; it was found that both data sets had strengths and weaknesses. The limited band combinations of SPOT 5 images restricted the use of indices such as the bare soil index. While the low resolution of Landsat data (30 m) was unable to distinguish gullies less than the pixel size. The study concluded that of all the algorithms tested that the SVM technique produced the most accurate results. The use of eCognition to identify gullies was later tested by Mararakanye and Le Roux (2012) in the T35 catchment in Eastern Cape Province. However, they discontinued the study due to the large amount of pre-processing needed especially when applied at a provincial scale. GIS and Remote Sensing technologies have been frequently used to assess soil erosion features in the Americas, Europe and Australia. However, in SA, there has been a lack of information regarding the spatial extent of gullies at a national scale. Mararakanye and Le Roux (2012) created a 1:10 000 gully location map of South Africa using remote sensing and GIS techniques on SPOT 5 images. This was the first study of its kind conducted in South Africa. The study highlighted the need for automatic, accurate gully mapping techniques based on high-resolution satellite imagery with global coverage which are applicable over large areas in order to reduce the time spent by researchers in manually digitising gullies (Mararakanye & Le Roux, 2012).

As with sheet and rill erosion, methods are needed to predict the extent and patterns of gully erosion across large catchments (*eg*. Hughes & Prosser, 2012). Identifying gullies from aerial and satellite imagery is the first step to creating a methodology to accurately calculate sediment yield from gully erosion in a catchment. Not all sediment produced from gullies end up in the river or dam at the catchment outlet as some of the sediment is deposited in sinks (Ndomba *et al.*, 2009; Le Roux *et al.*, 2015). Furthermore, not all gullies have equal potential to deliver sediment to the catchment outlet. Factors such as

vegetation cover inside the gully, connectivity and continuity (see Appendix 1) all determine the amount of sediment a gully will produce and channel through the catchment (Le Roux *et al.*, 2015). Various studies have tested numerous methods to estimate sediment yield from gullies. These studies used either indices, rule-based models/decision trees, and/or gully densities to estimate the overall eroded material followed by an estimated average gully delivery ratio in order to approximate the sediment yield contribution from gully erosion.

Le Roux *et al.* (2015) modelled the sediment yield derived from sheet, rill and gully erosion in the Mzimvubu Catchment in South Africa. The study used SPOT 5 images to map the changes in gully size between 2007 and 2012. They then applied a delivery ratio which ranged from 0% for disconnected gullies to 40% for potentially connected gullies and 60% for partially connected gullies, up to 100% for fully connected gullies. The potentially and partially connected gullies had unique delivery ratios based on connectivity rules in a GIS (Le Roux *et al.*, 2015).

Hughes and Prosser (2012) predicted patterns of gully density a catchment in Australia. They used aerial photographs to map the gullies across part of the Basin and then applied a multivariate statistical model for a range of environmental factors. They managed to predict gully density across the catchment, using a 10 km grid resolution. Although the gully density varied across the catchment they found that the average gully density across the catchment was 0.08 km/ km^2 and the resulting sediment yield contributions from gullies was about 27,106 t/yr. They concluded that the model was reasonably successful at predicting the variations in mapped gully density when compared with similar attempts to predict erosion processes a similar scale (Hughes & Prosser, 2012).

Ndomba *et al.* (2009) used a delivery ratio of 50% to estimate sediment yield from gully erosion in a catchment in north-east Tanzania. The study used aerial photos from selected years to estimate gully size and morphology changes over time. A delivery ratio was then applied to estimate the sediment yield rate. Sediment yield contribution from gully erosion was estimated as a ratio between gully erosion sediment yield and total sediment yield at the catchment outlet. Gully density in the catchment was found to be 0.016 km/

km². The final results produced, estimated sediment yield from gully erosion to be 140 000 – 280 000 t/yr (Ndomba *et al.*, 2009).

2.3. Effects of changing climate and land use on soil erosion

Climate change is predicted to have various direct and indirect effects on soil erosion (Mullan *et al.*, 2012). Climate change will impact the hydrological cycle through changes in rainfall events as well as lead to increased global temperatures and carbon dioxide concentrations in the atmosphere. It will result in changes to the amount, erosive power and temporal pattern of rain storm events (Mullan *et al.*, 2012). Soil erosion has a non-linear response to hydrological changes and so even a small increase in rainfall amount or intensity can result in widespread soil loss. This scenario is aggravated if the soil is unprotected or with bad land use practices (Simonneaux *et al.*, 2015). Climate change could lead to an increase or decrease in biomass along with a change in growing patterns of plants. This coupled with a temporal shift in rainfall or change in rainfall intensity could aggravate soil losses but it could also protect soil if the vegetation cover increases before the rainy season. Thus different catchments will have different responses to climate change and some may have a decrease in total soil loss (Bates *et al.*, 2008).

The indirect effects of climate change include changes in land use and management practices as well as the effect of increased atmospheric carbon dioxide (CO_2) on crop growth. More carbon dioxide in the atmosphere will have a complex effect on crop growth, some plant types may benefit from increased CO_2 and display faster growth rates (Franks *et al.*, 2013). Increased CO_2 needs to be supported by increase in water as well as other nutrients in order for plants to grow. Furthermore, increased CO_2 concentrations in the atmosphere will lead to complex changes in plant biomass. This can lead to faster residue decomposition from increased microbial activity and thus decreased soil erosion rates through an increase in soil surface canopy cover and biological ground cover (Routschek *et al.*, 2014).

Changes in rainfall of temperature could shift the growing season of many crops and so land management practices will have to shift with this in order to continue harvesting sufficient produce. In addition, climate change may cause

some areas under cultivation to be no longer conducive and may lead to land abandonment, which has shown to negatively affect soil erosion. Some cultivated areas may need to change the type of crop that is cultivated and some crops result in more soil loss than other crops. On a positive note, climate change may allow some areas not currently conducive to large scale agriculture to be cultivated.

Climate change will influence a variety of physical and chemical properties of the soil, which will affect infiltration rates and thus soil erosion processes. Soil moisture regime, organic carbon content and canopy cover are the most climate-sensitive properties of the soil (Chmielewski *et al.*, 2004). The most dramatic increases in erosion, however, are likely to result from a change in land use to more erosion-prone crops and less protective vegetation (Routschek *et al.*, 2014).

An increase in the atmospheric temperature is predicted to lead to an increase in atmospheric water-holding capacity at a rate of 7% per 1-degree change. This will lead to an increase in the water vapour content of the atmosphere and ultimately a more vigorous and volatile hydrological cycle with more intense rainfall events (Mullan *et al.*, 2012).

General circulation models (GCM) are a key basis for predicting future climate change and the effects on various parts of the environment. GCM's are numerical models representing the physical processes in the atmosphere, ocean, cryosphere and land surface and they are at present the most suitable models for projecting future climate change scenarios (Mullan *et al.*, 2012). GCM's, however, have a coarse spatial resolution so when needed for models which use fine scale resolution such as soil erosion, methods are needed for generating higher resolution climate change projections in order to more robustly model future erosion rates for individual catchments. Thus downscaling techniques have been developed in order to bridge the spatial and temporal resolution gap between the information that is provided by GCMs and the requirements of soil erosion models (Mullan *et al.*, 2012).

There have been a number of modelling studies which have investigated the impact of future climate change on soil erosion. These studies have identified three fundamental limitations to modelling climate and soil erosion. (1) The spatial scale at which climatic changes are represented; (2) the temporal scale

at which climatic changes are represented; and (3) the representation of changes in land use and management (Mullan *et al.*, 2012).

This study aims to focus on the relative change in sediment yield with projected climate change. Although this is not a perfect representation of the future scenario in the upper Tsitsa catchment there are numerous benefits to calculating relative change rather than exact change. By calculating the relative rates of soil erosion the change in erosion from present day rates owing to future climate change can be examined and it can even be more useful than calculating absolute rates. Even if SWAT fails to precisely simulate the absolute soil loss rates from projected climate change, it should better simulate relative changes. Most importantly since the results from calculating relative changes are influenced only by the altered parameters, in this case the weather inputs, they are better able to isolate the impacts and contribution of climate change to the future erosion problem (Mullan *et al.*, 2012). It should be noted that findings from the IPCC Technical Report VI showed that climate change would lead to greater rates of soil erosion and soil loss (Bates *et al.*, 2008).

2.4. Soil erosion in South Africa

Soil erosion is a major problem facing land resources in South Africa. Previous studies have found that over 70% of South Africa's land is affected by various degrees and forms of soil erosion (Le Roux *et al.*, 2007). Soil erosion not only poses a threat to land resources but also South Africa's water resources as much of the soil removed by erosion ends up in streams and rivers (Msadala *et al.*, 2010). Sediment loading in watercourses results in loss of water quality, affects the biodiversity and leads to dam siltation. It is predicted that soil erosion in southern Africa will likely worsen due to population increase (Flugel *et al.*, 2003). It is estimated that 360 million tons of soil are lost in South Africa annually (Beckedahl *et al.*, 1988). Poor farming methods along with the erodible nature of South African soils are cited as the main reasons for the extreme amounts of soil erosion in the country (Le Roux *et al.*, 2007).

Soil erosion in South Africa is subject to extensive spatial and temporal variation. This is due to the variation in topography, climate, soil and land use/ management practices across the country (Beckedahl *et al.*, 1988). The most

notable areas of soil erosion in South Africa are Kwa-Zulu Natal, Limpopo and the Eastern Cape Provinces (Beckedahl *et al.*, 1988; Le Roux *et al.*, 2007).

South Africa has been a focus point for soil erosion research in the sub-continent for the past fifty years and has thus a rich knowledge base accumulated on the topic (Msadala *et al.*, 2010). Numerous studies on soil erosion in South Africa have carried out observations of soil erosion yet, the derived statistical relationships from individual erosion measurements are limited to local conditions. These do not provide an adequately extensive range of input data for regional soil loss monitoring (Le Roux *et al.*, 2007).

Since 1991, the Department of Agriculture and the Water Research Commission have funded a number of studies on soil erosion in South Africa. The Global Assessment of Soil Degradation (GLASOD) was one of the first regional scale soil erosion studies of its kind. Funded by the United Nations Environmental Programme (Sonneveld & Dent, 2009), GLASOD was composed of several studies conducted by recognized experts in 50 countries around the world, including South Africa. GLASOD divided soil erosion areas into uniform units based on the most important erosion processes (Le Roux *et al.,* 2007). The study produced a relative ranking of human-induced soil erosion per area as well as a soil erosion risk map at the continental scale (Le Roux *et al.*, 2007). GLASOD has subsequently been the most influential global appraisal of land quality in terms of environmental policy (Sonneveld & Dent, 2009).

As of 1993, remote sensing and computational models have been used to identify areas of erosion or land degradation. USLE, RUSLE and SLEMSA were the most widely applied models in South Africa. The Erosion Susceptibility Map (ESM) was the first attempt to integrate the main soil erosion risk factors at a national scale in a GIS framework. A second attempt came about in 1998 where the Predicted Water Erosion Map (PWEM) was created. This improved on the ESM as it included long-term rainfall erosivity data. The PWEM highlighted that 60% and 56% Limpopo and the Eastern Cape Provinces were under extreme threat of erosion. ESM and PWEM were criticized as been an oversimplification of the USLE model because they combined the soil and slope factors with sediment yield data. Since then improvements have been made on the ESM and PWEM such as specific

attention to the soil erodibility and topography input factors (Le Roux *et al.*, 2007).

The mapping and monitoring of natural resources in Mpumalanga and Gauteng was completed in 2001 and later in 2004 for the northern Eastern Cape province and KwaZulu-Natal. The South African National Biodiversity Institute compiled a national soil degradation review using information obtained from 34 workshops throughout South Africa, held during 1997 and 1998 (Le Roux *et al.*, 2007).

Mararakanye and Le Roux (2012) produced a national gully location map, where all gullies in South Africa were manually identified and mapped in a GIS. This study was the first of its kind in South Africa and highlighted the importance of creating an automated gully identification algorithm in order to streamline the task. More recently, Le Roux *et al.* (2015) conducted a study in the Mzimvubu Catchment in the Eastern Cape Province. The study showed that the province was prone to extreme soil erosion in particular gully erosion. The reasons for which were explained as insufficient land management and poor soils.

2.5. Sediment yield mitigation strategies

Various strategies have been developed and tested which mitigate the effects of soil erosion and sediment yield on water courses and reservoirs, the most influential been preventing upstream soil erosion. Preventing upstream soil erosion has a substantial benefit on the lifespan of a dam increasing it by up to 25 years (Plamieri *et al.*, 2001). Soil erosion prevention techniques can include conservation agriculture or no-till practices. Prosdocimi *et al.* (2016) found that annual soil erosion rates were approximately 20% lower when soil conservation techniques were applied. Another study by Vogel *et al.* (2016) showed that conservation farming techniques had the highest erosion reduction potential and was promising in terms of reducing both on-site and off-site damage. Other practices can include field margins or the use of vegetation for mixed and inter-cropping (Vogel *et al.*, 2016). There are also mechanical techniques such as terracing and parcelling which can be used to limit soil erosion (Hudson, 1993).

Other methods to prevent the negative effects of soil erosion can be built into the reservoir such as the construction of sediment traps. According to Ferreira and Waygood (2009) who looked at sediment traps for mines in South Africa sediment traps or basins can be used to trap sediment. Another option suggested by to Ferreira & Waygood (2009) is to construct a settling facility with enough capacity such that the deposition of the residue is allowed for over the lifespan of the dam so that regular cleaning out is not required. In order to avoid the silting up of the dam, attenuation and settlement time are still important design considerations to ensure a high efficiency for the facility. Ferreira and Waygood (2009) also stated that an important input in the design process is a careful assessment of the silt loading that is expected over the design life. An underestimation will result in costs being occurred at a later stage; either to build a new dam or to clear the silt from the existing dam. On the other hand, an overestimation will result in a greater initial capital cost up front on an already expensive solution (Ferreira & Waygood, 2009). Plamieri *et al.*, (2001) suggested the construction of underwater dike or massive tunnels, which allow for annual sluicing. These measures, however, are expensive and their benefits should be weighed against the cost of implementing them (Plamieri *et al.,* 2001). Wang and Hu (2009), found the method of storing clear water and releasing turbid water to be the best management practice to increase the dam lifespan, which can be up to 36%. This method allows for the hydropower benefits and ecological stability to be maintained.

A final design strategy is the use of containment systems. The Government of Alberta (2011) launched a study to help prevent the siltation of dams. They focussed on the use of containment systems which trap sediment. The study noted that a 100% reduction of all incoming suspended particles is not feasible due to practical limits of storage space and available settling time. Therefore, the efficiency of a containment system is based on the efficiency of sedimentation of a target soil grain size. The sediment containment system should be designed so that the outflow rate during the design rainfall event is equal to or smaller than the inflow rate of sediment-laden runoff (Government of Alberta, 2011).

3. Introduction to the Study Area

3.1. Location

The study area is the upper Tsitsa River Catchment, upstream of the Ntabalenga village in the Eastern Cape Province, South Africa (Figure 3.1). It drains a catchment area of approximately 200 km². Catchment boundaries fall between 27.981 and 31.078 E and 28.721 and 31.009 W and between 28.134 and 30.786 N and 28.061, -31.151 S (Figure 3.1). The Tsitsa River, along with the Tina, Mzintlava, Kinera and Mzimvubu rivers, is a tributary to the greater Mzimvubu River. The source of the Mzimvubu River is in the Drakensberg range approximately 3000 m above sea level, it then flows down the Drakensberg escarpment to its outlet to the Indian Ocean at Port St Johns. The Tsitsa River joins up with the Mzimvubu River after a flow length of about 150 km.

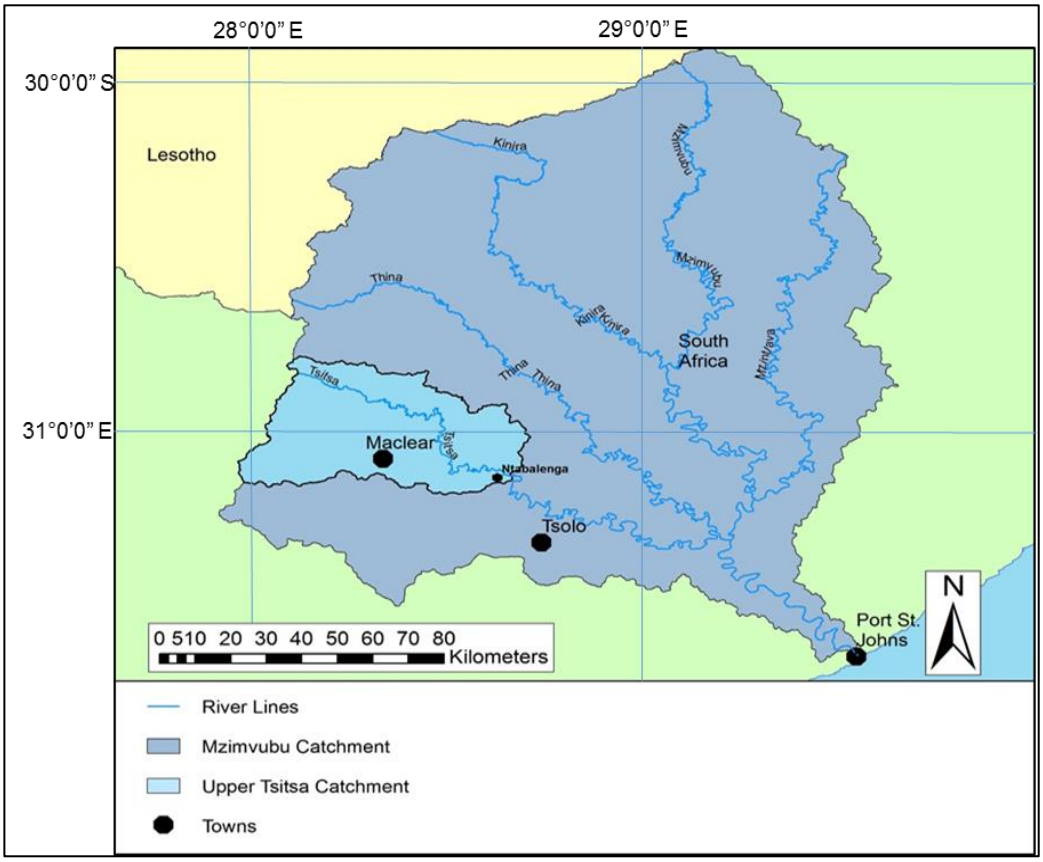

Figure 3.1: The Mzimvubu River Catchment in the Eastern Cape Province with the five major tributary rivers and the upper Tsitsa Catchment shown in light blue, along with the main towns near the upper Tsitsa Catchment.

Land use in the upper Tsitsa catchment is dominated by rural subsistence farming, larger commercial farms and plantations, with smaller urban centres scattered around the catchment the largest being the town of Maclear. Although there are some commercial farms and plantations, the Tsitsa Catchment is one of the poorest and least developed regions of South Africa. During the Apartheid era, a large part of the catchment fell within the Transkei homeland. Although the homeland policy was abolished in 1994 the area remains poor with a shortage of infrastructure and employment opportunities thus the majority of the population rely on rural subsistence farming for their livelihood.

3.2. Geology

The upper Tsitsa Catchment has a varied geology. Mafic and felsic sedimentary rocks are dominant throughout the catchment along with scattered intrusions of igneous dykes and sills. Upper reaches of the catchment are underlain by extrusive igneous rock of the Drakensberg formation (Figure 3.2). This basaltic layer is made up of tholeiitic (sub-alkaline) basaltic lava flows, subvolcanic plexus of intrusive dolerite dykes and sills estimated to be between 1300 m and 1800 m thick (Botha & Singh, 2012). It was formed during the Jurassic age approximately 180 million years ago through the break-up of Gondwanaland (McCarthey & Rubidge, 2005). A mantle plume under the continent caused a massive up-doming. This up-doming created a tensional tectonic regime, resulting in the break-up and emplacement of large volumes of magma into higher levels of the crust by convective upwelling. A massive amount of flood basalts flowed over the surface forming the Drakensberg basaltic layer (Botha & Singh, 2012).

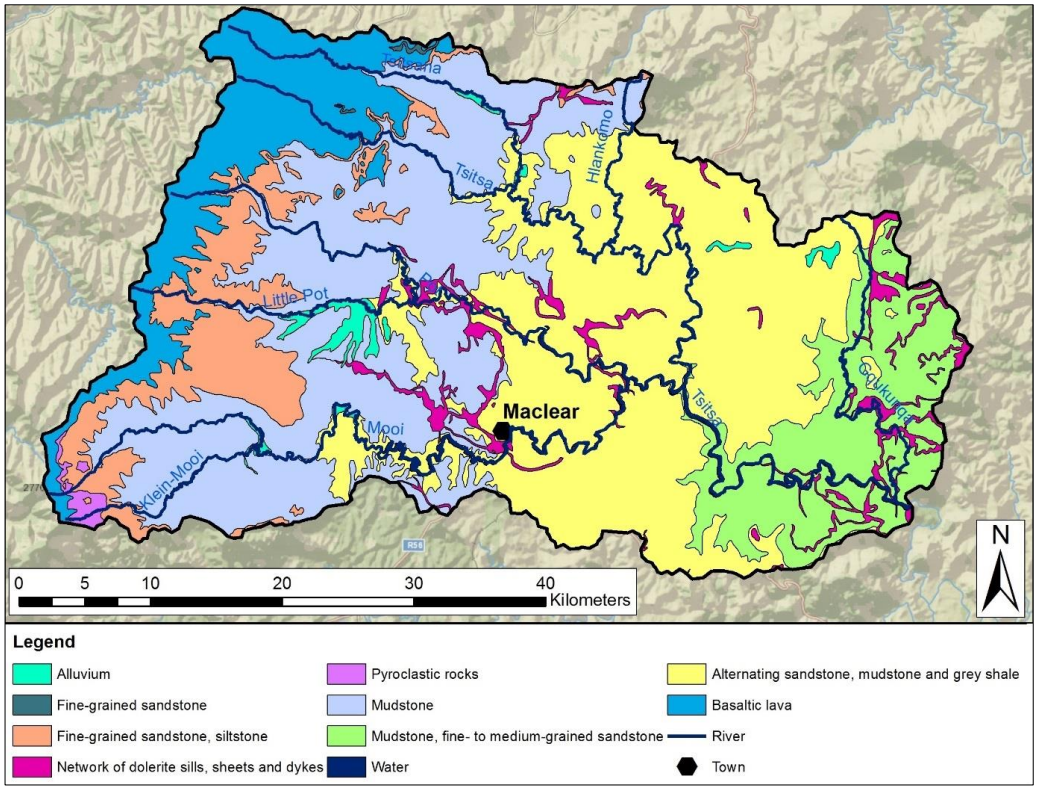

Figure 3.2: The geology of the upper Tsitsa Catchment in the Eastern Cape Province, South Africa. Adapted from vector data supplied by the Council for Geoscience (2008).

Numerous dolerite dykes and sills intruded the Drakensberg formation exploiting the pre-existing weaknesses. These acted as conduits for magma, into the higher-level fissures from which younger lava flows accreted on the surface (Botha & Singh, 2012). Dolerite dykes are composed mainly of plagioclase, feldspar and pyroxenes (Duncan *et al.*, 2015). They are homogeneous and have a similar geochemical composition to the basaltic lava except that they are coarser grained due to slower crystallisation rates at hypabyssal depths below the surface (Botha & Singh, 2012).

The Drakensberg Formation overlays a series of sedimentary rocks from the Clarens, Elliot, Molteno and Beaufort Formations. The uppermost layer of sedimentary rocks are red- yellowish sandstones of the Clarens Formation laid down during the late Triassic era (McCarthey & Rubidge, 2005). These rocks are composed of fine to medium-grained quartz-rich sandstones, which were deposited as Aeolian sediments in the arid environment of the Late Triassic and Jurassic (Bordy *et al.*, 2005). The rocks also indicate wadi and playa lake

systems. This geology has a variable thickness due to local paleo-topography and erosion forces (Bordy *et al.*, 2005). It is also known as cave sandstones due to its weathering patterns.

The Elliot Formation is found below the Clarens Formation and is composed of felsic mudstones and sandstones approximately 350 m thick thinning noticeably towards the north. Deposition of these rocks took place in a markedly drier period from the late Triassic to the early Jurassic era. Distinctive red and purple colours, caused by the high oxidising nature of the environment, characterises the Elliot Formation (Botha & Singh, 2012). three distinct environments of increasing aridity are indicated in the Elliot formation. The lower Elliot Formation shows a perennial, meandering fluvial system, associated with marshy floodplains, deposited in semi-arid climatic conditions, which became increasingly drier through time (Bordy *et al.*, 2005). Ephemeral streams and semi-arid floodplains are indicated in the middle era of the Elliot formation. While the upper Elliot formation shows greater acidification characterised by playa lakes and Aeolian dunes (Botha & Singh, 2012).

Below the Elliot formation lies the Molteno formation, which is composed of felsic sandstone with interlayers of mudstones and shales. Deposition of these rocks took place during the mid-Triassic Era in a perennially braided river system associated with braid plain areas. In this era, the climate was seasonally warm and humid. This layer indicates a transitional era into the desert climate of the later Elliot and Clarens formations (Bordy *et al.*, 2005). The Molteno Formation is approximately 200 m thick thinning noticeably towards the north and is characterised by coarse-grained mauve coloured sandstones and greenish grey inter-layered mudstones, with unique sparkling sandstones caused by the minute quartz crystals, which bind the rock (Botha & Singh, 2012).

The oldest layer is the Beaufort Group and in particular the Tarkastad Formation. These rocks are characterised by sandstones and mudstones deposited during the late Triassic era. The Tarkastad Formation is approximately 250 m thick and consists of three to five layers of sandstone, up to 10 m thick each, interlayered with finer mudstones (Botha & Singh, 2012). The rocks were deposited as fluvio-lacustrine sediments on gently subsiding

alluvial plains. Riparian vegetation along the river meanders sustained a variety of reptiles in particular "mammal-like reptiles" in a semi-arid climate with highly seasonal rainfall (Botha & Singh, 2012).

3.3. Topography

The larger Mzimvubu catchment begins in the high Drakensberg and flows down the great escarpment through the coastal plains and into the Indian Ocean at Port St Johns. The upper Tsitsa Catchment falls in the upper region of the Mzimvubu catchment and does not reach the coast (Figure 3.3). Basalts of the Drakensberg formation form the great escarpment and this area is characterised by steep slopes and narrow floodplains (Bäse *et al.*, 2006). The mountain range has a steep initial drop-off of approximately 1500 m until it levels out into the rolling hills of the "little berg". These steep slopes result in slope instability, mass movements and floods in the gradient streams (Botha & Singh, 2012). From here, the gradient of descent is more gradual until it reaches the flat plains of the coast.

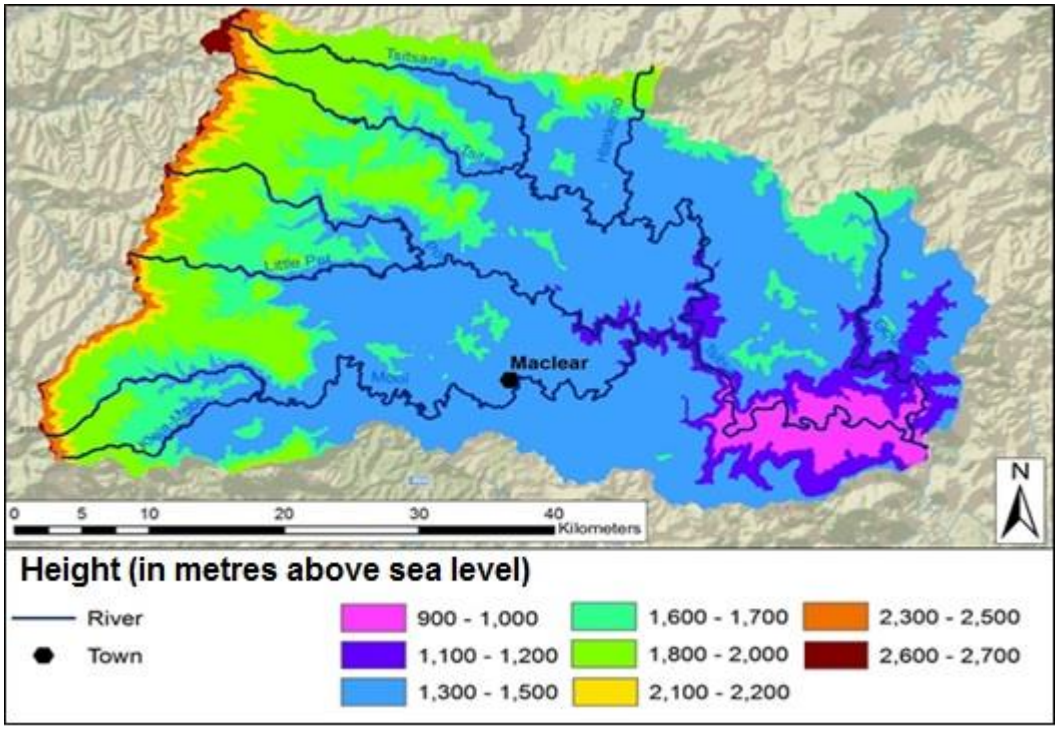

Figure 3.3: The topography ranging from 900 m asl to over 2700 m asl of the upper Tsitsa River Catchment in the Eastern Cape Province, South Africa.

The upper Tsitsa catchment ranges from 3000 m asl to 900 m asl at the dam outlet at Ntabalenga (Figure 3.3). It comprises the steep Drakensberg slopes and rolling hills of the 'Little berg". Numerous dykes and sills cut through the Drakensberg formation. Structural control of these dykes on tributary stream valleys have left a distinctive aspect of deeply incised river valleys in the catchment (Botha & Singh, 2012). The underlying Molteno Formation results in a 'terraced' hillslope topography with outcrops of large, flat slabs of coarse-grained sandstone scattered on the lower slopes (Botha & Singh, 2012).

3.4. Climate

The upper Tsitsa Catchment falls in a summer rainfall region with the climate been described as temperate, sub-humid or sub-tropical (Le Roux *et al.*, 2015). Average summer temperature is 25 degrees Celsius with January been the hottest month. Winters in the catchment are cold with July been the coldest month. Average winter temperatures are 14 degrees Celsius; snow is common on the higher mountains in winter (Agrometeorology Staff, 1984-2008). Summer has an average of 130 mm of rain in its peak month, January, mostly in the form of thunderstorms. Average annual rainfall is 850 mm (Agrometeorology Staff, 1984-2008). The average maximum hourly rainfall rate in mm/ hour is 13 mm with the maximum occurring in September at 17 mm/hour (Agrometeorology Staff, 1984-2008). These are described as high-intensity rainfall events and result in higher erosion rates in the catchment (Fraser *et al.*, 1999). Spatio-temporal variability in the rainfall is due to the varied topography across the catchment (Bäse *et al.*, 2006). Higher reaches in the Drakensberg receive more rain than the lower lying areas at the catchment outlet (Agrometeorology Staff, 1984-2008).

3.5. Land use/land cover

Vegetation in the catchment is classified as sub-escarpment grassland and sub-escarpment savanna bioregions. Four main bioregions are found in the catchment namely Drakensberg grasslands, sub-escarpment grassland, freshwater wetlands and zonal/intra-zonal forests (Figure 3.4).

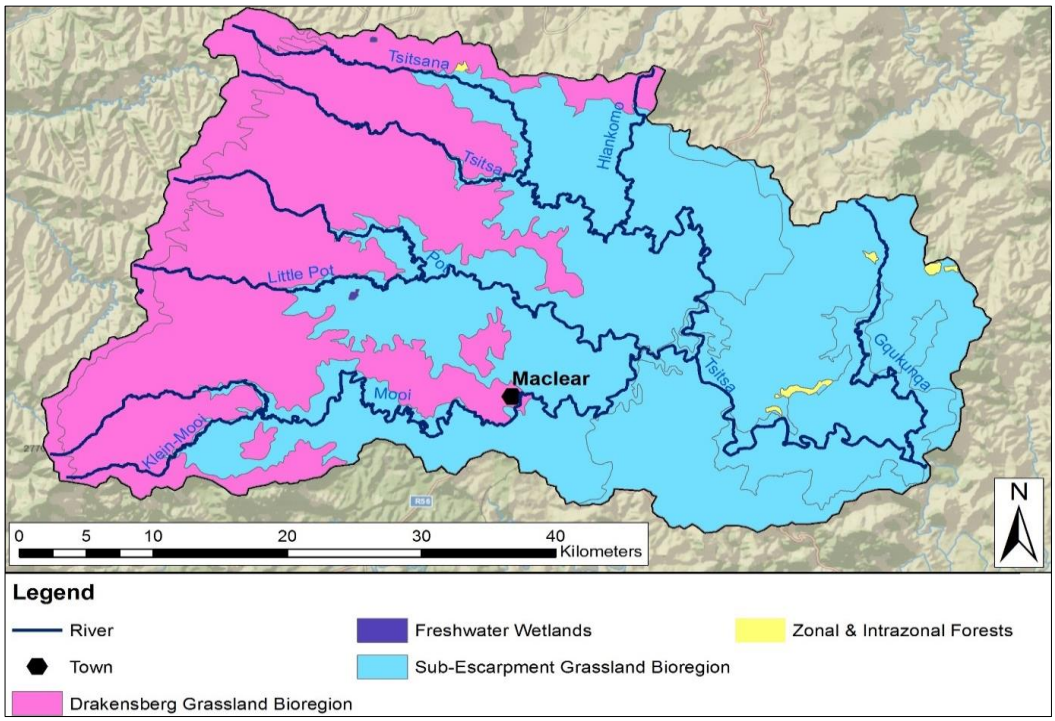

Figure 3.4: The various bioregions found across the upper Tsitsa River Catchment in the Eastern Cape Province, South Africa at a scale 1: 1000 000 (Mucina & Rutherford, 2009).

The bioregions can be further divided into several vegetation types namely: Drakensberg foothill Moist Grasslands, East Griqualand Grassland, Eastern Temperate Freshwater Wetlands, Lesotho Highland Basalt Grassland, Southern Drakensberg Highland Grassland and Southern Mist belt Forest along the drainage lines (Figure 3.5) (Le Roux & van den Berg, 2014; Duncan *et al.*, 2015). At the valley floor, East Griqualand Grassland and Drakensberg Foothill Moist Grassland are the most prominent vegetation types where acacias and euphorbias dominate (Le Roux & van den Berg, 2014). Higher up on the slopes Southern Drakensberg Foothill Moist Grassland and Lesotho

Highland Basalt are the most common vegetation types with patches of southern mist belt forest found as well (Duncan *et al.*, 2015).

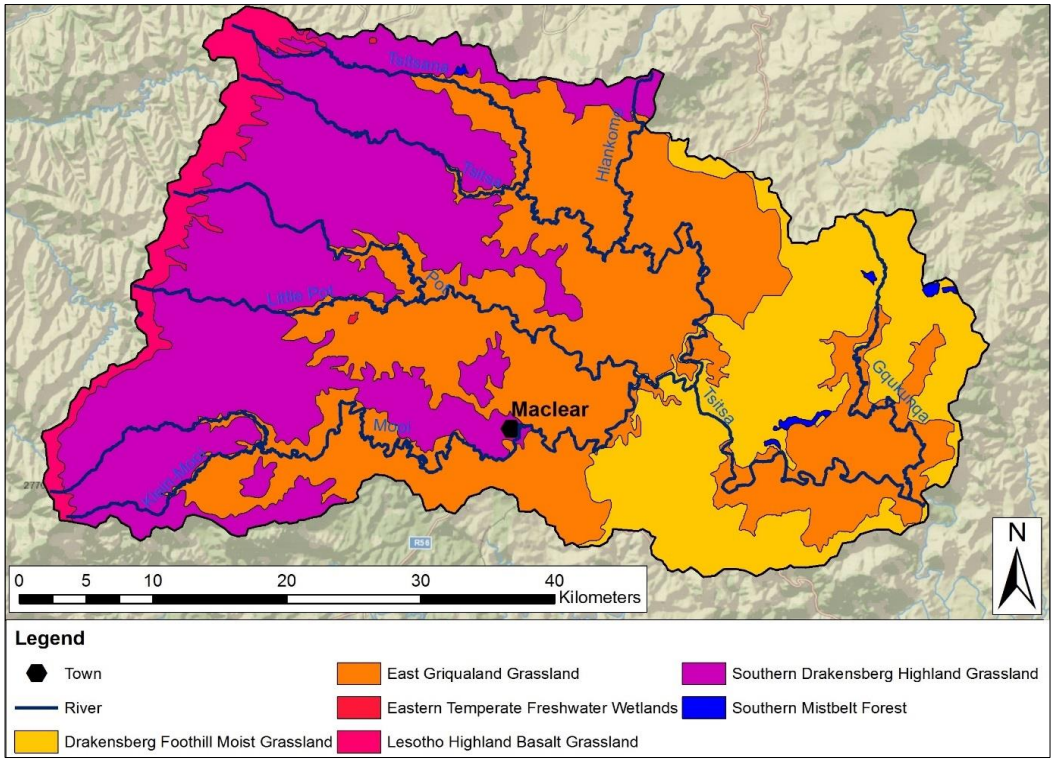

Figure 3.5: The various vegetation types occurring across the upper Tsitsa Catchment in the Eastern Cape Province, South Africa at a scale 1: 1000 000 (Mucina & Rutherford, 2009).

A land cover map created by Le Roux *et al.*, (2015) was used in the study (Figure 3.6). Natural vegetation makes up 72% of the land cover in the catchment, this is composed of grassland (90%), thicket (6.9%), forest (3%) and shrubland (0.1%). Commercial and subsistence agriculture and livestock grazing are the predominant anthropogenic land use in the catchment making up 15% of the land cover. Plantations, towns, forests and waterbodies make up the remaing 13% of land use in the catchment. Commercial farms in the region are mainly cattle for dairy and meat. Plantations are also a valuable land use higher up in the catchment above Maclear and around the towns of Elliot and Ugie. The lower section of the upper Tsitsa Catchment falls in the former Transkei Homeland and although the homeland policy was abolished in 1994, it remains one of the poorest and least developed regions of South Africa with

the majority of the population relying on subsistence farming and social grants for their livelihood (Figure 3.7).

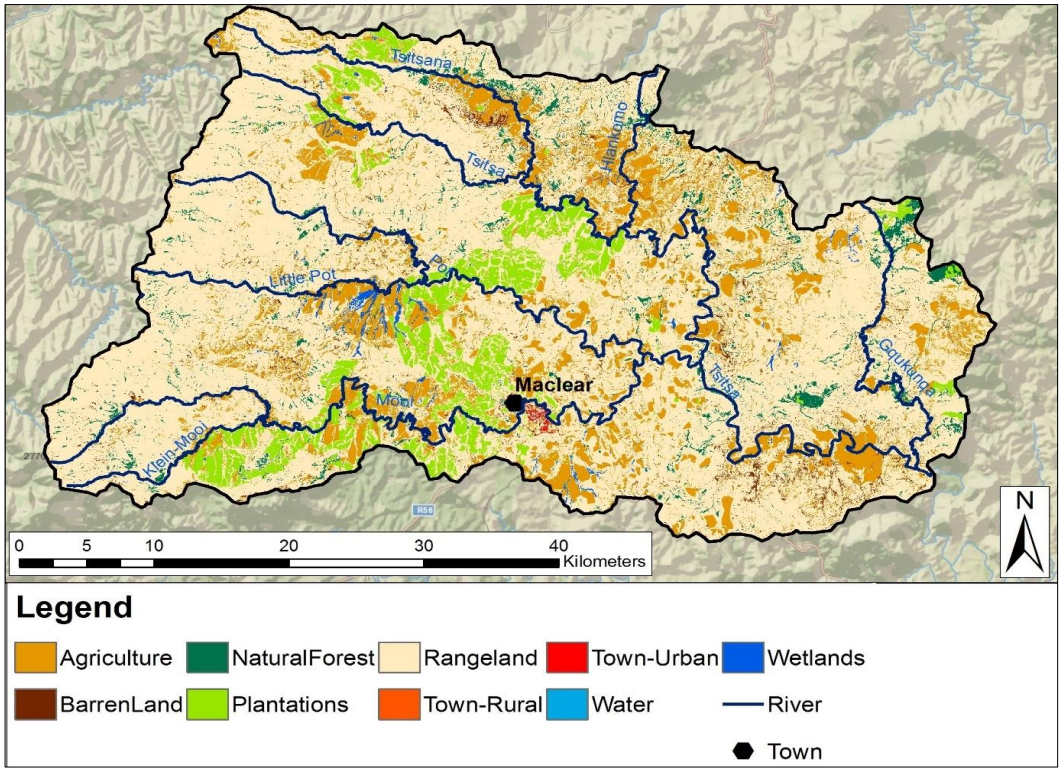

Figure 3.6: The land cover map showing the various land cover classes in the upper Tsitsa Catchment in the Eastern Cape Province, South Africa (Le Roux *et al.*, 2015).

Figure 3.7: The rural housing and communal farming found in the upper Tsitsa Catchment in the Eastern Cape Province, South Africa.

3.6. Pedology

Characteristics and properties of the soils in the upper Tsitsa River Catchment vary considerably across the catchment and are derived from the diverse geology as well as the varied rainfall and temperature in the catchment (Figure 3.8). The majority of the soils are highly acidic due to the siliceous nature of the lithology from which they are derived along with the high rainfall the region receives in the higher reaches (van Huyssteen *et al.*, 2005). Average pH of the soils dips lower than 5.5, with soils of pH between 5.5 and 6 found mainly near the catchment outlet. Soils also characterised as having a low cation exchange capacity (CEC) and thus a low base status. Many of the soils show signs of periodic wetting and drying such as mottling (van Huyssteen *et al.*, 2005).

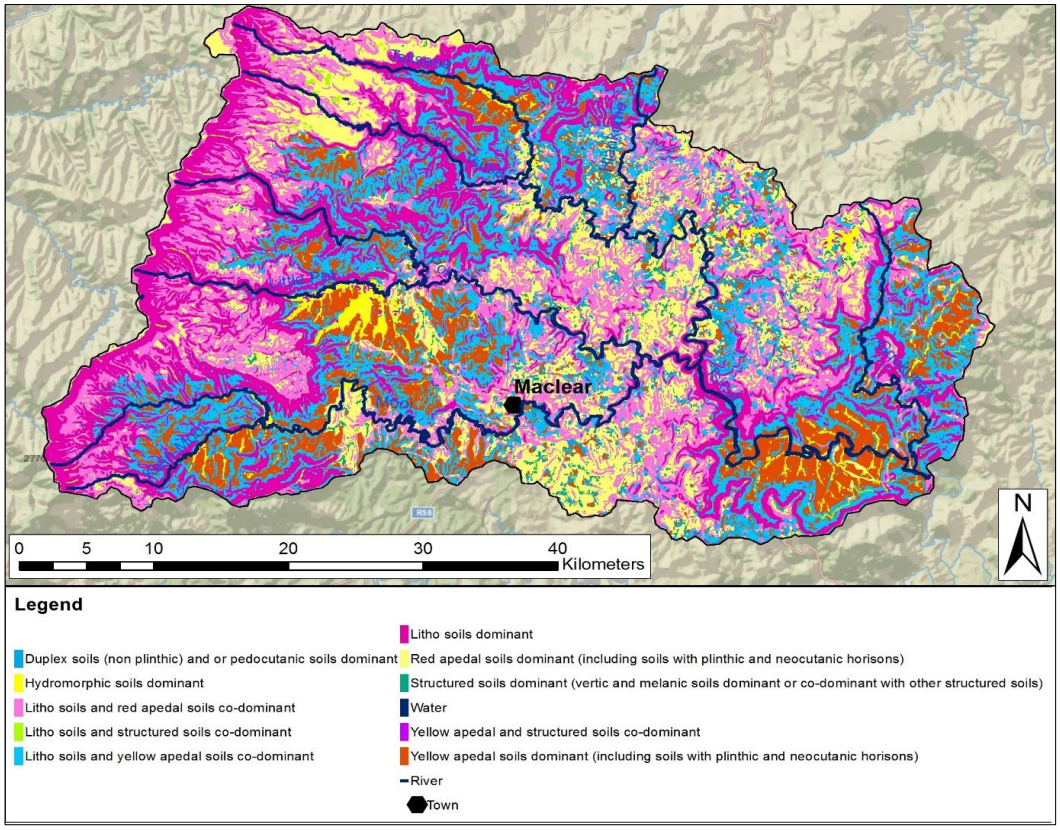

Figure 3.8: The soil association classes of the upper Tsitsa Catchment in the Eastern Cape Province, South Africa developed by van den Berg and Weepener (2009).

Although the soils are very varied across the catchment the most common soils are shallow (<30 cm) to medium depth (50 cm) loams. Less common but still of significance are moderately (50 cm – 70 cm) deep to deep (70 cm – 115 cm) sandy loams which make up the Hutton soils (Le Roux *et al.*, 2015). Soils derived from the Tarkastad, Molteno and Elliot Formations commonly form duplex soils. Duplex soils are described as having a sharp distinction between the topsoil and sub-soil layers due to the higher clay content found in the subsoil caused by leaching (Duncan *et al.*, 2015).

The soils in the catchment vary with the majority being of clayey or loamy or a clayey loam structure with some sandy loam and sandy clay structures. Texture of the topsoil is described as sandy loam gradually transferring to sandy clay loam in the subsoils with reference to the weakly structured soil forms such as Clovelly, Avalon, Pinedene, Magwa, Hutton, Bainsvvlei, Inanda, Griffin, Kranskop, Constantia, Longlands, Oakleaf, Tukulu and Vilafontes. Soils in the catchment, which have the duplex character, include the Kroonstad, Sterkspruit, Escourt, Swartland and Valsrivier forms. Soils with little development of a sub-horizon are common and include the forms such as Mispah, Glenrosa, Cartref, Mayo and to a lesser extent, the Nomanci soil-form (Esprey, 1997).

Soil depths range from 10 cm to 200 cm with the shallow soils (<30 cm) occurring on the rocky and steeply sloped areas. Deeper soils (>50 cm) are mainly located on flatter terrain covering the lower foot slopes and valley bottoms. Most of the catchment has a leaching status of mesotrophic with eutrophic soils found near the catchment outlet. Van den Berg and Weepener (2009) developed a semi-detailed soil map for three catchments in South Africa including the upper Tsitsa Catchment. The map produced from the study categorised the soils in the upper Tsitsa Catchment into six main classes which were: yellow apedal soils, red apedal soils, litho soils, hydromorphic soils, duplex soils and structured soils (Figure 3.8) (van den Berg & Weepener, 2009).

3.7. Soil erosion in the upper Tsitsa Catchment.

There is a high degree of soil erosion in the catchment, especially in the inter-fluvial regions adjacent to the stream channels. Majority of gully erosion occurs on the deep soils described as yellow apedal soils and litho/yellow apedal co-dominant soils by van den Berg and Weepener (2009). A fair amount of gully erosion also occurs on the hydromorphic soils; as hydromorphic soils occur along drainage lines where runoff is concentrated.

High rainfall intensities, steep slopes, erodible nature of the soils and land use practices are cited as the main causes for soil erosion (van Tol *et al.*, 2014; Le Roux *et al.*, 2015). Over-grazing and over-cultivation on steep terraced slopes also cause a loss of vegetation cover and root stability, which aggravates sheet and rill erosion (Duncan *et al.*, 2015). Gully erosion is the most prominent and concerning erosion phenomena in the catchment. Gullies in the catchment vary in shape from U to V-shaped and range from 0.5 – 30 m deep and 0.5 – 300 m wide, stretching for up to 5 km in length in certain areas (Figure 3.9) (Le Roux & van den Berg, 2014).

Figure 3.9: Examples of extensive soil erosion and gullying found in the upper Tsitsa Catchment in the Eastern Cape Province, South Africa.

The ability of a soil to resist erosion is largely determined by its resistance to disaggregation and/or dispersion, which is controlled by the physical and chemical properties of the soil. Two most important positive factors in soil stability are soil organic matter and the presence of iron and aluminum oxides, while the presence of sodium causes soil dispersion (Laker, 2004). It has been

widely established that sodium is by far the most dispersive major cation in soils and since dispersion predisposes a soil to erosion, it is considered one of the most important ions which enhance soil erosion (Laker, 2004). In soils derived from the Beaufort group, such as those found in the Tsitsa catchment, the presence of organic matter is the principle factor in retaining the soil structure and thus removing organic matter through overgrazing and bad agricultural practices will cause increased soil erosion. Another cause for the high dispersion rates of soils in the catchment was explained by Laker (2004); the clay fractions of soils derived from Beaufort mudstones and shales contain significant amounts of clay-sized quartz, which are directly inherited from the underlying geology. The findings indicate that the most inert members of the clay fraction are most actively involved in the process of disaggregation. It was also shown by Buhmann *et al.* (1996) that the dominant soil constituents of silty soils, such as chemically inert quartz and feldspars increase their susceptibility to erosion and dispersion. It is thus clear that other factors may strongly override the effects of sodium on dispersion and erosion. Soils derived from igneous rocks such as Drakensberg basalts and dolerite have much higher iron content and thus do not rely so heavily on organic matter to promote the aggregation of soil particles creating the soil structure (Laker, 2004). This explains the lack of gullies higher up in the catchment where soils derived from the Drakensberg Basalt are dominant.

The upper Tsitsa River Catchment also has an abundance of duplex soils, which are cited as a primary reason for the extensive gully erosion by van Tol *et al.* (2014) and Le Roux *et al.* (2015). Duplex soils are defined as soils with an abrupt change in texture between the horizons in the soil profile. Texture varies significantly from a lightly textured topsoil (coarse sandy loam) to a heavier, fine textured lower soil (clay). Duplex soils are prone to tunnelling and gully erosion due to the lateral subsurface flow between the horizons, which is aggravated in highly dispersive soils (van Zijl, 2010). Van Zijl (2010) found that in Lesotho, the most the wide, deep and active gullies were found on duplex soils. It is hypothesised that the cause of gullying in duplex soils is due to the formation of a capillary fringe at the contact zone between the top horizon and the sub-horizon. This enhances the dispersive chemical reactions, which create free clay particles. These particles clog the pores of the lower finer textured horizon and prevent the downward movement of water into the sub-soil.

Removal of dispersive clay is caused by the movement of excessive water which is then pushed into the cracks of the upper, soil horizon, this leads to the initiation and widening of cracks in this layer. These cracks widen until they join up forming an underground pipe (van Zijl, 2010). Sometimes the topsoil above these pipes collapses, initiating a gully (Le Roux & Sumner, 2012).

4. Methods

4.1. Overview

This study aimed to model the major soil erosion processes and determine the sediment yield in the upper Tsitsa catchment which was achieved through two approaches. (1) Model the sediment yield contribution from sheet-rill erosion using ArcSWAT, a graphical user interface for SWAT and ArcMap® software along with climate, land use, soil and topography data. (2) Determine the sediment yield contribution from gully erosion using the remote sensing technique, OBIA, along with GIS. Finally, projected land use and climate change data were used to determine the effects of such change on the sediment yield. Each approach will be dealt with separately in the Methodology chapter.

4.3. SWAT methodology

SWAT (Figure 4.1) was used to model the current sediment yield from sheet and rill erosion in the upper Tsitsa Catchment for the five-year period 2007-2012. An updated land use, soil and DEM along with measured weather records were used as input data.

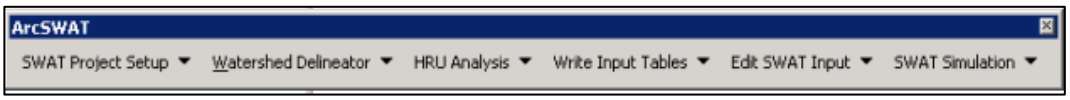

Figure 4.1. The SWAT graphical User Interface as a toolbar in ArcMap.

4.2.1. Model set up

SWAT requires specific information about soil, weather, land use and topography in order to properly model the watershed (Nietsch *et al.*, 2011; Winchell *et al.*, 2013). ArcSWAT requires a DEM as the first input to create the model. For the model set up in this study the hydrologically improved STRM DEM created by Weepener *et al.* (2012) was used. In the second phase of setting up the model, SWAT requires land use and soil data to determine the area and the hydrologic parameters of each land-soil category simulated within each sub-watershed. The land cover input used for this study was the land cover map produced by Le Roux *et al.*, (2015) see (chapter 3). A national Land

Type map created by the ARC-ISCW see (chapter 3) was used as the soil input. In order to link the input map and the SWAT database, the categories specified in the land cover map need to be reclassified into SWAT land cover and plant types. The user has three options for reclassifying the categories (Winchell *et al.*, 2013). For this study, the land cover types were reclassified by typing in the 4-letter SWAT land cover/plant type code for each category (Table 4.1). It should be noted that in the upper Tsitsa Catchment the land use is largely communal and communal grazing along with subsistence crop farming is practiced interchangeably without formal boundaries. This makes identifying and modelling such land use difficult and thus these areas were modelled collectively in the SWAT model as rangelands.

Table 4.1: The various SWAT land cover classes used in the study with a description and the percentage of land the catchment each class occupies.

SWAT Class	Description	Land cover Percentage
WATR	Water	0.092
WETN	Wetlands (non-forested)	0.543
FRSD	Deciduous forest	3.775
RNGE	Rangeland-Grass	71.764
AGRC	Agriculture	15.792
FRSD	Evergreen forest	6.329
BARR	Barren	1.526
URMD	Urban (medium density)	0.086
URML	Urban (low density)	0.094

The reclassification process needs to be repeated for the soil input which needs to be linked to the User Soils database. The User Soils database is a custom soil database designed to hold data for soils which are not included in the U.S. soil database. Four options are available to link the map to the user soil database. In this study, the MUID (Multiple Unit Identity) number was used. Finally, climate data are needed to complete the basic SWAT model. Climate

data are used in SWAT to simulate the moisture and energy inputs that control the water balance. SWAT needs data for precipitation, temperature, solar radiation, wind speed and relative humidity as input climate variables. Weather data used as the inputs were measured data from ARC weather stations in the catchment (Agrometeorology Staff, 1984-2008). Once the basic model has been set up the user can change land management and other operations.

In USLE-based models such as SWAT, land cover and land management are the most important factors controlling soil erosion (Wischmeier & Smith, 1978). The SWAT model considers plant cover as a more dominant factor in soil erosion than the effects of rainfall, slope and the soil profile (Le Roux, 2009). Therefore, site-specific vegetation parameters must be accurately derived to ensure successful model performance. This can be done by the user once the model has been set up by simply editing the land cover database. These changes are then transferred to the SWAT database from which it reads the information.

4.2.2. Model calibration

Model simulation was conducted over a five-year period from 2007-2012. Flow measurements from seven stations from the Department of Water and Sanitation were used to validate and calibrate the model for the whole Mzimvubu catchment by Le Roux *et al.* (2015). Unfortunately, a major limitation to the use of continuous time models such as ArcSWAT in developing countries is the lack of recorded flow and sediment data for calibration and validation (van Zyl, 2007). Due to the absence of data on sediment loads, model calibration concentrated on the hydrological part of the model. This was done by adjusting sensitive model parameters similar to other studies by Tibebe and Bewket (2011). Calibration of the hydrological component was done by modifying the curve number and base-flow coefficients, whereas the erosion component was calibrated by adjusting the USLE soil erodibility and support management factors (Le Roux *et al.*, 2015). These model calibrations were then used for the smaller study area on the upper Tsitsa River.

4.3. OBIA methodology

4.3.1. Overview

A major limitation to the SWAT model is that it does not account for gully erosion. This can cause a severe underestimation of sediment yield in catchments such as the upper Tsitsa, where gully erosion is prominent. Thus in order to properly assess sediment yield in the catchment, it is important to map the gullies and determine gully growth over the five-year period 2007-2012. This was done using SPOT 5 images from 2007 and 2012 and eCognition software to conduct OBIA.

4.3.2. Description of inputs used

SPOT 5 images from April 2012 and February 2007 were used due to their generally good spatial resolution as well as the ability to sense wavelengths in a range of bands (Table 4.2). This was useful in calculating the normalised difference vegetation index (NDVI) and the normalised difference water index (NDWI) or the modified normalised difference water index (MNDWI). eCognition developer was used for image analysis and ArcMap was used for post processing of the image objects. eCognition Developer is distributed by Trimble and is a powerful development tool for OBIA. Furthermore, eCognition has been widely used in earth sciences to develop rule sets for the automatic analysis and classification of remote sensing data. Feature extraction, change detection and object recognition can all be computed in eCognition. The object-based approach can facilitate analysis of a variety of data sources, such as medium to high-resolution satellite data, high to very high-resolution aerial photography, LiDAR, radar and even hyperspectral data (Trimble Navigation Limited, 2014).

Table 4.2: The different SPOT 5 spectral bands with their respective resolution and wavelengths. Adapted from (Weepener *et al.*, 2014).

Spectral bands	Pixel size	Spectral resolution
Panchromatic	2.5 m	0.48 - 0.71 µm
Green	10 m	0.50 - 0.59 µm
Red	10 m	0.61 - 0.68 µm
Near infrared	10 m	0.78 - 0.89 µm
Shortwave infrared (SWIR)	20 m	1.58 - 1.75 µm

By developing a classification approach on widely available satellite imagery as the input, it is envisioned that the ruleset created will be applicable to other SPOT 5 images and can be used for other catchments. This can be beneficial for comparing different areas, upscaling the ruleset to the larger catchment or used for multi-temporal analysis, as the classification approach is not location dependent (d'Oleire-Oltmanns *et al.*, 2014). It is important to note here, the influence of scale; all satellite data are limited by its respective pixel resolution. In this case, 2.5 m for pan-sharpened SPOT 5 images. The minimum spatial extent of the object which needs to be identified, in this case, gullies, has to match the resolution of the satellite image (d'Oleire-Oltmanns *et al.*, 2014). SPOT 5 is considered one of the higher spatial resolution satellite imagery available, with a pan-sharpened image of 2.5 m x 2.5 m resolution. Image analysis will not be able to detect gullies less than 2.5 m because they will become embedded within the pixels (Mararakanye & Nethengwe, 2012). While pan-sharpening a SPOT 5 image may result in some loss of spectral information, it is still considered a good representation and compromise between the spectral information and spatial resolution that is required for gully detection.

4.3.3. Support data

Manually digitised gully location maps were used to conduct an accuracy assessment of the eCognition generated gully objects prepared in this study. Gullies were captured through manual digitising from 2007 Spot 5 images by Mararakanye and Le Roux (2012) and updated with SPOT 5 images of 2012 by Le Roux *et al.* (2015). Manual digitising of new gullies was done by delineating the outer boundary of the gully from the background using SPOT 5 imagery at a scale of 1: 10 000, gully growth was also captured by delineating the newly formed gully boundaries. The gullies were visually identified according to drainage pattern, shape, size, colour and tone (Mararakanye & Nethengwe, 2012).

4.3.4. Developing the ruleset

The ruleset in eCognition was based on a "top-down" approach where the smallest level is pixel-based and the largest level is the "entire scene", creating three levels of differing segment sizes from large too small.

In eCognition, the SPOT 5 image was segmented using a region-based approach in order to create objects for further classification. The segmentation process divides the image into smaller objects each with their own unique spectral and spatial properties. A region-based approach to the segmentation was taken, which partitions the image into regions or polygons that are similar according to a set of user-defined conditions. Region-based segmentation looks for homogeneity within a sub-region, based on properties such as intensity, colour, or texture (Shruthi *et al.*, 2012). Segmentation was aimed at the extraction of gullies as target objects, rather than a complete classification of the satellite image. Initial segmentation settings were adjusted to be optimal for gullies; the values for shape and compactness were set to 0.3 and 0.8, respectively. In order to give colour, or rather spectral properties, a strong influence on the objects a low value of 0.3 for shape was set. Setting the value for compactness to 0.8 aimed at delineating more compact objects such as plantations, croplands and large areas of bare soil. Due to their heterogeneous nature, gully-affected areas contain a low degree of compactness and were over-

segmented. This allowed for differentiation against the homogeneous areas surrounding the gullies (d'Oleire-Oltmanns *et al.*, 2014).

Using eCognition's customised algorithm function the NDVI (Equation 4.1.) was calculated using the red and near infrared bands of the SPOT 5 image, at the image object level i.e. for each image object rather than per pixel. Figure 4.2, shows the reflectance's of vegetation, water and soil for the various wavelengths and the bands of SPOT 5 image, green (1), red (2), NIR (3) and SWIR (4) in grey. The spatial variation of NDVI values across the upper Tsitsa Catchment for 2007 and 2012 are shown in in the maps in Figure 4.3 and Figure 4.4 respectively.

Equation 4.1. $$NDVI = \frac{\sum_{i=1}^{n} \left(\frac{(NIR_p - R_p)}{NIR_p + R_p}\right)}{n}$$

Where n = number of pixels in the object

NIR_p = Near Infrared value of given pixel

R_p = Red value of given pixel

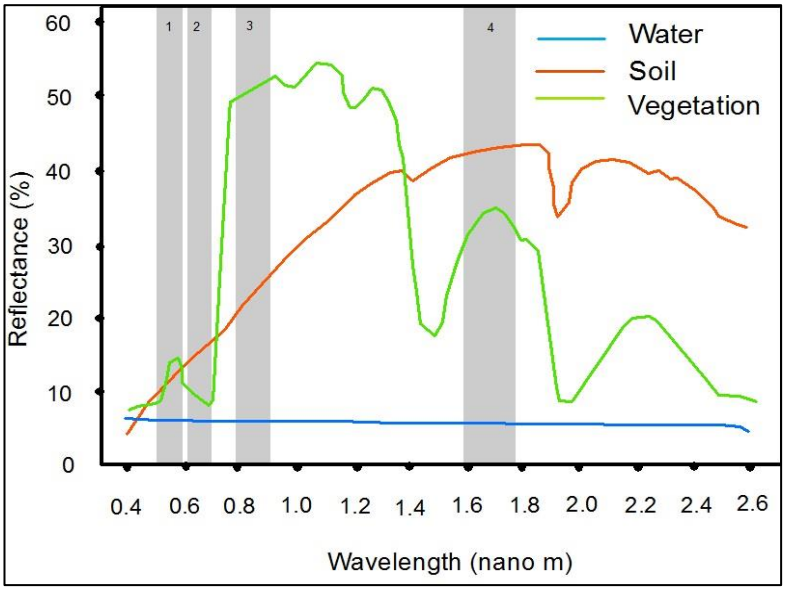

Figure 4.2. The reflectance's of vegetation, water and soil for the various SPOT 5 bands. Adapted from (Weepener *et al.*, 2014).

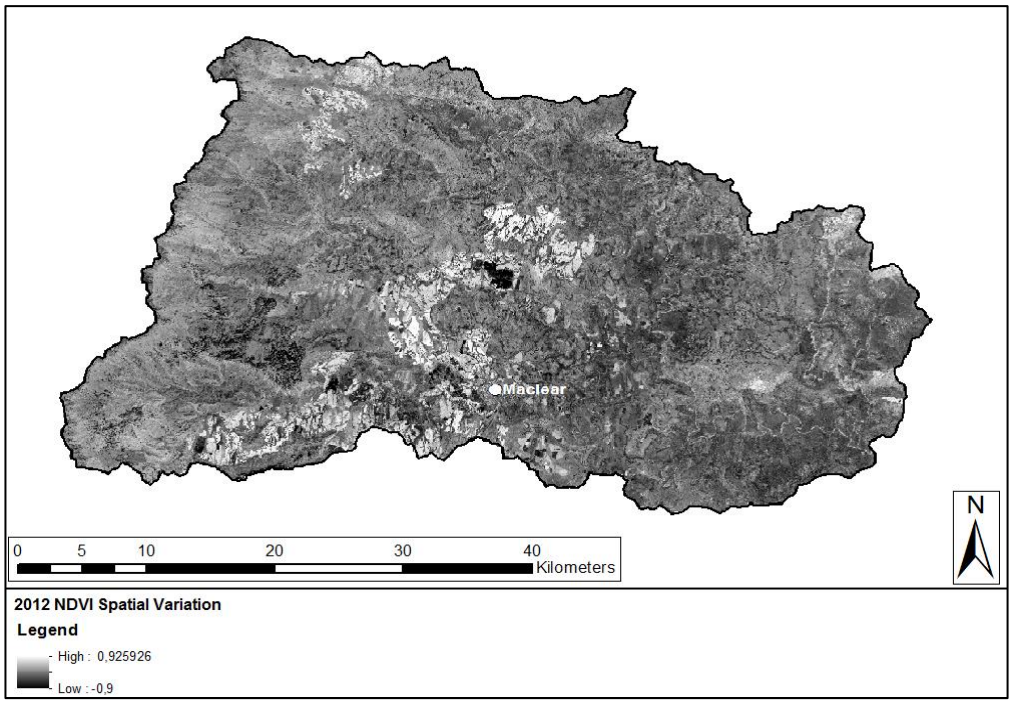

Figure 4.3. The spatial variation of NDVI values derived from the 2012 SPOT 5 dataset in the upper Tsitsa Catchment, Eastern Cape, South Africa.

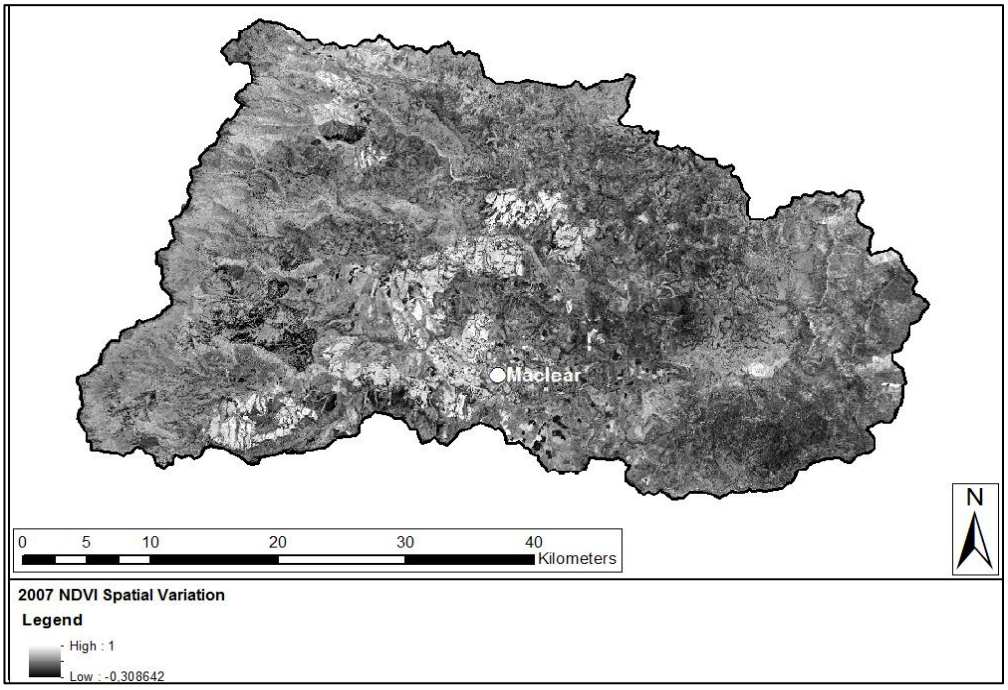

Figure 4.4. The spatial variation of NDVI values derived from the 2007 SPOT 5 dataset in the upper Tsitsa Catchment, Eastern Cape, South Africa.

Due to chlorophyll's absorption of light in the blue and red part of the spectrum, vegetation displays a low reflectance of these two wavelengths. However, vegetation strongly reflects light in the near-infrared part of the spectrum (Govaerts & Verhulst, 2010). By using the red and NIR bands of the SPOT 5 image it is possible to create an index which gives positive values to vegetation cover. NDVI is sensitive to vegetation and areas of denser vegetation appear as increasingly positive values in the resulting NDVI layer (Gao, 1996).

A separate calculation was used to calculate the MNDWI (Equation 4.2), using the green and short wave infrared bands of the image for each image object similar to the methodology used by (Xu, 2006; Ji *et al.*, 2009). Water reflects the strongest in the green band of the SPOT 5 image while absorbing more in the NIR and SWIR bands (Figure 4.1). It was proven by Xu (2006) that using SWIR bands instead, of the NIR band as Mcfeeters (1996) used in the normalized difference water index (NDWI), allowed for the distinction between water and buildings and gave a more accurate classification. The MNDWI is a normalized index similar to NDVI but the resulting layer has positive values for water bodies. These two indices were used to remove water and vegetation cover in the first step of the classification process. This allowed for a large portion of the image to be removed from the rest of the classification process, helping to streamline the results.

Equation 4.2. $$MNDWI = \frac{\sum_{i=1}^{n} \left(\frac{(G_p - SWIR_p)}{G_p + SWIR_p}\right)}{n}$$

Where n = number of pixels in the object

G_p = Green value of given pixel

$SWIR_p$ = Shortwave Infra-red value of given pixel

The threshold for NDVI was set to 0 in the first step, this was not a significantly high NDVI threshold as objects containing both areas of vegetation and bare soil may have an average NDVI value lower than 0. However, it has been noted that many gullies in the upper Tsitsa catchment contain patches of vegetation

on the side walls and channel base. If the NDVI threshold was set too sensitive these areas would have been removed in the first step removing many gullies from the classification process. Similarly, MNDWI was used to remove the rivers and farm dams from the classification process. A threshold of 0.25 was set for MNDWI as many gullies form along smaller river channels. Setting a very sensitive threshold would have removed these gullies from the classification process. The water in the gullied channels is generally shallow and contain large amounts of sediment that allows the water in these channels to be distinguished from the main river channels.

Through the segmentation process, the gullied areas were separated into areas of light soil and areas of dark soil or shadows. Once the vegetation had been classified, a series of rules were written based on soil brightness to establish areas of bare soil, sparsely vegetated soil, light shadows and very dark shadows. All these spectral properties can be found in a gully, which makes a single classification algorithm difficult. Thus a series of rules based on size and brightness were written in order to merge areas of bare soil and shadow to create the gully outline. This method also classified tilled croplands in gully classes and in order to remove these errors, the texture of the gullies was taken into account. Gullies contain areas of light and dark patches in random arrays depending on the angle of the sun or objects creating shadows. In contrast, tilled land creates shadows of continuous straight lines along the areas of tillage. Thus the texture after Haralick algorithm was used to distinguish between the two land types (Haralick *et al.*, 1973).

A grey level co-ordinance matrix (GLCM) of contrast at all angles across band one was calculated to derive the texture values. A threshold of 1.2 was found to best distinguish between gullies and tilled land after a series of trials were run. This was all done in eCognition using the inbuilt texture algorithm function. A series of rules were then written to merge the areas classified as soils and shadows in order to create unified gully objects. Houses were also classified as gullies using the earlier rules and the separation of gullies from houses was achieved in this step. Houses are generally small, square objects less than 150 pixels in size, thus areas classified as gullies smaller than 150 pixels were reclassified as houses. A relational border algorithm was then used to incorporate small gullied areas misclassified in the previous step; all objects

that shared a border of more than two pixels with gullies were then changed to gullies.

The final challenge was to separate rock outcrops from the gullied areas. The texture algorithm after Haralick was used because of challenges encountered with the similarities between the brightness values of the rock outcrops and gullied areas. Rock outcrops tended to have a higher vegetation to rock ratio than the gullies and their homogeneity texture was thus different. A GLCM of homogeneity at all angles across band one was calculated to get the texture values. A threshold of 0.08 was found to best to distinguish rocks from gullies after a series of trials were run. The results were then exported as a shapefile to ArcMap for further processing. The ruleset can be found in Appendix 2.

Another error in the classification was road lines that were incorrectly classified as gullies. Majority of the roads in the catchment are unpaved and thus have a similar spectral signature to that of the gullies. In ArcMap, digitised road lines at a scale of 1:50 000 provided by the National Geospatial Information were used to create a buffer of roughly 40 m, as the error threshold of the data set is 40 m. The buffer was then used to erase the exported polygons falling along these lines.

4.3.5. Description of variables used

4.3.5.1. Texture after Haralick

Texture can be defined as fine, coarse, smooth, rippled, irregular or lineated (Haralick *et al.*, 1973). Using a GLCM 22 separate formulas can be derived, however, usually only five of these are considered as parameters of importance namely contrast, homogeneity, dissimilarity, energy and entropy (Gebejes & Huertas, 2013). A GLCM contains information on the distribution of co-occurring pixel values or the frequency of occurrence of two neighbouring pixel combinations across an image. GLCMs are created from greyscale images, by calculating how often the grey scale intensity value of a pixel occurs horizontally, vertically or diagonally adjacent to that pixel (Gebejes & Huertas, 2013). A GLCM is based on the assumption that the texture information in an image is contained in the overall spatial relationship which grey levels of

neighbouring pixels have to one another (Gebejes & Huertas, 2013). In this study, only two GLCMs were used namely contrast and homogeneity.

Contrast is based on Equation 4.3, where i and j represent the horizontal and vertical cell coordinates and p is the grey intensity value for that pixel. Contrast is simply the measure of intensity contrast of a pixel and its neighbour and is based on the local grey level variation in the GLCM. Thus a continuous object will have a contrast of 0. The grey level variations show the variation of the texture itself. If neighbouring pixels have very similar grey intensity values, the contrast in the object will be very low, which is the case for smooth soft textures; heavy textures will produce high intensity values (Gebejes & Huertas, 2013).

Equation 4.3. $$Contrast = \frac{\sum_{i,j}|i-j|^2 p(i,j)}{n}$$

Where

n = number of pixels in the object

p = grey level intensity pixel value

i = horizontal cell coordinates

j = vertical cell coordinates

Homogeneity measures the similarity of the distribution of elements in the GLCM to the diagonal of the GCLM. The homogeneity calculation, shown in Equation 4.4., uses the inverse of the contrast weight to give weights to each pixel value, then sums these weights and finds the average homogeneity for each image object. The GLCM homogeneity of any texture is high if GLCM concentrates along the diagonal, meaning that there are many pixels with the same or very similar grey level value. The larger the changes in grey values, the lower the GLCM homogeneity making higher the GLCM contrast. Homogeneity ranges between [0, 1]. If there is little variation across the object, then the homogeneity will be high where there is no variation the homogeneity is 1. Therefore, high homogeneity refers to textures that contain ideal repetitive structures, while low homogeneity refers to big variation in both,

texture elements and their spatial arrangements. An "inhomogeneous texture" refers to an object that has almost no repetition of texture elements and spatial similarity in it is absent (Gebejes & Huertas, 2013).

Equation 4.4. $$Homogeneity = \sum \frac{\frac{\sum_{i,j} 1\, p(i,j)}{1-(i-j)^2}}{n}$$

Where n = number of pixels in the object

p = grey level intensity pixel value

i = horizontal cell coordinates

j = vertical cell coordinates

4.3.6. Accuracy assessments

An accuracy assessment reflects the difference between the classified image and the reference data. Assessing the accuracy of the classification quantitatively requires the comparison of two maps namely the classification derived map (OBIA map) and the reference map (manually digitised map) (Lillesand *et al.*, 2008). It is important that the reference data are accurate and reliable as this might cause the accuracy assessment of the classified data to reflect a poor classification workflow, whereas, in reality, the classification might be very good (Yale's Centre for Earth Observation, 2003).

According to d'Oleire-Oltmanns *et al.* (2014) the delineation and accuracy assessment of geomorphological features, for example, gullies is not as simple as for other features such as crops or water. Borders of erosional features are often not clearly defined and may vary due to natural influences; this creates a problem when trying to define an object's boundaries. This problem is further compounded by the definition of gully erosion and the lack of three-dimensional data as gullies are often defined by depth, which distinguishes them from other forms of erosion (Poesen *et al.*, 2003).

Four separate accuracy assessments were conducted and their results compared. This allowed for the testing of various accuracy assessment

techniques against each other. Drăguț and Eisank (2012) highlighted the value of applying more than one method to determine the accuracy of the classification as no one technique can assess all the possible errors a classification can produce. User's and producer's accuracy, as well as the overall accuracy, was calculated using Equations 4.5, 4.6 and 4.7. Table 4.3 shows a confusion matrix, which the user (x) and producer's accuracies (y) are based on. The values of the user's, producer's and overall accuracy are usually not the same. Overall accuracy determines the number of correctly classified pixels in the image from the total number of pixels in the image. User's accuracy also referred to as the commission error is defined as the reliability of the map, in other words, how well the pixels on the map represent the feature in reality. Producer's accuracy or omission error refers to how well a certain feature can be classified (Yale's Centre for Earth Observation, 2003).

Equation 4.5. $$User's\ Accuracy = \frac{Number\ of\ correctly\ classified\ pixels\ for\ class}{Total\ Number\ of\ classified\ pixels\ in\ class}$$

Equation 4.6. $$Producer's\ Accuracy\ \frac{Number\ of\ correctly\ classified\ pixels\ for\ class}{Total\ Number\ of\ ground\ truth\ pixels\ in\ class}$$

Equation 4.7. $$Overall\ Accuracy = \frac{Number\ of\ correctly\ classified\ pixels}{Total\ Number\ of\ pixels}$$

Table 4.3: A confusion matrix used to conduct accuracy assessments. Where the 'actual' refers to the reference data and 'predicted' refers to the classified data. Adapted from Fielding and Bell (1997).

	Actual	+	-	User's Accuracy
Predicted	+	a	b	*y*
	-	c	d	*y*
Producer's Accuracy		*x*	*x*	

4.3.6.1. Random point sampling method

This method was based on one conducted by Mararakanye and Nethengwe (2012) who assessed the accuracy of classified gullies by comparing them with a manually digitised gully location map using random points. A sample of 144 random points, generated through ArcMap's random point generator function, were placed in the exported OBIA gully map and the accuracy was calculated by determining whether the points which fell inside the gullies were also represented by gullies in the reference dataset. Thus, this method only tested the OBIA identified gullies and if OBIA missed gullies it would not show up in the accuracy assessment. Thus, a further 144 random points across the entire catchment, not specific to gullies, were then assessed in the same manner. Wang *et al.* (2014) used 144 random sample points for a catchment in China. Mararakanye and Nethengwe (2012) chose 150 points for the gullies and 150 points for the catchment in a study area approximately three times bigger than the catchment area of this study thus 144 points were assumed to be adequate.

4.3.6.2. Total area of overlap

The principle behind the total area of overlap method was to determine the total area of gullies which overlapped between the digitised data set and the data extracted through OBIA. This was achieved by conducting a simple raster calculation between the digitised gullies and the gullies extracted through

OBIA. In ArcMap, both data sets were converted to raster files as follows: no data values (i.e. areas where no gullies were found) were given a value of one, while areas where gullies had been identified, were given a value of two for the OBIA extracted data set and 10 and 20 for the digitised data set. Ten represented an area of no gullies while 20 represented a gullied area. The two data sets were then added, which gave four classes namely 11, 12, 21 and 22. These classes represented the various combinations of gullies and no gullies between the two data sets, as shown in Table 4.4. This was done for both the 2012 and 2007 data sets. Results of the error matrix were interpreted using the producer's accuracy, user's accuracy, overall classification accuracy equations stated above.

Table 4.4: The four classes of the basic accuracy assessment.

Value	Description
11	Neither data set found gullies
12	The digitised gullies showed no gullies yet the ruleset found gullies
21	The digitised data set found gullies where the ruleset found no gullies
22	Both data sets identified gullies

4.3.6.3. Boundaries of leniency

Boundaries of leniency considered the distance of the error or the distance that the closest true positive (reference data) fell from a false positive (error in OBIA data set). Euclidean Distance, in ArcMap, was used to carry out this assessment in order to determine the accuracy of the classified gullies within a given radius of the manually digitised gullies. According to Fielding and Bell (1997), there is good reason in calculating errors based on the spatial locations of the two data sets. As it can be assumed that false positives which fall in close

proximity to true positives may create less serious errors than those which are found far from true positives (Fielding & Bell, 1997).

A common problem with a conventional confusion matrix accuracy assessment observed by Wang *et al.* (2014) is that it fails to provide the spatial distribution of the classification error. There are two common and easy methods (shown by Equations 4.8. and 4.9.) to determine the accuracy of false positive errors by weighing their relative proximity to actual positive cases of the reference data. In the first technique, the distance weight is calculated as the number of adjacent true positives based on Equation 4.8. Equation 4.9. represents a second technique where errors are weighted by their distance from the nearest positive case. Using these weights, an adjusted confusion matrix may be constructed from which adjusted error measures are calculated. If the ratio of adjusted errors to actual errors is calculated, it will provide information about the spatial characteristics of the prediction errors (Fielding & Bell, 1997).

Equation 4.8. $$Weight = 1 - \frac{Postive\ neighbours}{9}$$

Equation 4.9. $$Weight = 1 - \frac{1}{2(Distance\ from\ positve\ value)}$$

4.3.6.4. Object comparison

Object comparison was conducted by considering each gully as a single object rather than a grouping of pixels. Intersection of the manually digitised gullies and the gullies extracted through OBIA was calculated by converting both vector sets to raster and giving the one data set a value of 1 for gullies and 0 for no gullies. In the other data set, a unique value was given to each gully object. The two data sets were then multiplied using the raster calculator. Objects were considered accurate when they intersected the reference data set.

4.4. Gully Erosion

4.4.1. Calculation of gully growth

In order to determine whether the gully systems were active and if so at what rate the gullies in the catchment were expanding, two SPOT 5 images five years apart were compared. Any gully was considered active if it had increased in size laterally between 2007 and 2012. The OBIA ruleset was used to extract gullies in the SPOT 2007 and SPOT 2012 images in eCognition. The two vector data sets were then overlaid in ArcMap and the surface area difference was calculated using a simple raster calculation. This calculation only accounted for lateral growth and did not account for an increase in gully depth. However, it is assumed that gullies will incise downwards until reaching the bedrock below from then on they will only expand laterally so all gullies which have expanded laterally would have already reached the bedrock below and would have no further increase in depth (Le Roux *et al.*, 2015) (Equation 4.10).

Equation 4.10. $Surface\ area\ growth = gully\ surface\ area_{(2012)} - gully\ surface\ area_{(2007)}$.

The results were then divided by the five years in order to determine how fast the gullies were expanding annually. Using this method active gullies could be identified.

4.4.2. Calculation of gully volume

As gullies can either be classified as “V” or “U” shaped depending on the type of erosion (Das & Saikia, 2013) (Figure 4.5). The volume of sediment produced from the gullies was calculated as a range. Assuming all gullies in the catchment had the “V” shape would produce the minimum sediment contribution scenario, whereas assuming all the gullies in the catchment had the “U” shape would produce the maximum sediment contribution scenario. Bulk density was assumed to be 1.6 over the catchment and that gullies erode down to bedrock before expanding laterally (Le Roux *et al.*, 2015). Thus the land types data with soil depth for the catchment were used to calculate the

size of each gully in the catchment under the "V" and "U" scenarios. The volume of a square and triangle was used to calculate the volumes for the two "V" and "U" shaped scenarios respectively.

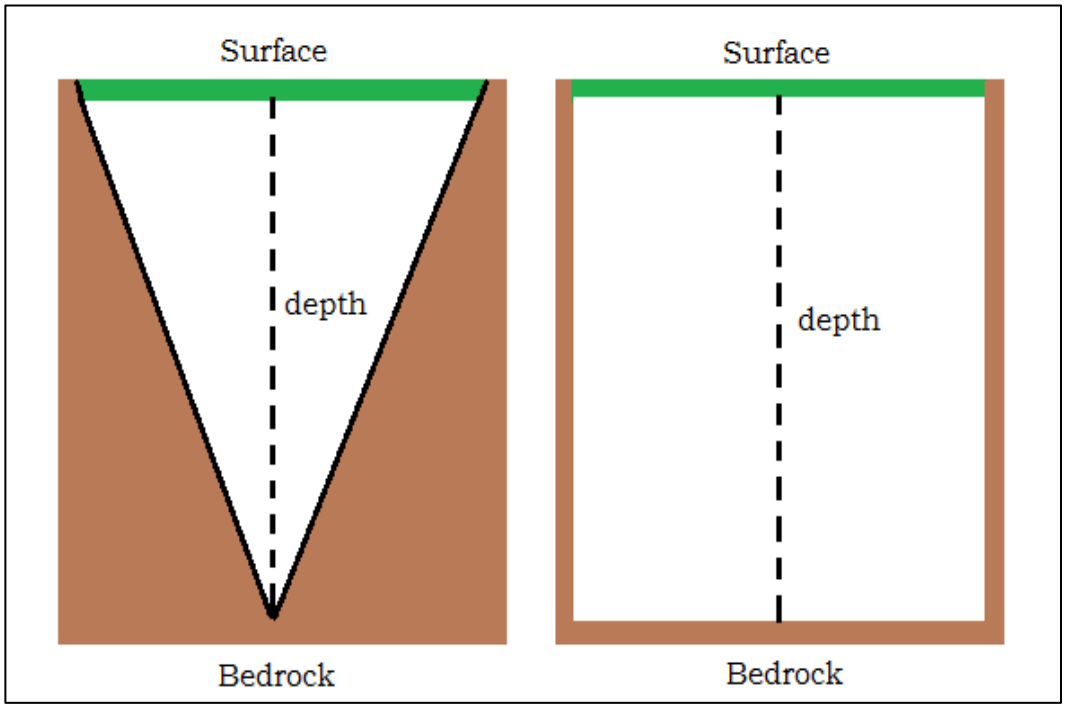

Figure 4.5: Cross section of a U (right) and V (left) shaped gully system.

For a U-shaped gully the equation to calculate the volume of a rectangle was used shown in Equation 4.11 below.

Equation 4.11. $Volume = Width * length * height$

Where $Width$ = width between the gully walls

$Length$ = length of gully

$Height$ = depth to base

For a V-shaped gully the volume of a triangle was calculated shown in Equation 4.12 below.

Equation 4.12 $$Volume = 0.5\ base * height * length$$

Width, length and height are the same as in Equation 4.11.

4.4.3. Calculation of sediment yield from gully erosion

As with sheet and rill erosion, methods are needed to predict the extent and patterns of gully erosion across large catchments (Hughes & Prosser, 2012). Identifying gullies from aerial and satellite imagery is the first step to creating a methodology to accurately calculate sediment yield from gully erosion in a catchment. However, not all sediment produced from gullies end up in the river or dam at the catchment outlet as some of the sediment will be deposited in sinks (Ndomba *et al.*, 2009; Le Roux *et al.*, 2015). Furthermore, not all gullies have equal potential to deliver sediment to the catchment outlet. Factors such as vegetation cover inside the gully, connectivity and continuity (see Appendix 1) all determine the amount of sediment a gully will produce and channel through the catchment (Le Roux *et al.*, 2015).

During the field trip in June 2014, various properties of 24 gullies in the catchment were visually assessed and noted in Appendix 1. It was found of the gullies assessed in the field that half were connected and all were active. Connected gullies are defined as been able to channel coarse sediment during 'normal' flood events, 12 were identified in the field. Partially connected gullies defined as been able to transfer sediment only in extreme flood events and potentially connected gullies having competence to transport sediment but lack of supply were grouped and seven gullies fell in this class. Finally, five gullies were identified as disconnected gullies in which transfer is obstructed. (Hooke, 2003; Le Roux *et al.*, 2015). It was also found that 14 of the gullies were continuous.

A constant sediment delivery ratio (SDR) of 50% was applied to all the gullies in the catchment. Although Walling (1983) found that linking on-site rates of erosion in a catchment to the sediment yield at the catchment outlet using a sediment delivery ratio created uncertainties, various SDRs have been used and suggested in literature. As assuming all sediment produced by gully erosion in a catchment will end up at the outlet is too simplistic (Ndomba *et al.*, 2009) and numerous studies have indicated that not all eroded sediments that leave the gully end up in the river (Ndoma *et al.*, 2009; Hughes & Prosser, 2012; Le Roux *et al.*, 2015). Martinez-Casasnovas *et al.* (2003) found in their study in Spain, a SDR of 68.1% in a catchment of 0.688 km^2 . As the catchments increase in size so the SDR decreases (Walling, 1983; Ferro & Minacapilli, 1995). This inverse relationship has been used in many studies to estimate SDR and has been explained that there is decreasing slope and channel gradients and increasing opportunities for deposition associated with increasing basin size (Walling, 1983). Thus the upper Tsitsa Catchment will likely have a lower SDR than that found by Martinez-Casasnovas *et al.* (2003).

In a study conducted by Ndomba *et al.* (2009) a SDR of 50% was used for gully sediment yield predictions in a basin in Tanzania. After estimating the gully erosion rates (13 600 t/yr), Ndomba *et al.* (2009) then applied a constant delivery ratio of 50% in order to obtain 6 800 t/yr as the sediment yield contribution from gully erosion. In this study a delivery ratio of 50% was used following the study of Ndoma *et al.* (2009) and field observations that 50% of gullies were connected and 58% were continuous. With a delivery ratio of 50%, it was estimated that gully erosion contributes between 70 000- 140 000 t/yr to the sediment yield in the upper Tsitsa Catchment.

4.5. Modelling various climate scenarios

4.5.1. Overview

Due to the potential of climate change to increase soil erosion and lead to associated adverse impacts such as dam siltation, it is crucial to model future rates of erosion in order to access it as a potential future environmental problem and implement strategies to mitigate its effects. Climate and erosion prediction models have become vital tools used to assess soil erosion under

various scenarios. They are also the most practical means of assessing the effect of climate change on soil erosion (Mullan *et al.*, 2012). SWAT was used to incorporate the rainfall and temperature projections from Engelbrecht *et al.,* (2011) in order to gain insight into how sediment yield from sheet and rill erosion in the upper Tsitsa Catchment will be affected by climate change.

4.5.2. Incorporating climate projections in the SWAT model

For this study, maximum and minimum temperature and rainfall data were used from the study conducted by Engelbrecht *et al.* (2011) who downscaled the six GCM models for South Africa:

- GFDL-CM2.0
- GFDL-CM2.1
- ECHAM5/MPI
- UKMO
- MIROC3.2
- CSIRO

It is important to use multiple GCMs in a study involving the effects of climate change (Crosbie *et al.*, 2011). The use of multiple models helps account for the large potential uncertainties in future estimates of soil erosion and sediment yield. By choosing only the best performing GCMs the range of projections may be narrowed. Similarly, by choosing the extremes of the GCMs for rainfall may not produce the extremes of the sediment yield as different parametres within the model may outweigh the effects of rainfall. Thus it is best to use as many as possible, which has the added benefit of providing a range sediment yield forecasts (Crosbie *et al.*, 2011).

All the models are from the 'business as usual', A2, based on the Intergovernmental Panel on Climate Change (IPCC) Special Report on Emissions Scenarios (SRES) (Engelbrecht *et al.,* 2011). The A2 scenario represents a differentiated world. It is characterized by lower technological change, slow capital stock turnover and lower trade flows. Countries are more

independent with less international cooperation and there is a slow transfer of technology and ideas. A2 represents more self-reliance in terms of resources with less emphasis on economic, social, and cultural interactions between the different regions. Economic growth is uneven and the income gap between now-industrialized and developing parts of the world does not narrow. In the A2 scenario, the income per capita is largely maintained or increased in absolute terms. The A2 scenario places emphasis on family and community life and fertility rates decline relatively slowly, which makes the A2 population the largest among the various scenarios reaching 15 billion by 2100 (Intergovernmental Panel on Climate Change, 2000).

Data for each model were prepared for SWAT by combing them in separate text files, which were then run in the SWAT macro to calculate the weather statistics needed for the SWAT weather generator. From here the various climate scenarios were run in the SWAT model using the same land use and soil data on a generic agricultural land use scenario.

4.5. Modelling various agricultural scenarios

4.5.1. Overview

DAFF is considering the Eastern Cape including in the Tsitsa River Catchment for potential commercial farming of certain crops. If the dam is to be built it is important to predict sediment yield from sheet and rill erosion in the catchment under future land use conditions in order to adequately manage the dam and prevent siltation.

4.5.2. Running various crop types in SWAT

Once the SWAT model is set up and run under current land use and climate conditions, it is easy to change the land use inputs for various other scenarios. The land use input was changed for 12 different land use scenarios. It was run for agricultural land, cabbage, corn, sweet potato, sugar and avocado orchids under both a till and no-till system except for sugar and avocado which was

run only on a no-till scenario. Results were saved and the total sediment output for each scenario was analyzed.

4.5.3. SWAT tillage operations

SWAT considers mixing depth and mixing efficiency when it models tillage operations. SWAT requires the timing of the tillage operation as well as the type of tillage operation in order to model the effects of tillage on the soil (Nietsch *et al.*, 2005). In SWAT the user can manually change the SCS-CN for the HRU's according to the unique tillage operations of their catchment. These CNs represent the moisture value of the soil and SWAT can adjust the manually entered value for daily modelling to reflect changes in soil water content (Nietsch *et al.*, 2005). Mixing coefficient in SWAT defines the fraction a residue/nutrient/pesticide/bacteria pool in each unique soil layer that is then redistributed through the depth of the soil that is mixed by the tilling equipment (Nietsch *et al.*, 2005). In order to calculate the redistribution of nutrients/chemicals or residue during tillage, SWAT divides the depth of the soil layer by the tilling mixing depth which is then multiplied by the amount of mixed nutrient/chemical or residue. To calculate the final concentrations, the redistributed nutrients/residue or chemicals are added to the unmixed concentrations for that layer. The only difference for bacterial concentration calculations is that bacteria mixed into the layers below the surface layer are assumed to die (Nietsch *et al.*, 2005).

During tillage nutrients, pesticides and residue are redistributed in the soil profile. By disturbing the residue of the soil and destroying the structure increases the soil's vulnerability to erosion (Rust & Williams, n.d.). A study conducted by Wuest *et al.* (2009) conducted in a semi-arid environment in the USA showed that agriculture under no-till systems had considerably less erosion and surface runoff than agriculture under a system of tilling. As the upper Tsitsa catchment comprises many independent farms with various crop, soil and slope types there are numerous systems applied for tilling. As it was beyond the scope of the study to identify the various tillage systems each farmer used, for simplicity the tillage system modelled in SWAT was the 4-bed roller technique.

4.6. Field surveys

Le Roux *et al.* (2015) collected four grab samples during a field survey in October 2013, three at Tsitsa Bridge near the future dam site and two at the Tsitsa-Tina River confluence, Figure 4.3. A further four grab samples were taken in a field survey for this study in June 2014 (e.g. Figure 4.6.) These were taken at the Tsitsa Bridge near the future dam and the Tsitsa-Tina River confluence. One more grab sample was taken in January 2015 at the Tsitsa Bridge. All grab samples were sent to the analytical laboratories at the ARC-ISCW to be analysed for total dissolved solids. During the field surveys, observations of the gullies were also recorded this included gully position, depth, size, activity, continuity, vegetation cover (both internally and externally) as well as the manning's roughness (both internally and externally) and finally the connectivity. A sample of the observation form is shown in appendix A. the position of the gullies was mapped using a GPS camera. The limited road network in the catchment, as well as the quality of the roads, made accessing many of the gullies difficult.

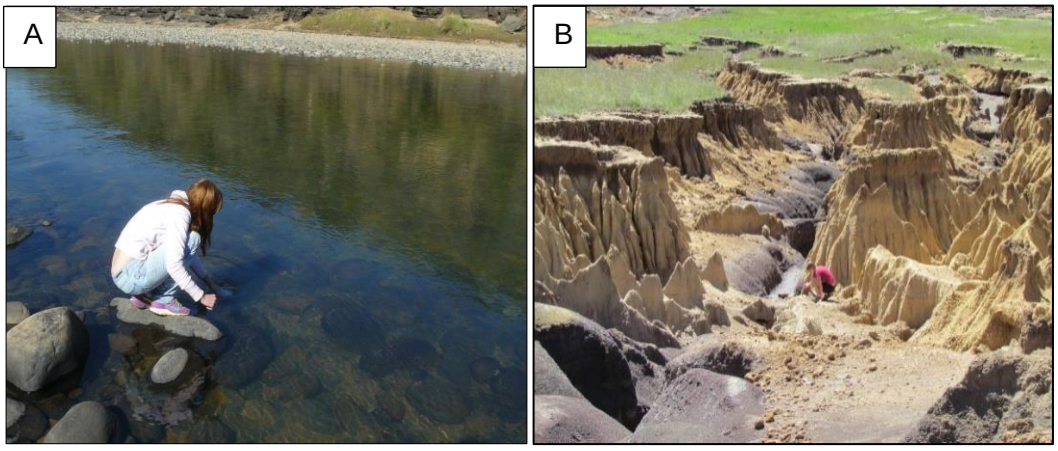

Figure 4.6. (A) Collecting grab samples at the Tsitsa-Tina confluence in June 2014. (B) Gully observations in January 2015 in the upper Tsitsa Catchment Eastern Cape Province, South Africa.

Bulk density samples were also taken on a field trip in January, due to the diversity of soils and the limited time in the field, it was not possible to sample all the soils according to the land types data used in the SWAT model (approximately 100). It was manageable to sample the bulk density of all the soils according to the soil association map created by van den Berg and

Weepener (2009), however, due to the large discrepancy between the two data sets it was impossible to link the bulk density of the soil association and the land type map used in the SWAT model. The average bulk density was found to be 1.4. A table of the sampled bulk densities can be found in Appendix 3.

5. Results

Results from the current scenario presented here (2007-2012) from both the SWAT analysis and the OBIA are presented first in the results section. SWAT was used to determine the sediment yield from sheet and rill erosion and OBIA was used to determine the sediment yield from gully erosion. Results from both analyses needed to be combined as the SWAT model does not account for gully erosion. The future climate and land use change scenarios are presented after the current scenario. Future land use is based on potential changing agriculture and a number of crops were identified as potential crops for the upper Tsitsa Catchment namely: corn, cabbage, sweet potatoes, sugarcane and avocado. Climate change data from six downscaled GCM's were also tested for the period 2015-2100.

5.1. SWAT Results

SWAT was used to model sediment yield from sheet and rill erosion under various land use and climate scenarios. First, the current land use and climate scenario was to modelled by using measured climate data from weather stations in the catchment for the period 2007 -2012 along with the National Land Cover map. These results gave the basis to which the results of the other scenarios could be compared.

The second scenario involved testing the impact of tillage operations on sediment yield from sheet and rill erosion this too was done using measured climate data and the National Land Cover map but the management operations in SWAT were changed to incorporate tillage. A third land use scenario was tested and this was based on proposals for large-scale agriculture of certain crops namely corn, cabbage, avocado, sweet potato and sugarcane. Both till and no-till operations using measured climate data were tested.

Finally, the effect of projected climate change on sediment yield from sheet and rill erosion was modelled. This was done by using rainfall and temperature data from the six GCM models CSIRO, GFDL, GFDL 2, MIROC, MPI and UKMO for the period 2015-2100. The period 2015-2100 was divided into three

19-year time period: short-term 2015-2034, medium-term 2045-2064 and long-term 2081-2100.

5.1.1. Current land use and weather (2007-2012)

Sediment yield from sheet and rill erosion in the upper Tsitsa Catchment for the 2007-2012 period was approximately 0.91 t/ha (Figure 5.1). Average annual sediment yield is thus 0.18 t/ha/yr. The sediment yield in the catchment increases dramatically by over five times after 2008 with two noticeable spikes in sediment yield in 2009 and 2011.

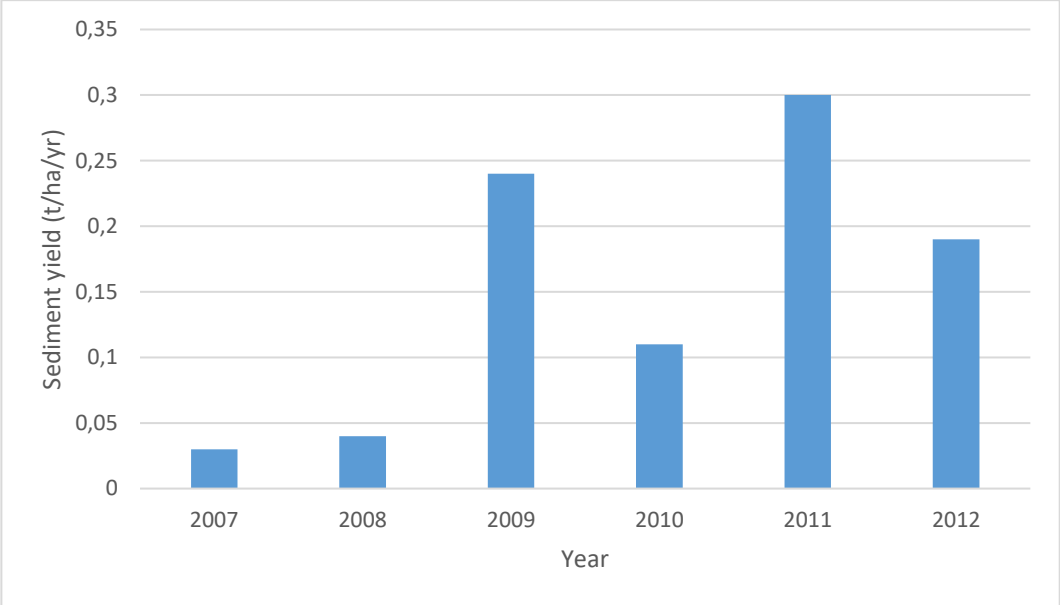

Figure 5.1: The average sediment yield from sheet and rill erosion in the upper Tsitsa Catchment, Eastern Cape, South Africa, for each year for the period 2007-2012 modelled in SWAT.

Average annual measured rainfall for the 2007-2012 period is shown in Figure 5.2. Rainfall is lowest in 2007, rising steadily to 2011 and then decreasing again in 2012. The trend supports the observations in Figure 5.1 for the low sediment yield modelled in 2007 and 2008 and high sediment yield in 2011 with a decrease again in 2012.

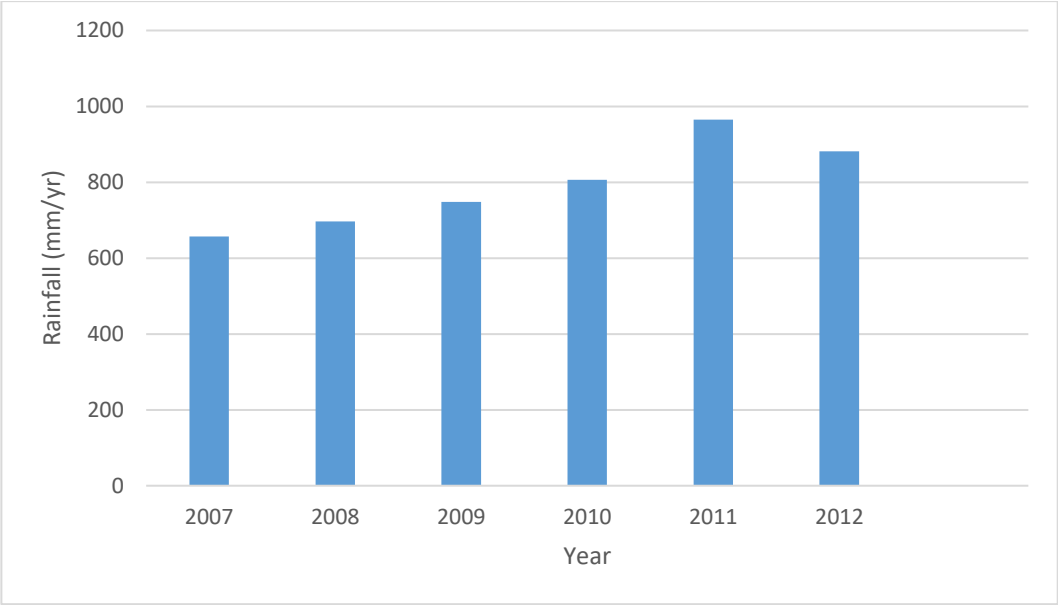

Figure 5.2: The average annual measured rainfall for each year during the period 2007-2012 in the upper Tsitsa Catchment, Eastern Cape, South Africa.

Figure 5.3 shows the number of 5 mm, 10 mm and 15 mm rainfall events over the 2007-2012 period. All the events increase in the years 2010-2011 and then show a decrease to 2012. This supports the increased sediment yield and rainfall in 2011 and decrease in 2012 shown in Figure 5.1 and Figure 5.2.

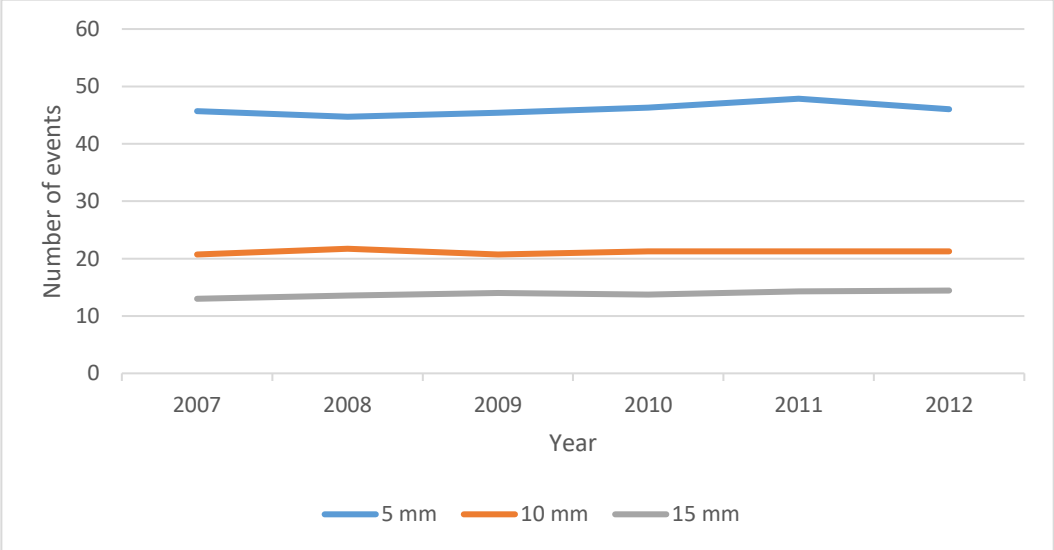

Figure 5.3: The number of 5 mm (blue), 10 mm (orange) and 15 mm (grey) rainfall events during each year for the 2007-2012 period in the upper Tsitsa Catchment, Eastern Cape, South Africa.

Average sediment yield from sheet and rill erosion per month shows that the majority of the sediment yield occurs between January and February decreasing towards June and August and then slowly rising towards December (Figure 5.4). A similar trend is observed in the monthly rainfall graph (Figure 5.2). In both Figures 5.4 and 5.5, there is a spike between June and August. The raw data shows that May 2011 was a wetter than average month with approximately 50 mm more rainfall than the other years. The result of this rainfall caused the spike observed in Figures 5.4 and 5.5.

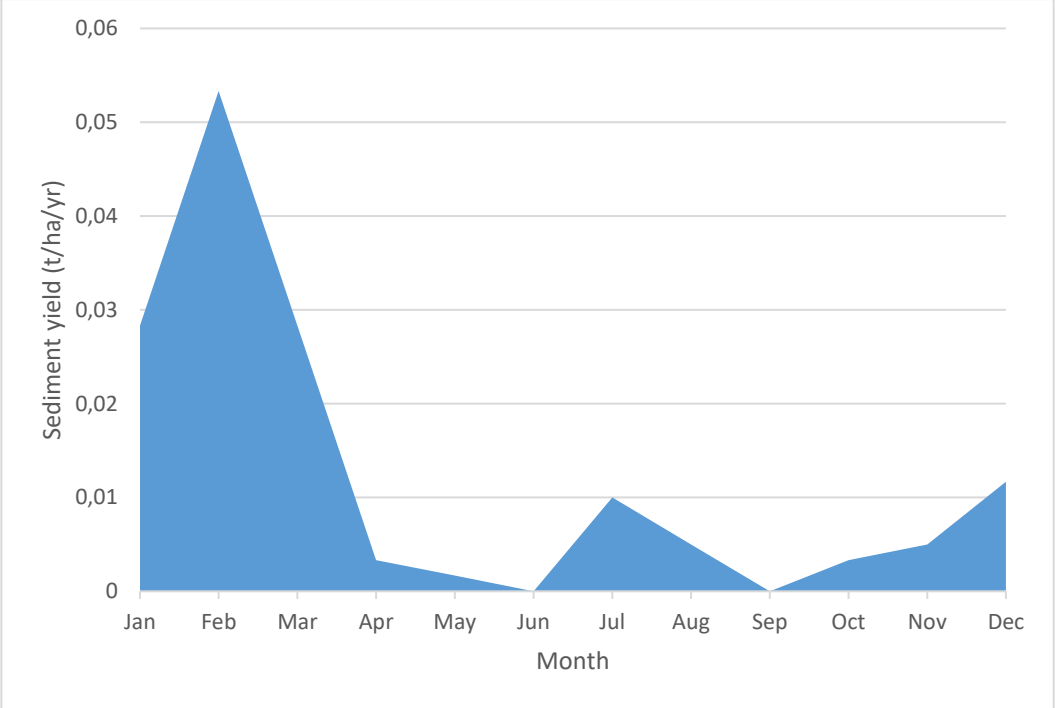

Figure 5.4: The average sediment yield from sheet and rill erosion in the upper Tsitsa Catchment, Eastern Cape, South Africa, for each month averaged over the 2007-2012 period.

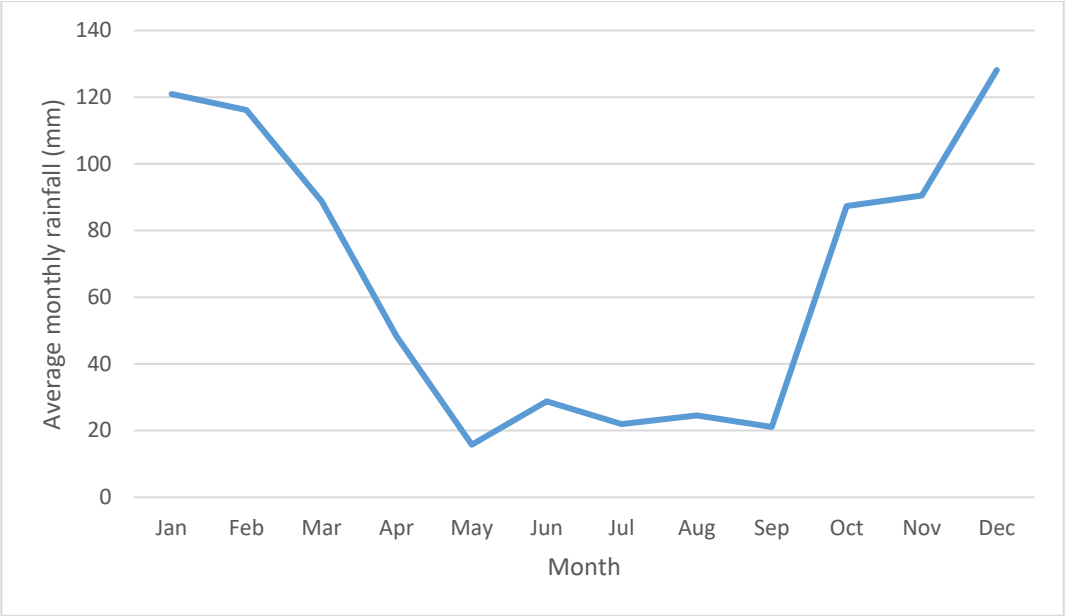

Figure 5.5: The average monthly rainfall averaged out over the period 2007-2012 in the upper Tsitsa Catchment, Eastern Cape, South Africa.

In order to account for the extreme rainfall in 2011 the Fournier's equation was used to graph the average monthly rainfall and sediment yield from sheet and rill erosion for the period 2007-2012 (Figure 5.6). Results show the same trend as Figure 5.4 and Figure 5.5 without the large spike caused by the 2011 outlier.

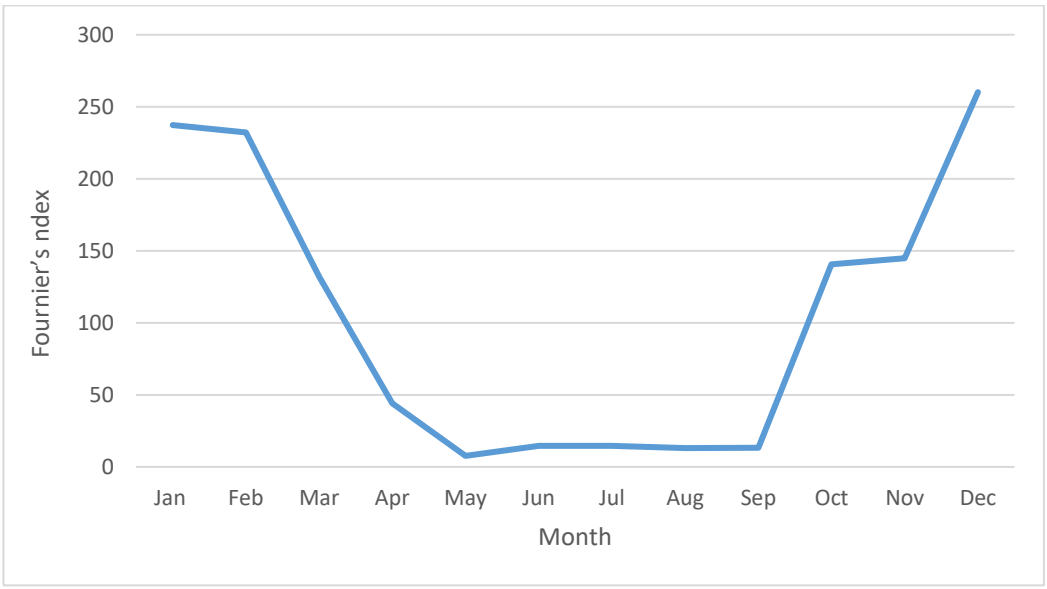

Figure 5.6: The rainfall erosivity calculated using Fournier's equation for the period 2007-2012 in the upper Tsitsa Catchment, Eastern Cape, South Africa.

5.2. OBIA results

eCognition was used to facilitate OBIA on two SPOT 5 images taken in 2007 and 2012 respectively. The objective of using OBIA was to identify and map the gullies in the upper Tsitsa Catchment on both images and then compare the gully sizes in order to determine the gully growth rate.

Once OBIA had been conducted it was important to determine the accuracy of the ruleset and thus the derived gully location maps. Since determining the accuracy of a gully location map is subject to bias, four separate accuracy assessments were conducted. The two derived gully location maps were overlaid and the increase in gully size was calculated. This was done using a basic model of gully development. It was found that sediment yield from gully erosion produced between 140 000-280 000 tons of eroded material in the five-year monitoring period. The rate of soil erosion from was calculated to be between 7 t/ha/yr and 14 t/ha/yr for the 200 km^2 catchment.

It was found that the gullies expanded in both area and length. Statistics for each were calculated in ArcMap. The gully erosion increased by $4e^6$ m^2 over the catchment. The maximum area of gully expansion was 240 000 m^2 and minimum 0.000375 m^2 and on average the gullies expanded by 42000 m^2.

5.2.1. Gully location maps of the catchment

Figures 5.7 and 5.8 show the extent of gully erosion over the catchment for the years 2007 and 2012 respectively. The 2012 map has more gully erosion particularly in the northern part of the catchment. It was also found that the 2012 algorithm misclassified a large portion of rock outcrops (circled in red). On both images, the majority of the gullies appear in the lower areas of the catchment with only one or two gullies identified in the higher reaches of the Drakensberg.

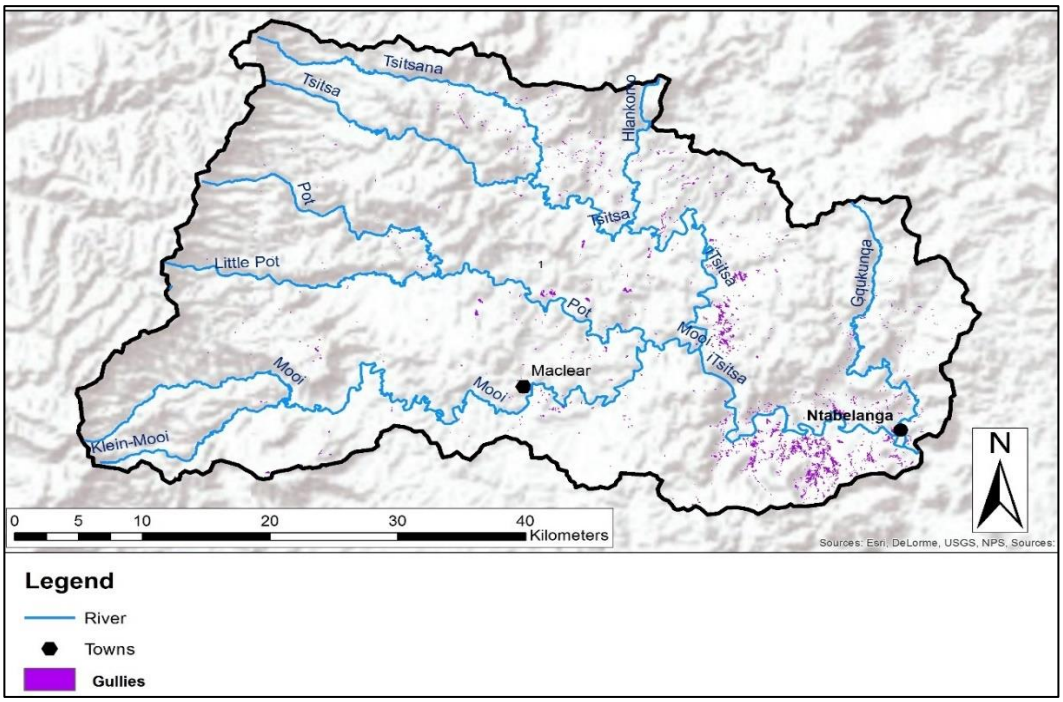

Figure 5.7: The extent of gully erosion in 2007 from the OBIA classification in the upper Tsitsa Catchment, Eastern Cape, South Africa.

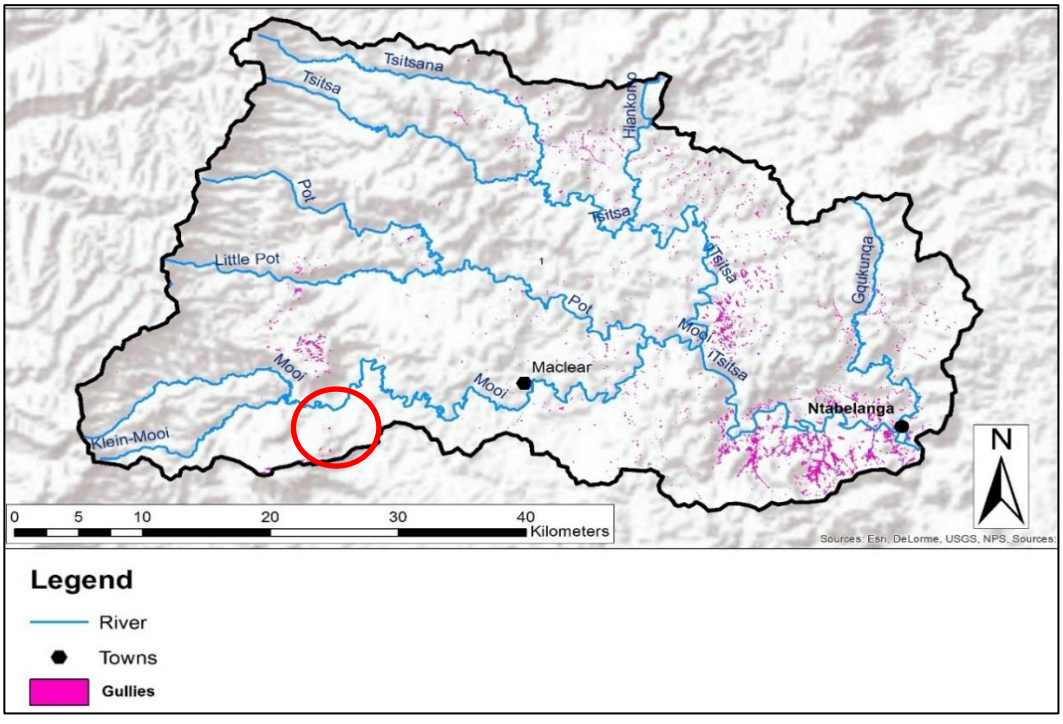

Figure 5.8: The extent of gully erosion in 2012 from the OBIA classification in the upper Tsitsa Catchment, Eastern Cape, South Africa, with the miss-classified rock outcrops circled in red.

5.2.2. Individual gully assessment

Visual assessment of the individual classified gullies shows satisfactory accuracy. The accuracy of the classification is qualified further in Section 5.2.3 through four separate accuracy assessments. It also highlights some benefits over the manually digitised gullies. Classified gullies formed more accurate boundaries around the gullies, "hugging" the edges more closely than that of the manually digitised gully boundaries. They were also able to distinguish between the inter-gully and the gully area more accurately than the manual interpretation. Figure 5.9 shows an area where there is a high similarity between the manually digitised gully (red) and the classified gully (pink). With the manually digitised gullies, the interpreter drew boundaries around the whole gully system, where the classified gullies distinguished areas in the gully system which were vegetated and not part of the gully shown. Finally, it was noted that OBIA ruleset was able to better identify larger gully systems than smaller disconnected gullies.

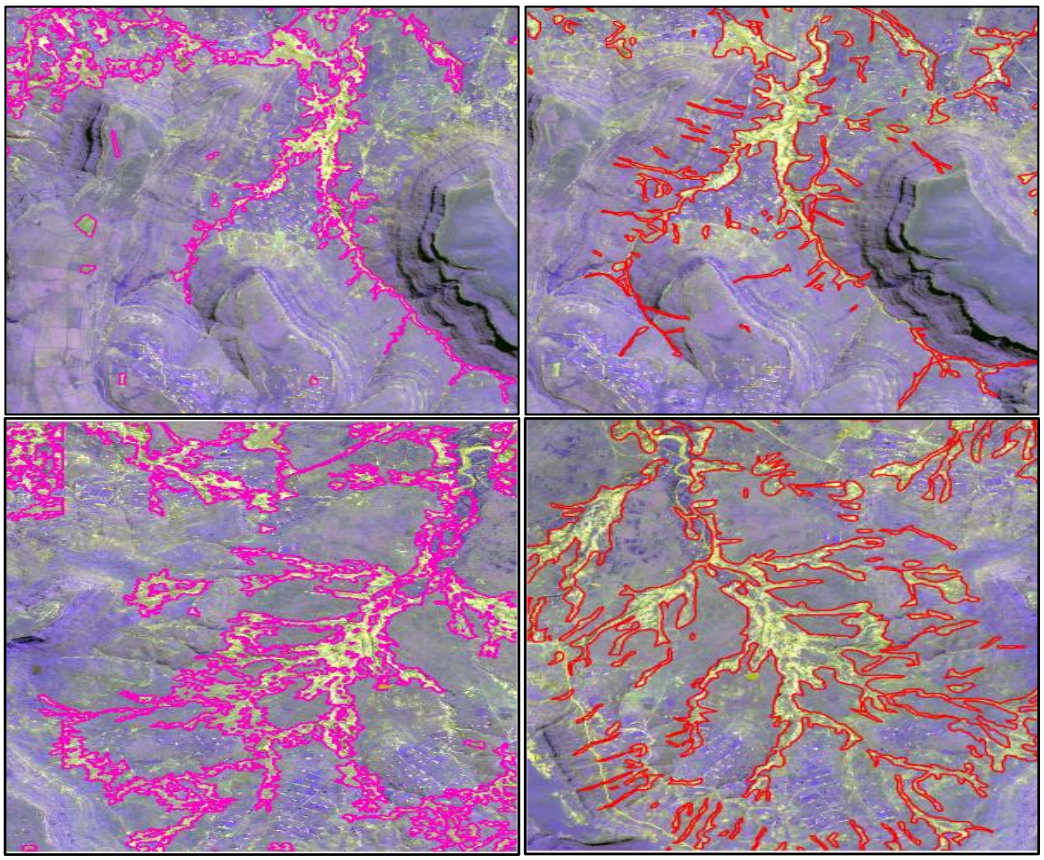

Figure 5.9: Segments of the SPOT 5 images of gully systems identified through OBIA classification (pink) and manual interpretation (red) in the upper Tsitsa Catchment, Eastern Cape, South Africa.

From visual interpretation, it was also noted that errors were made by both the manual interpreter and OBIA ruleset. Major errors for each are shown in Figure 5.10 and 5.11. Figure 5.10 shows the common errors made by the manual interpreter namely classifying rock outcrops and densely vegetated gullies. The latter may not be considered a too serious error, however, Casanovas and Zaragova (1996), as well as Le Roux *et al.* (2015), determined that highly vegetated gullies do not contribute significantly to the sediment load in the catchment. This is due to a number of reasons; first, during a rain storm the leaf canopy intercepts the drops and dissipates their kinetic energy, which prevents the droplets from causing physical disaggregation of the soil by hitting the soil at a high speed. Second, the dense basal cover provided by the vegetation reduces the runoff and the velocity of the runoff as it slows down the water flow. Finally, vegetation cover contributes to the organic matter that stabilizes the soil structure (Laker, 2004). Thus digitising densely vegetated gullies and calculating the sediment load generated from these gullies through the same method as that for non-vegetated gullies will give an overestimation of sediment yield.

Figure 5.11 shows the various types of classification errors made through OBIA. OBIA erroneously identified certain rock outcrops, sedimented parts of the river and roads as gullies even after a thorough ruleset had been created. OBIA also under classified some gully systems and discontinuous gullies. OBIA was better able to identify larger, connected gully systems than smaller disconnected gullies. The various types of errors made by the OBIA classification will be quantified and explained further in Section 5.2.3.2.

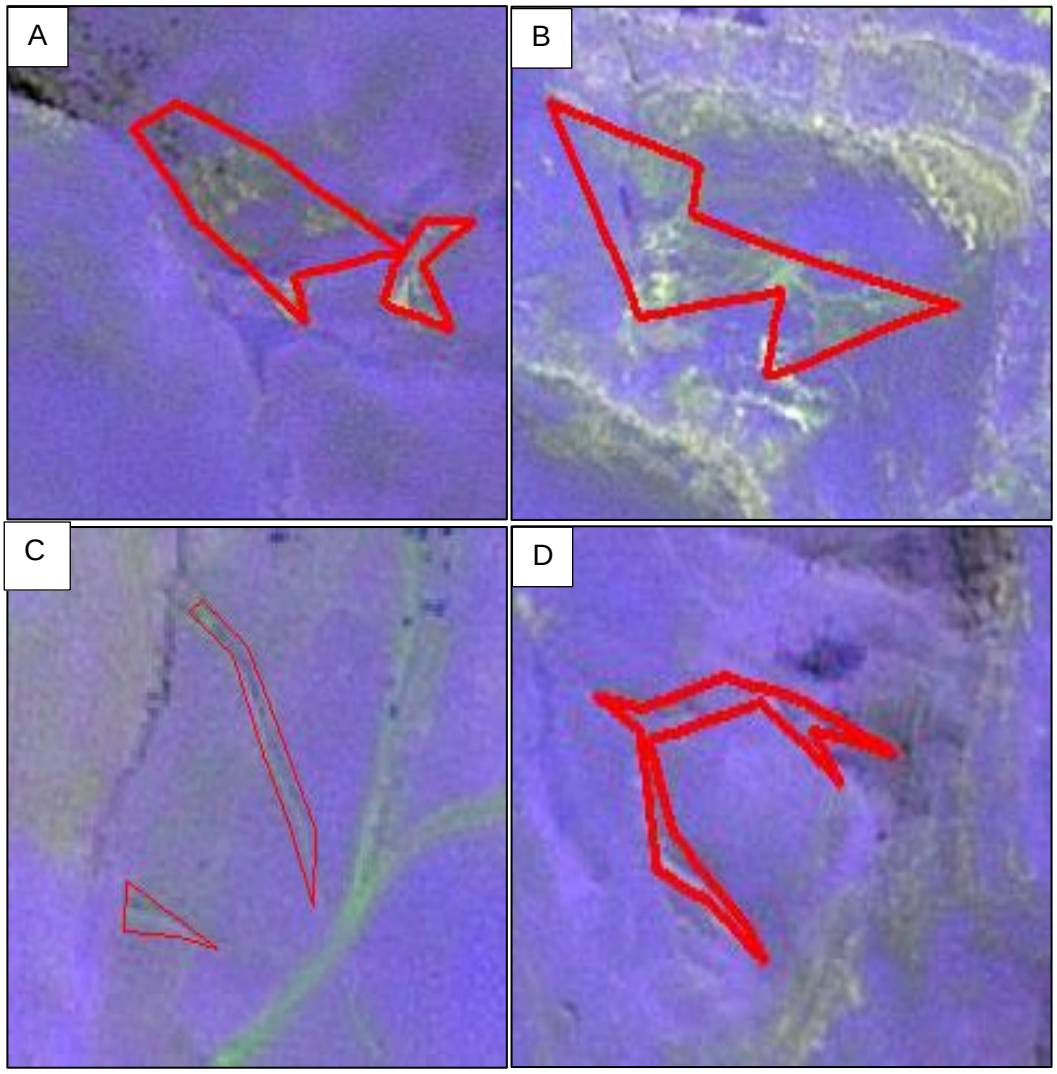

Figure 5.10: The errors made by the manual interpreter in red on the spot 5 image of the upper Tsitsa Catchment, Eastern Cape, South Africa. (A), (B) showing the delineation of rock outcrops as gullies. (C), (D) showing the delineation of densely vegetated gullies.

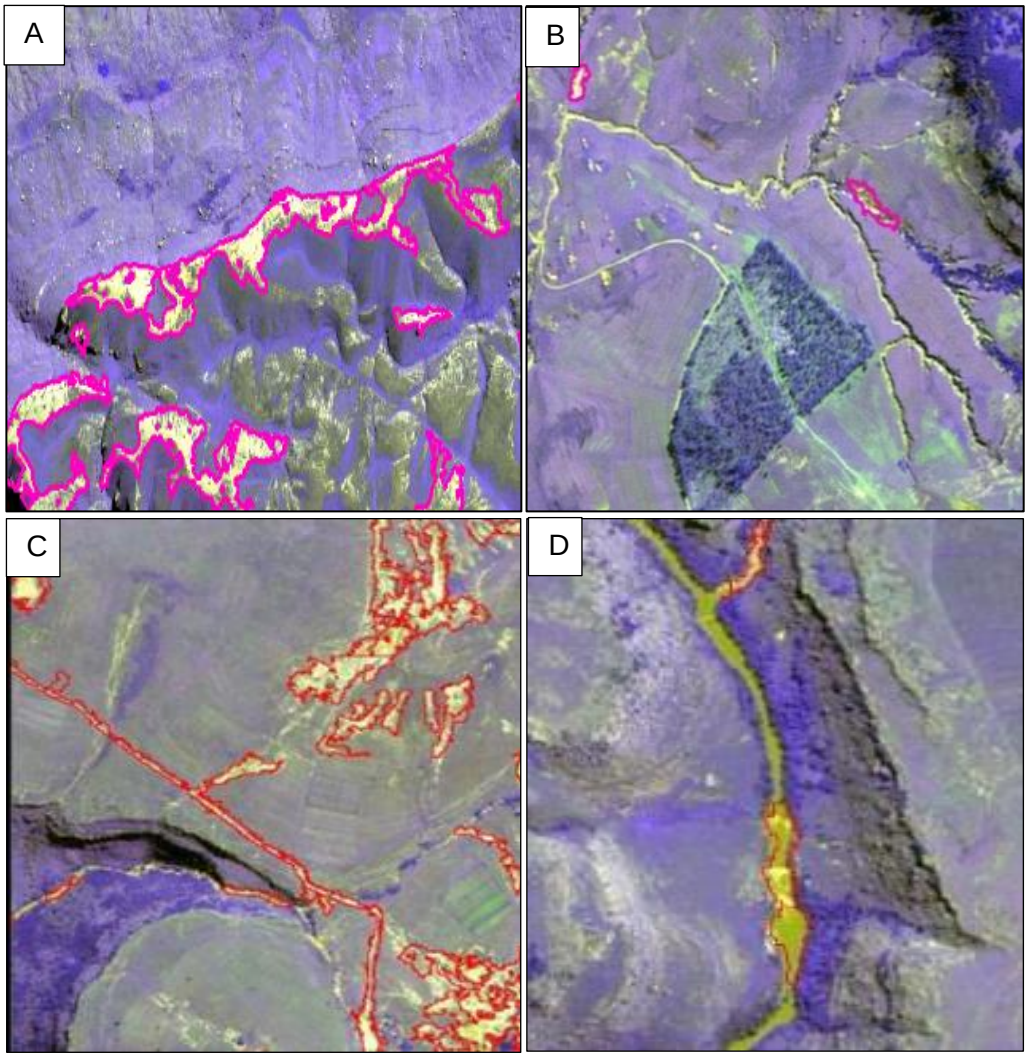

Figure 5.11: The errors made through OBIA on segments of the SPOT 5 image of the upper Tsitsa Catchment, Eastern Cape, South Africa. (A) showing the delineation of rock outcrops. (B) showing an under classified gully system. (C) showing the error made by classifying the roads. (D) showing the incorrect classification of the river.

5.2.3. Results of the accuracy assessments

5.2.3.1. Random point sampling

Results of the random point sampling accuracy assessment for the 2012 data set whereby 144 random points inside the gullies were assessed against the SPOT 5 image, gave an overall accuracy of 59.7%. This method also allowed for the types of errors to be categorized. It was found that of the classification errors made through the OBIA 79.3% was falsely classifying rock outcrops, 10.3% was falsely classifying sheet erosion and the rest was made up of errors in footpaths and sediment in the rivers and grass patches. When the 144 random points were extended to the entire catchment it gave an overall accuracy of 97.2%. Mis-represented gullies made up 2.1% and gullies which were not represented accounted for 0.6% of the error.

5.2.3.2. Total area of overlap

Results of the total area of overlap accuracy assessment gave an overall accuracy of 98% for the 2012 data set and 99% for the 2007 data set. The user's and producer's accuracy was less correct. For the 2012 data set, the user's accuracy was 23% and the producer's accuracy was 28%. The 2007 data set had an overall accuracy of 99% with the user's and producer's accuracy 25% and 61% respectively. Table 5.1 shows the types of errors encountered through the OBIA classification for each data set. Both the 2007 and 2012 data sets agreed 99% and 98% respectively with the manual interpretation in finding no gullies. OBIA error in the 2007 and 2012 data sets composed of respectively 0.21% and 0.34% in classifying objects which the manual interpreter did not find to be gullies. In most cases, OBIA identified rock outcrops, sedimented parts of the river and tilled land as gullies, there were a few cases where OBIA found gullies which the manual interpreter missed. OBIA failed to identify 0.49% and 0.67% of the gullies that the manual interpreter found in the 2007 and 2012 images respectively. In some of these cases the manual interpreter falsely classified rock outcrops or classified highly vegetated gullies which OBIA could not identify.

Table 5.1: The percentage of gullies extracted through OBIA falling in each of the four classes of the basic accuracy assessment for the 2007 and 2012 data set.

Value	Description	Percentage (2007)	Percentage (2012)
10	Neither data set found gullies	99,1	98,7
11	The digitised gullies showed no gullies yet the ruleset found gullies	0.21	0,34
20	The digitised data set found gullies where the ruleset found no gullies	0.49	0,67
21	Both data sets identified gullies	0.24	0,3

5.2.3.3. Boundaries of leniency

The boundaries of leniency accuracy assessment showed that 30% of the gullies extracted through OBIA corresponded exactly with the manually digitised gullies. It was decided that an error range of 40 m was acceptable as this was the standard of the National Geospatial Information for all their digitised files. It was calculated that 52% of the gullies extracted through OBIA fell within a 40 m range of the manually digitised gullies. Table 5.2 shows the percentage of gullies falling in each range between 0 and 40 m.

Table 5.2: The percentage of gullies extracted through OBIA falling within a specified range of the manually digitised gullies.

Range (m)	Percentage
0-10	44,3
11-20	3,8
21-30	2,6
31-40	2,1

5.2.3.4. Objected comparison approach

The object comparison accuracy assessment showed a 48% overlap of the extracted gullies to the manually digitised gullies. When the formula was converted and the manually digitised gullies were compared to the extracted gullies the overlap accuracy was 16%.

5.2.4. Sediment yield from gully erosion

Using the area of the gully erosion extracted through OBIA between 2007 and 2012 it was determined that the gully erosion increased by 4 km^2 over the catchment. The manually digitised data set showed an increase of 5.6 km^2, which is a 28% difference between the two data sets.

Using lateral gully expansion and soil depth for both U-shaped and V-shaped gully profiles it was calculated that gully erosion produced between 7 t/ha/yr and 14 t/ha/yr, which results in between 140 000 t/yr and 280 000 t/yr been produced in the catchment. When using a delivery ratio of 50% for gully erosion the estimated sediment yield resulted in between 70 000 and 140 000 t/yr.

5.2.5. Total sediment yield for the catchment.

Sediment yield results from the sheet and rill erosion calculated in SWAT showed that sheet and rill erosion contributed 3600 t/yr of sediment. This was then added to the sediment yield contribution from gully erosion calculated using OBIA in eCognition which was found to be between 140 000 and 280 000 t/yr. When using a delivery ratio of 50% for gully erosion, it was found that between 73 600 t/yr and 143 600 t/yr of sediment was generated in the upper Tsitsa Catchment.

5.3. Results of the field surveys

Nine grab samples were collected on various field trips four by Le Roux *et al.* (2015) and five for this study. These were analyzed at the ARC-ISCW analytical laboratory. Results are shown in Table 5.3. Samples 1-4 were taken in November (Le Roux *et al.*, 2015), samples 5-8 were taken in June and sample 9 was taken in January. The grab samples confirmed that the suspended sediment load is much higher in summer than in winter which indicates that it is related to increased event discharge. Two grab samples taken in winter showed no suspended sediment. It should be noted that the results of the grab-samples could not be used to validate the model directly due to the limited number of samples and because the samples were taken after 2012 which falls outside the timeframe of this study.

Table 5.3: Total suspended solids (mg/L) of grab samples taken during the field trips.

Grab sample number	Location	Total suspended solids (mg/L)
1	Mzimvubu River Mouth	574.2
2	Mzimvubu River Mouth	689.4
3	Tsitsa-Tina River Confluence (Tsitsa side)	3131.6
4	Tsitsa-Tina River Confluence (Tina side)	688.0
5	Tsitsa Bridge near dam site	0.0
6	Tsitsa Bridge near dam site	0.6
7	Tsitsa-Tina River Confluence (Tsitsa side)	0.0
8	Tsitsa-Tina River Confluence (Tina side)	0.4
9	Tsitsa Bridge near dam site	259.2

Ground truthing of the gullies was done during two field trips in June 2014 and January 2015. Due to the remoteness of the catchment ground truthing was limited to areas accessible by road. Roads in the catchment are also unpaved, which makes travelling to remote areas difficult. Thus the ground truth points taken were limited to gullies that intersected with the roads. Figure 5.12 shows the photos taken in the catchment with a GPS camera and the gullies that were identified for ground control points are shown in green. Results of the gully observation field work can be found in Appendix 1.

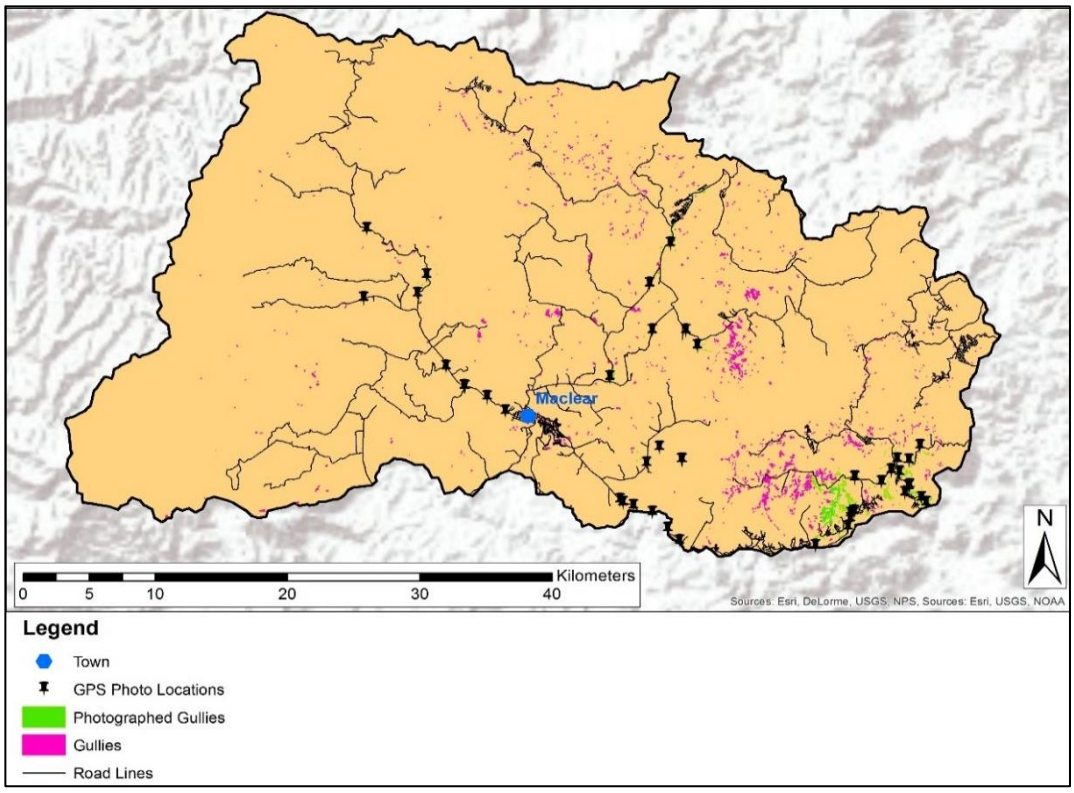

Figure 5.12: The locations in the upper Tsitsa Catchment, Eastern Cape South Africa, where ground truthing was done in June 2014 and January 2015.

5.4. Future scenario modelling results

5.4.1. Land use change results

Results showed that tillage operations increased the sediment yield from sheet and rill erosion for all the land uses tested by an average of 7% from the current no-till, land use scenario (Figure 5.13). Corn and generic agriculture showed the largest increase in sediment yield with tillage 0.19 t/ha/yr and 0.18 t/ha/yr respectively. Under no-till management cabbage will produce the most amount of sediment yield with 0.17 t/h/yr. Avocado orchards and sugarcane will cause the least amount of sediment yield with 0.14 t/ha/yr.

The largest increase in sediment yield was with the generic agricultural land use and the corn land use, which increased by 13% and 15% respectively with tillage operations. Tillage had the smallest effect on sediment yield with sweet potato crops causing a 1% increase. A comparison of all crop types under no-till showed that sugarcane and avocado orchards resulted in a 5% decrease in sediment yield from the current land use scenario. While the other crop types showed an average of 5% increase in sediment yield from the current land use scenario.

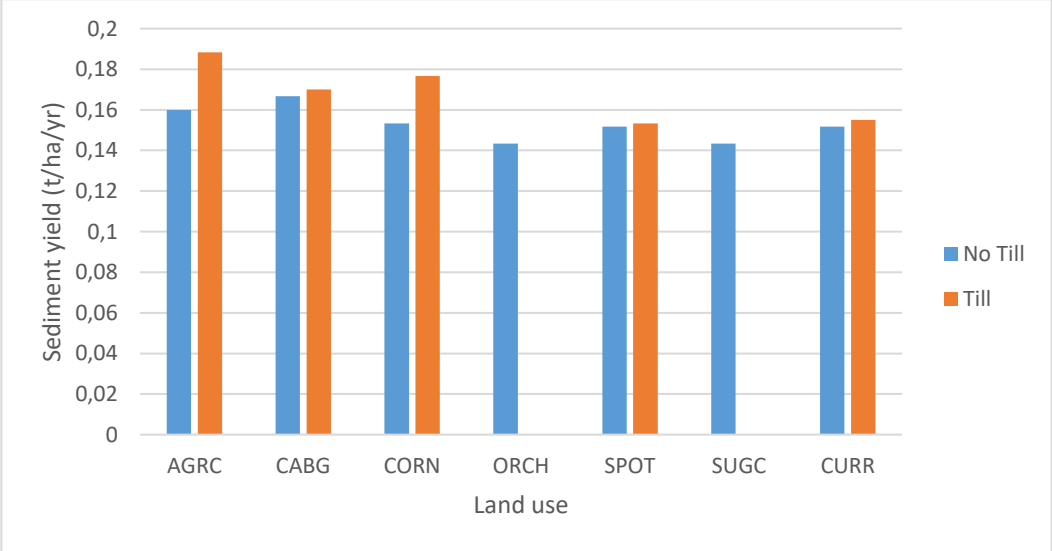

Figure 5.13: The average annual sediment yield from sheet and rill erosion in the upper Tsitsa Catchment, Eastern Cape, South Africa for the various land types tested in SWAT under till and no-till management (AGRC= Generic Agriculture, CABG= Cabbage, CORN= Corn, ORCH= Avocado, SPOT= Sweet Potato, SUGC= Sugarcane, CURR= Current land use).

5.4.2. Climate change results (2015-2100)

Sediment yield from sheet and rill erosion increases substantially towards 2100 for most models, with the main exception being the UKMO model (Figure 5.14). UKMO shows considerably more sediment yield in the first two periods (2015-2034 and 2045-2064) and then decreases noticeably between 2045 and 2100. Future sediment yield for the century can range between 0.3 t/ha/yr and 0.02 t/ha/yr.

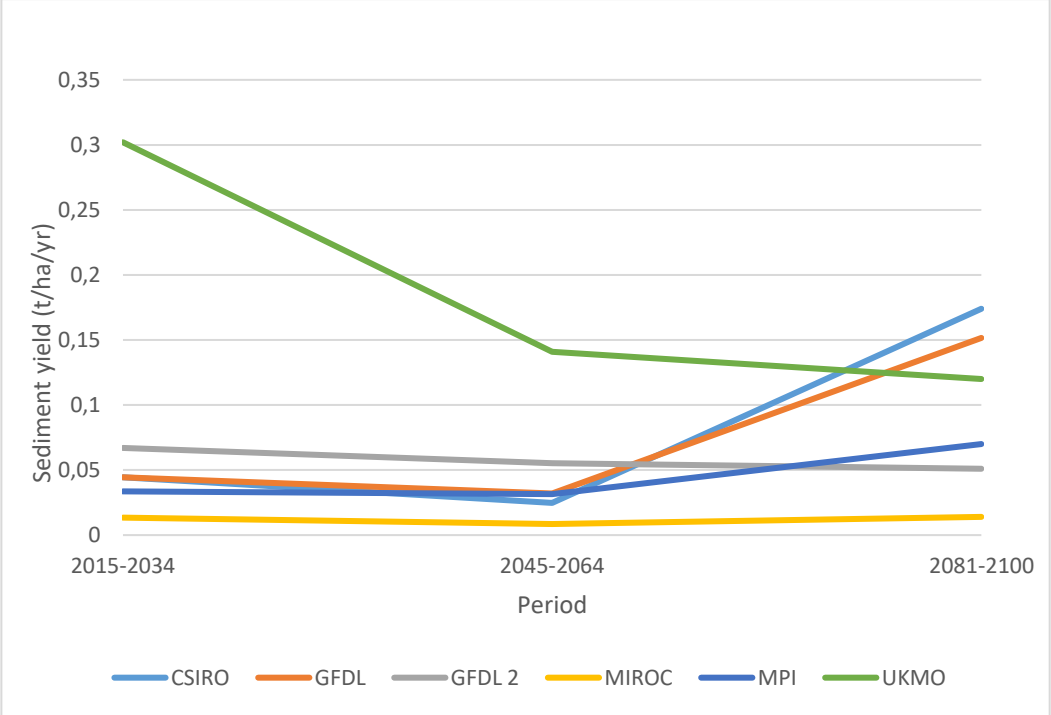

Figure 5.14: The sediment yield from sheet and rill erosion in the upper Tsitsa Catchment, Eastern Cape, South Africa, modelled in SWAT by each of the General Cirulation Models (GCM) for the period 2015-2100.

Average annual rainfall of the six GCMs for the three periods show an increase throughout the century (Figure 5.15). The largest rainfall is expected in the 2045-2064 period which increases by 8% from the previous period. Rainfall then decreases in the 2081-2100 period by 2% yet is still 6% higher than in the 2015-2034 period.

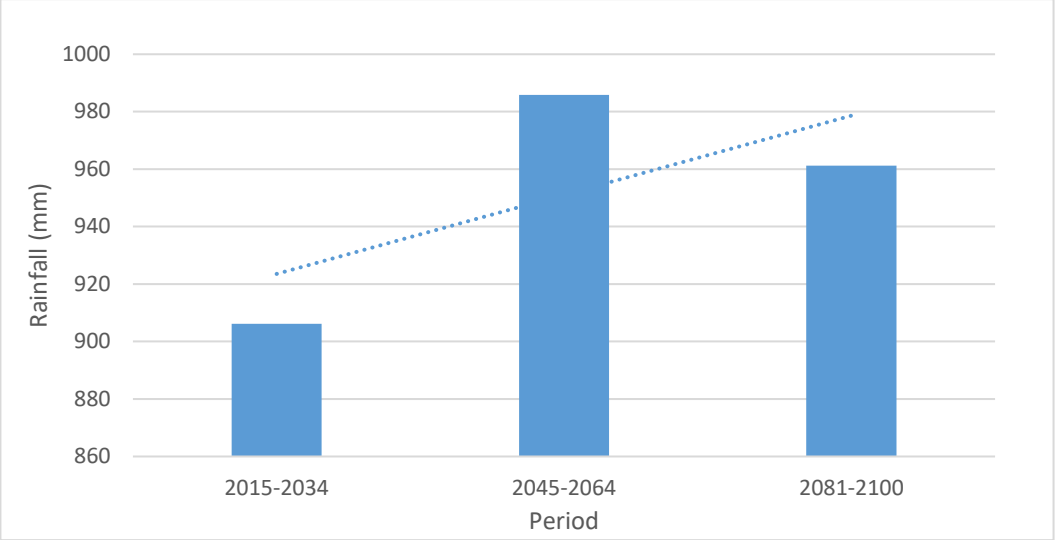

Figure 5.15: The average rainfall of the six GCM models in the upper Tsitsa Catchment, Eastern Cape, South Africa for each period.

Average sediment yield predicted by the six models for each of the periods is shown in Figure 5.16. There is a 42% decrease in sediment yield from sheet and rill erosion from the period 2015-2034 to the period 2045-2064. Sediment yield then increases by 49% from the period 2045-2064 to the period 2081-2100. The trend line also shows an increase in sediment yield throughout the period 2015-2100.

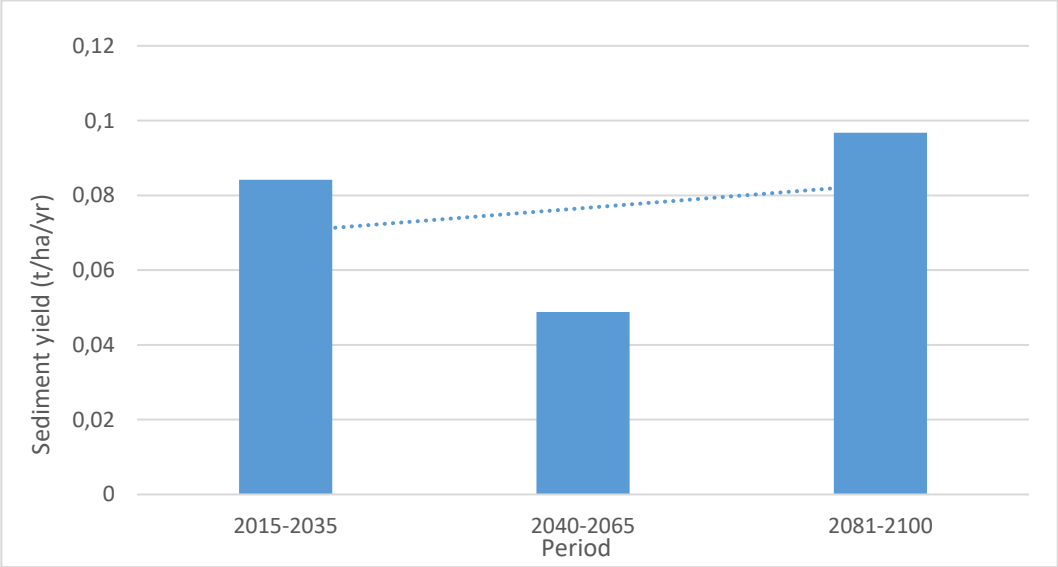

Figure 5.16: The average sediment yield from sheet and rill erosion in the upper Tsitsa Catchment, Eastern Cape, South Africa, for the three periods along with the current scenario modelled in SWAT.

Figure 5.17 shows the average erosivity calculated using the six models for each of the three modelled periods. Erosivity decreases from the first to the second period by 1% and then increases by 4% in the final period. The overall trend shows an increasing erosivity throughout the period 2015-2100, in line with the results shown in Figures 5.15 and 5.16.

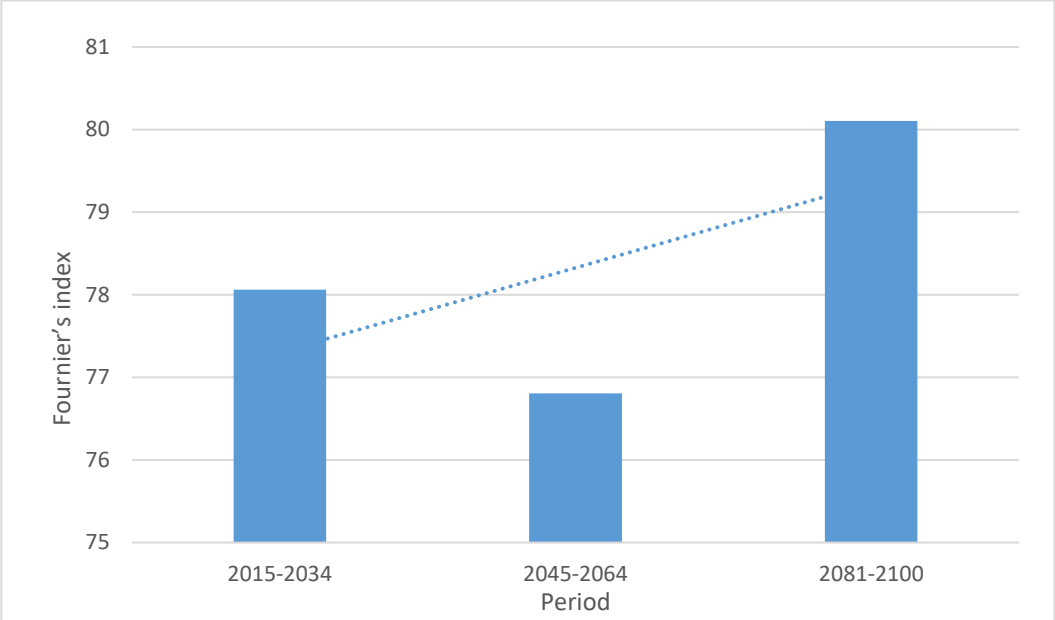

Figure 5.17: The average rainfall erosivity in the upper Tsitsa Catchment, Eastern Cape, South Africa for each period, calculated using Fournier's index for the six GCM models.

Figure 5.18 shows the sediment yield from sheet and rill erosion for each model for each of the three modelled periods 2015-2035, 2040-2065 and 2081-2100. For the 2015-2035 period, the UKMO model predicts much greater sediment yield than the other models. MIROC predicts the least sediment yield from sheet and rill erosion. Average sediment yield predicted by the models for the period was 0.084 t/ha/yr. There is a similar trend in the 2040-2065 period with UKMO predicting the greatest sediment yield from sheet and rill erosion and MIROC the least. Average sediment yield predicted by the models for the period was 0.05 t/ha/yr. CSIRO predicts the most sediment yield from sheet and rill erosion while the MIROC model still predicts the least sediment yield for the period 2081-2100. The average sediment yield for the period is 0.097 t/ha/yr.

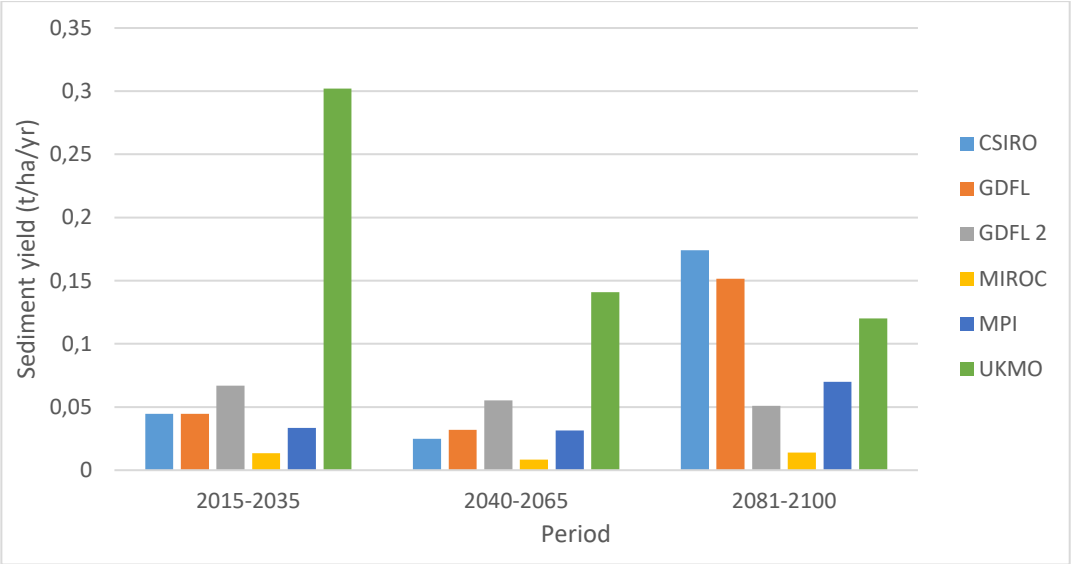

Figure 5.18: The average annual sediment yield from sheet and rill erosion in the upper Tsitsa Catchment, Eastern Cape, South Africa, modelled for each GCM in SWAT for the period 2015-2100.

Average of the six climate models monthly rainfall for each of the three time periods in shown in Figure 5.19. In January and December, the rainfall peaks with the minimum rainfall occurring in the winter months April –August. The graph shows a noticeable shift in rainfall with rainfall lessening from April in 2065-2100.

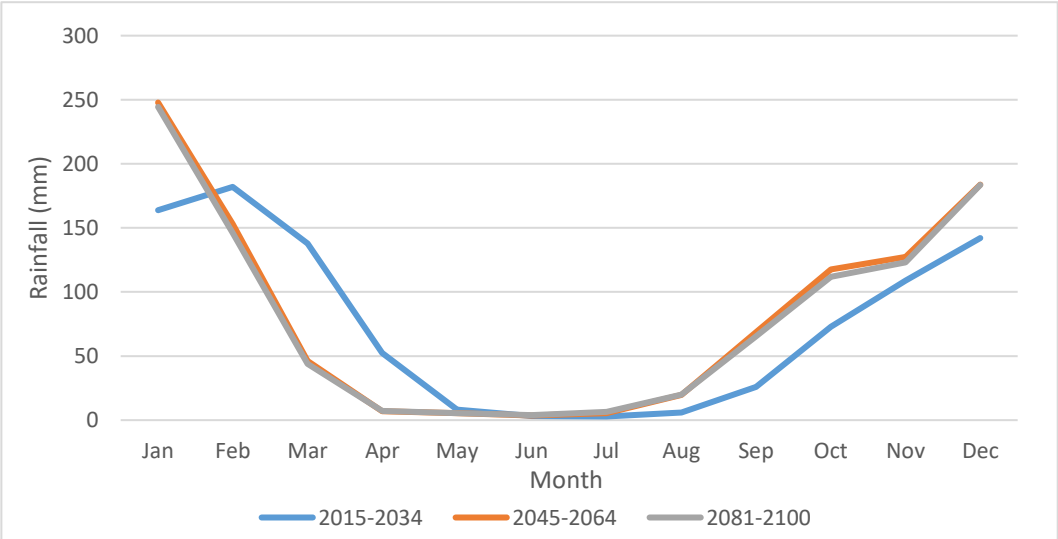

Figure 5.19: The average of the six GCM models' monthly rainfall in the upper Tsitsa Catchment, Eastern Cape, South Africa, for the periods 2015-2035 (blue) 2045-2064 (orange) 2081-2100 (grey).

Average sediment yield from sheet and rill erosion for each month for each of the three modelled periods is shown in Figure 5.20. The three periods depicted in the graph show similar trends with the majority of sediment yield generated in January-February with the least in the winter months May-August. Sediment yield from sheet and rill erosion in November-December decreases between the first two periods by approximately 50% but then increases in the final period 2081-2100.

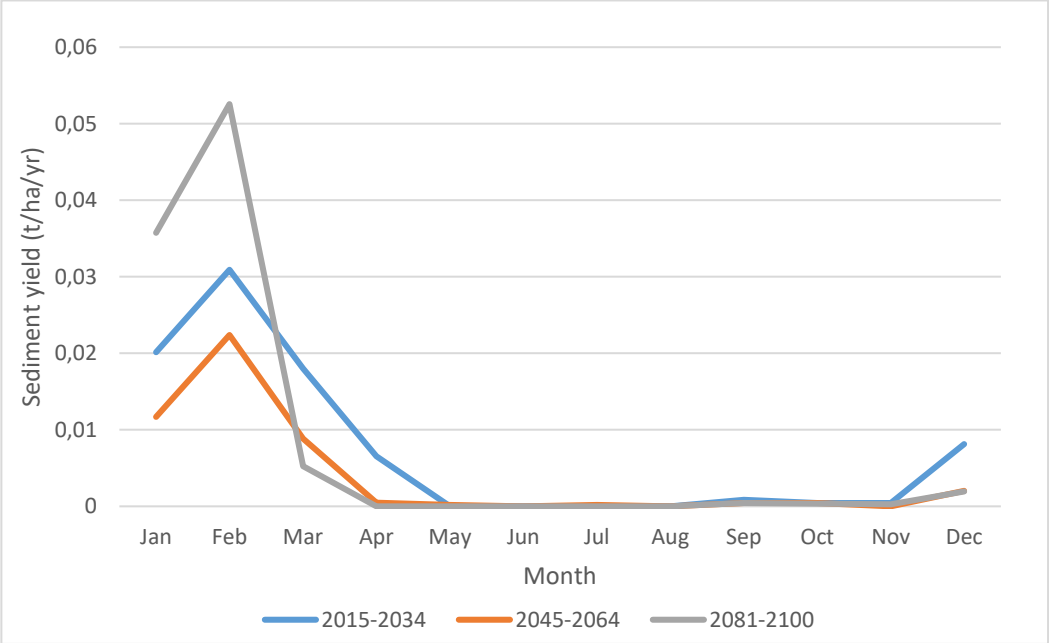

Figure 5.20: The average monthly sediment yield in the upper Tsitsa Catchment, Eastern Cape, South Africa, modelled in SWAT from the average of the six GCM models for the periods 2015-2035 (blue) 2045-2064 (orange) 2081-2100 (grey).

In the short term 2015-2034, the months with the most erosive rainfall are September to April. However, from the mid to long term this shifts earlier by a month so that the months with the most erosive rainfall becomes August to March (Figure 5.21). Erosivity also increases, in the short term peak erosivity is approximately 180, while from the medium to long term the erosivity increases to 250.

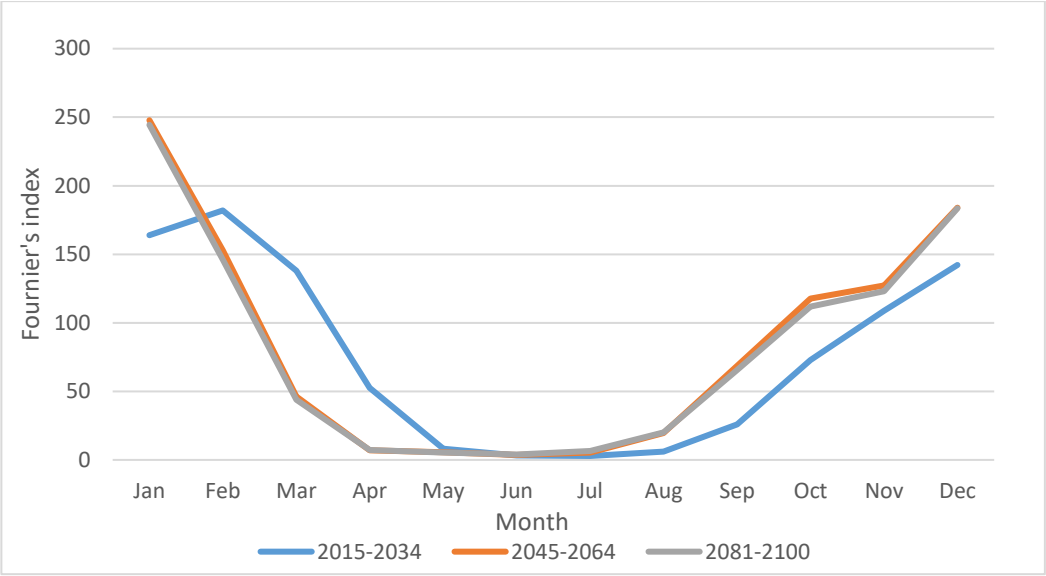

Figure 5.21: The average rainfall erosivity in the upper Tsitsa Catchment, Eastern Cape, South Africa, calculated using Fournier's Equation from the average of six GCM models for each month for the periods 2015-2035 (blue) 2045-2064 (orange) 2081-2100 (grey).

Figure 5.22 shows the average annual erosivity for each of the six climate models for each period. There is no distinct variation or outlier in any model for the period. There does appear to be an increase in erosivity towards 2100.

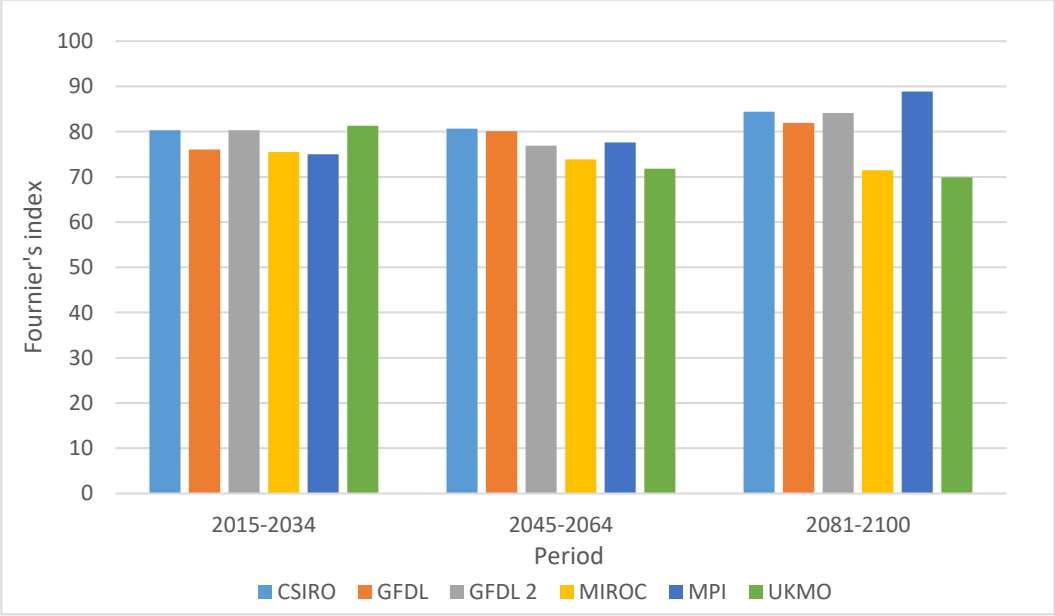

Figure 5.22: The average annual rainfall erosivity in the upper Tsitsa Catchment, Eastern Cape, South Africa, for each of the six GCM models for the periods 2015-2035, 2045-2064, 2081-2100.

5.4.2.1. Extreme Event Results

Figures 5.23- 5.26 show how the average number of extreme events are predicted to change over the period 2015-2100. Most noticeable change is the increase in the number of extreme events towards 2100 for the 10 mm and 15 mm events. The models also deviate considerably for 10 mm and 15 mm predictions.

Three of the six models show an increase of extreme events above 15 mm except for the CSIRO GFDL and UKMO models. For 10 mm events, five of the six models predict an increase in extreme events. UKMO is the only model which shows a slight decrease. Finally, for 5 mm events, all the models show a slight increase but so slight that it can almost be considered negligible changes.

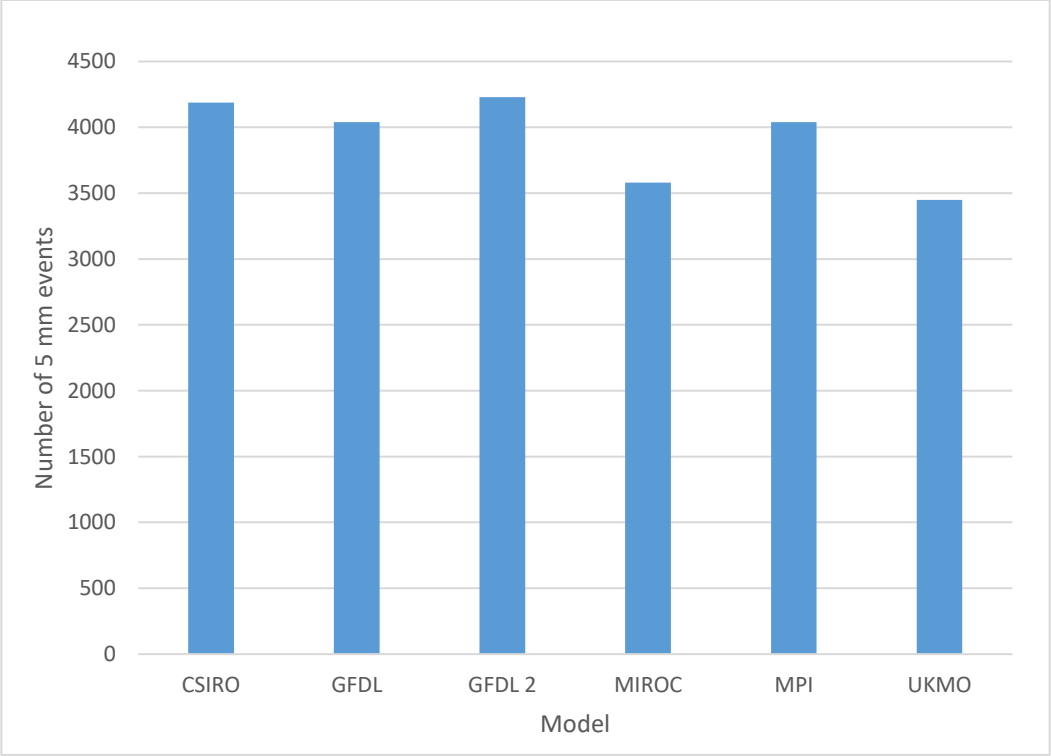

Figure 5.23: The number of projected rainfall events in the upper Tsitsa Catchment, Eastern Cape, South Africa, over 5 mm for each of the GCM models for the period 2015-2100.

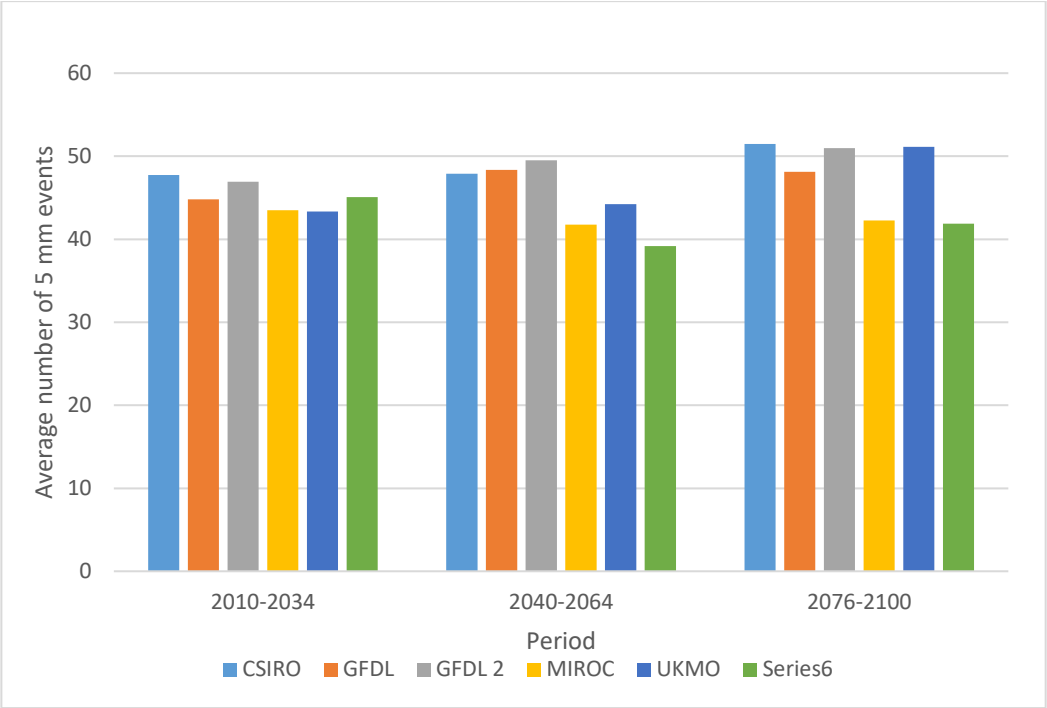

Figure 5.24: The number of 5 mm rainfall events in the upper Tsitsa Catchment, Eastern Cape, South Africa, for the periods 2015-2035, 2045-2064, 2081-2100 for the six GCM models.

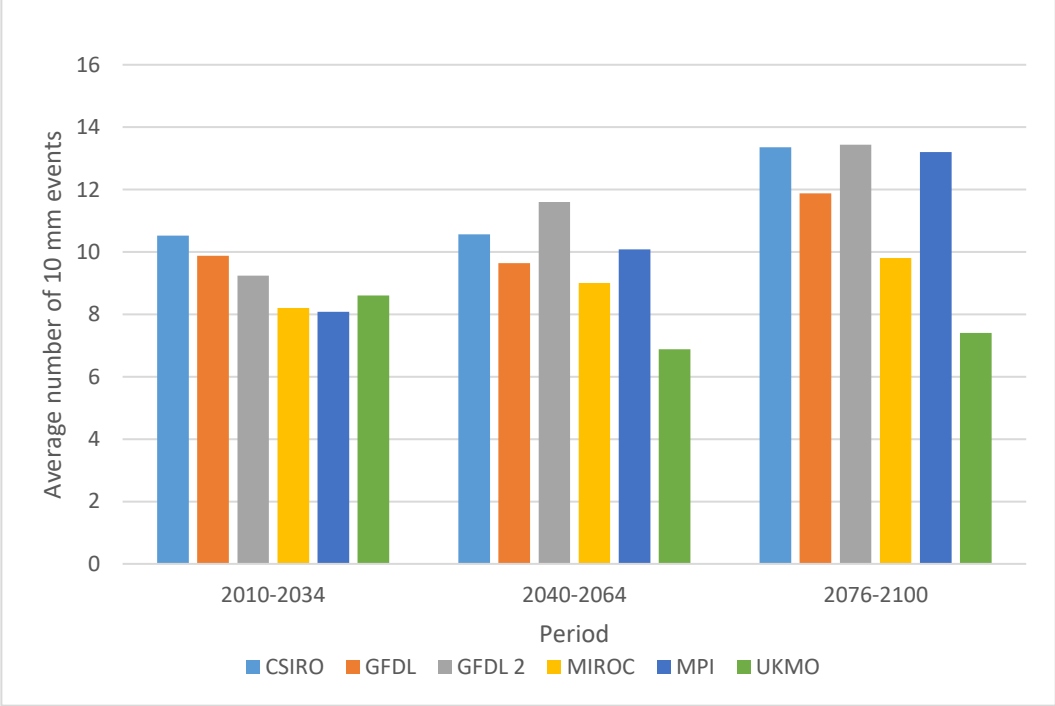

Figure 5.25: The number of 10 mm rainfall events in the upper Tsitsa Catchment, Eastern Cape, South Africa, for the periods 2015-2035, 2045-2064, 2081-2100 for the six GCM models.

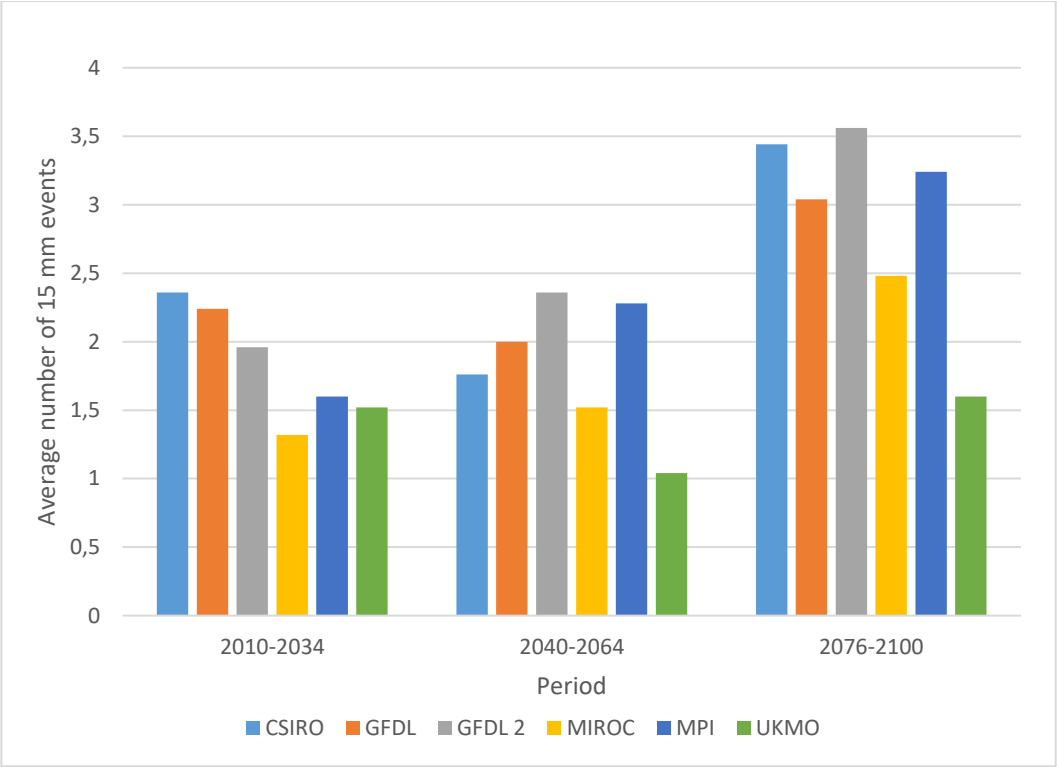

Figure 5.26: The number of 15 mm rainfall events in the upper Tsitsa Catchment, Eastern Cape, South Africa, for the periods 2015-2035, 2045-2064, 2081-2100, for the six GCM models.

5.4.2.2. Rainfall Results

Three of the graphs show an increase in average annual rainfall throughout the period CSIRO, GFDL, MPI whereas, GFDL2, MIROC, UKMO graphs show a decrease in the rainfall throughout the period. CSIRO predicts the highest rainfall over the period, whereas the MIROC model predicts the least rainfall over the period. The main observation in Figure 5.27 is that the average annual rainfall increases slightly between 2065 and 2100.

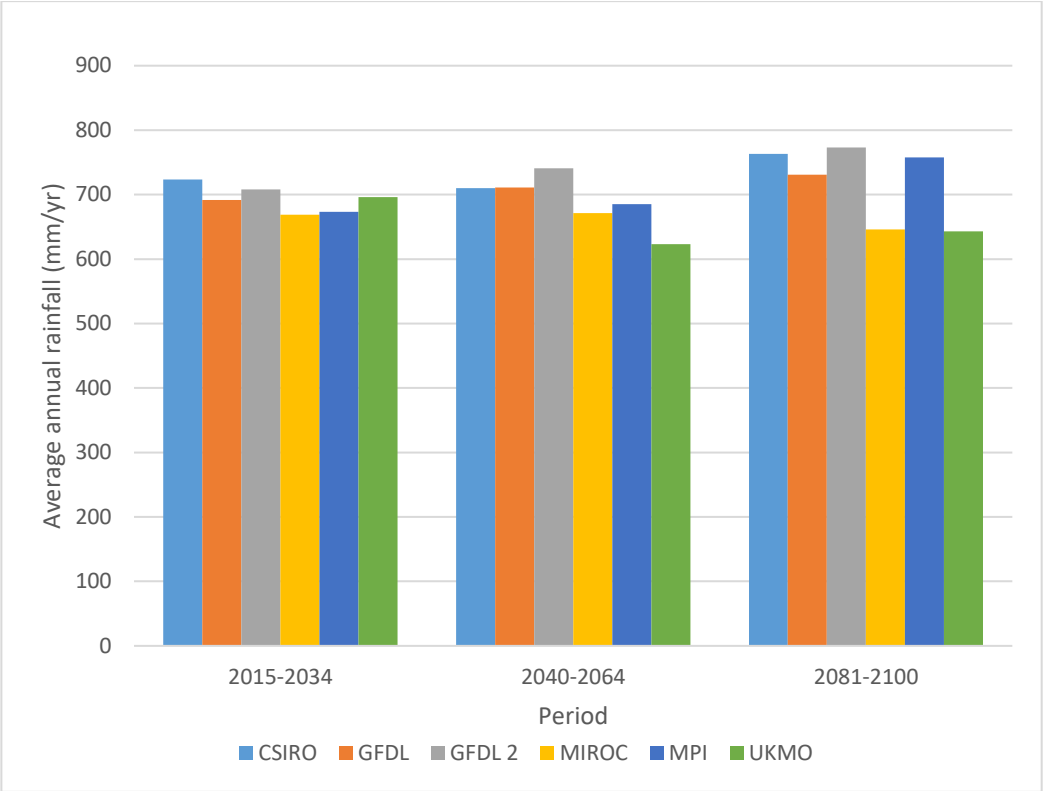

Figure 5.27: The average annual rainfall projections for the upper Tsitsa Catchment, Eastern Cape, South Africa, for the six GCM models from 2015-2100.

As the models show large variations in projected rainfall and associated variables. The range of average annual rainfall predicted by the six GCMs was calculated in order to determine best and worst case annual rainfall scenarios. It was found that maximum average annual rainfall may exceed 1000 mm while minimum annual rainfall could be below 400 mm (Figure 5.28).

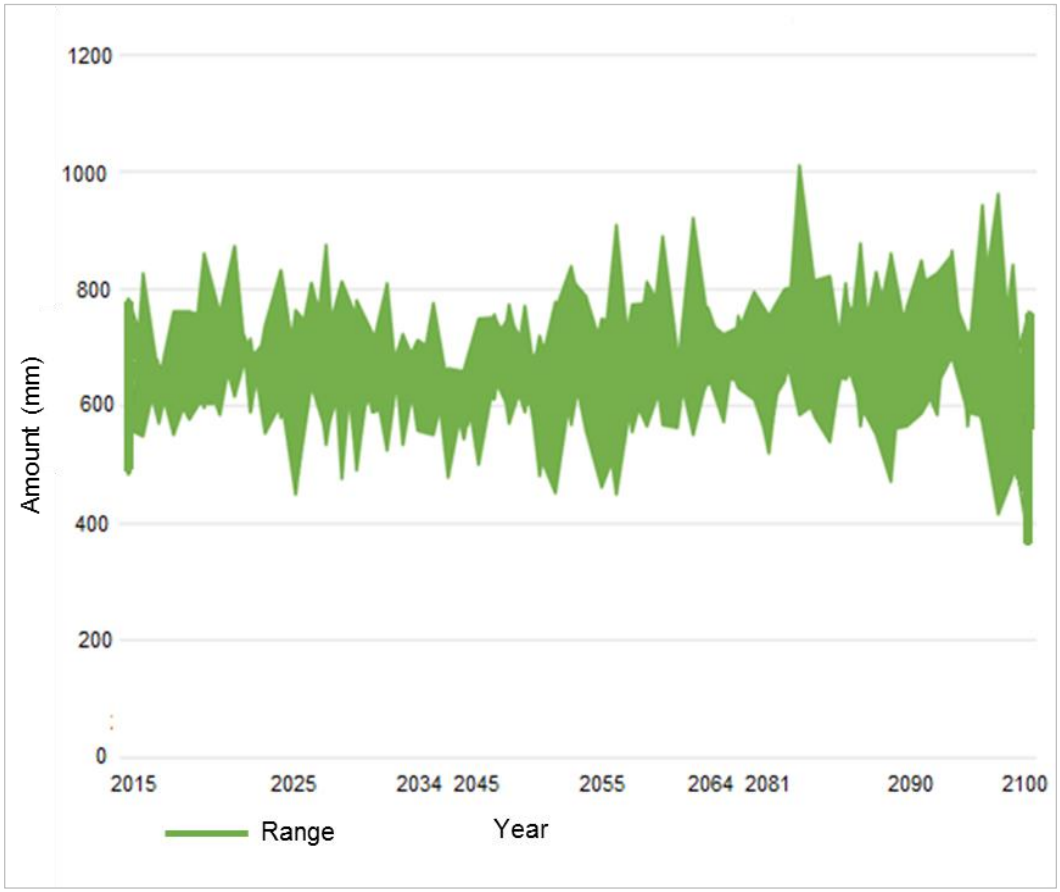

Figure 5.28: The range of average annual rainfall in the upper Tsitsa Catchment, Eastern Cape, South Africa, for the six GCM models over the period 2015-2100. The maximum amount is over 1000 mm while the minimum amount is less than 400 mm.

In order to determine which GCM model most closely represents reality, rainfall projections for the six GCMs for the current period, 2007-2012, along with the observed rainfall data were compared (Figure 5.29). No model predicted closely the current conditions, yet CSIRO, MPI and UKMO were the most similar to the observed data showing an increase in rainfall from 2007-2011. GLFD, GLFD 2 and MIROC did not resemble the observed data very well with GLFD showing the least resemblance to the observed data.

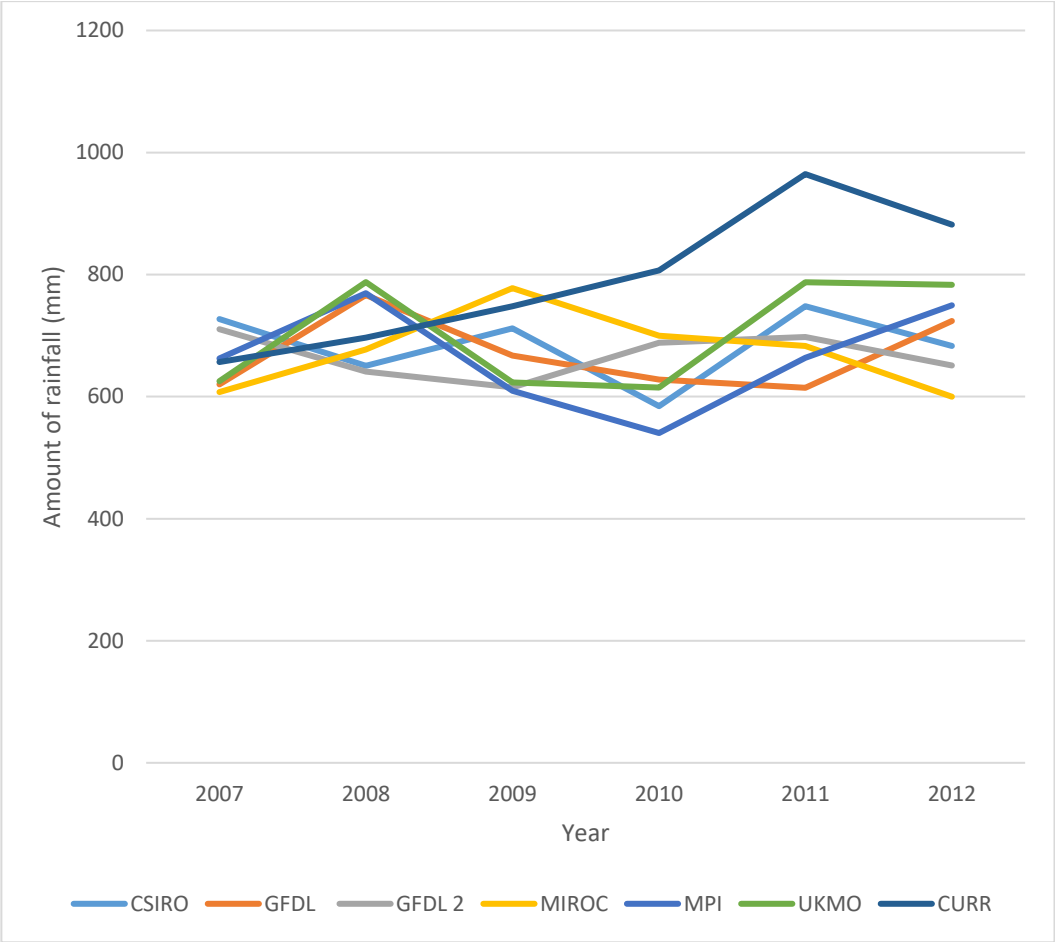

Figure 5.29: The average annual rainfall in the upper Tsitsa Catchment, Eastern Cape, South Africa, predicted by the six GCM models along with the observed measurements for the period 2007-2012.

5.5. Summary of results

Results showed that sediment yield from sheet and rill erosion in the upper Tsitsa Catchment between 2007 and 2012 was 0.91 t/ha with an average annual sediment yield is being 0.18 t/ha/yr or 3600 t/yr. Gully erosion resulted in between 7 t/ha/yr and 14 t/ha/yr of sediment in the same time period. This equates to between 140 000 t/yr and 280 000 t/yr of sediment been produced in the catchment. When using a delivery ratio of 50% for gully erosion the estimated sediment yield resulted in between 70 000 and 140 000 t/yr. Adding the sediment derived from sheet, rill and gully erosion results in between 73 600 t/yr and 143 600 t/yr of sediment been generated in the upper Tsitsa Catchment in the 5-year monitoring period.

Tillage operations increased the sediment yield from sheet and rill erosion for all the land uses tested by an average of 7% from the current no-till, land use scenario. Corn and generic agriculture showed the largest increase in sediment yield with tillage 0.19 t/ha/yr and 0.18 t/ha/yr respectively. Under no-till management cabbage will produce the most amount of sediment yield with 0.17 t/h/yr. Avocado orchards and sugarcane will cause the least amount of sediment yield with 0.14 t/ha/yr.

Projected climate change shows an 15% increase in sediment yield from 2015-2100. The increase is not uniform and there is a decrease in sediment yield and erosivity from the short term to medium term. Rainfall showed an increase in this period. From the medium term scenario to the long term scenario there is an increase in sediment yield and erosivity while rainfall decreased. Average number of 5 mm, 10 mm and 15 mm events are all projected to increase throughout the century.

The following chapter will discuss the results in more detail.

6. Discussion

6.1. Current scenario results

6.1.1. Results of SWAT

Results of the sediment yield from sheet and rill erosion for the period 2007-2012 show an average annual sediment yield of 0.18 t/ha/yr, which equates to 3600 t/yr generated in the upper Tsitsa catchment. Le Roux *et al.* (2015) calculated a total yield of 80 000 t/yr for the entire Mzimvubu catchment. These results correspond to that of Le Roux *et al.* (2015) who found an average of 0.1-0.18 t/ha/yr for the upper Tsitsa Catchment when modelling it as part of the larger Mzimvubu Catchment. Yesuf *et al.* (2015) found similar erosion rates of between 0.2 to 3.5 t/ha/yr from sheet and rill in their study of a 113 hecatre catchment in north-east Ethiopia. The study is similar as both catchments had a variety of land use mixed between agriculture and rangeland with rangeland been the dominant land use. Both catchments also had a mix of slope terrains.

It is noticeable that the current land use scenario for sheet and rill erosion, 2007 and 2008 had low sediment runoff while 2009 and 2011 had a very high sediment runoff. When considering the average annual rainfall for this period 2007 and 2008 had lower rainfall but not by a considerable amount when compared to 2009. There was a 20% higher average annual rainfall in 2011 than the other years in the study period, which is reflected in the sediment yield from sheet and rill erosion. It is possible to understand these trends when the number of extreme rainfall events is considered. 2011 saw a spike in extreme events especially in the number of 5 mm rainfall events whereas the number of 5 mm events dropped in the 2007/2008 period. The number of 10 mm events remained consistent during the first part of the period yet from 2009 onwards, increased quite noticeably. The number of 20 mm events remained even throughout the period 2007-2012 with a slight increase in the last few years from 2009.

When factors other than rainfall are held constant, soil losses due to water erosion are directly proportional to the level of rainfall erosivity (Yu & Rosewell, 1996). The strong relationship between rainfall events and erosivity is due to two main reasons. First, impact of raindrops on the soil surface during high-intensity storms events cause an increase in soil particle detachment.

Second, higher rainfall intensity events result in higher infiltration rates, excess runoff and a greater ability to transport suspended sediment load (Mohamadi & Kavian 2015). There is a long standing debate in geomorphology about whether extreme intensity yet low frequency rainfall events cause greater erosivity and sedimentation than frequent, moderate or low intensity rainfall events. Various studies have shown that sediment production in high-intensive, low frequency events is significantly greater than sediment yield produced from moderate–intensive yet more frequent events (Arnaez *et al.*, 2007; Mohamadi & Kavian 2015). In South Africa, Russow & Garland (2000) found that a single flood event in 1987 caused the siltation rates of the Hazelmere Dam to more than double the normal rate. Although low frequency, extreme events results in greater erosivity, the effects of moderate to low intensity frequent rainfall events cannot be overlooked as they do lead to large rates of soil erosion (Arnaez *et al.*, 2007). Mohamadi & Kavian, (2015) conducted a detailed study of storm characteristics on erosivity and found that the relationship between soil loss and rainfall intensities can be characterized by two types of functions: (1) in low rainfall intensity, high frequency events a linear function is fitted to soil loss-rainfall intensity, and (2) in high rainfall intensities, low frequency events non-linear functions are fitted to soil loss-rainfall intensity (Mohamadi & Kavian 2015). During the 2007-2012 period for this study no extreme, low frequency rainfall event was recorded. Thus, the term extreme event in used in this thesis relates to the events during which greater than average rainfall totals were recorded. These were defined in three grades of severity as 5mm, 10 mm and 15 mm events. Numerous low to moderate intensity (5 mm, 10 mm and 15 mm) and frequent rainfall events were recorded throughout the study period (405 of 1052 total rainfall events). As Mohamadi & Kavian (2015) found these events result in a linear response of soil erosion to rainfall intensity. Thus, these 405 recorded events would have resulted in greater soil loss in the catchment than the other events. Trends between Figure 5.1, 5.2, 5.3 agree with these studies and show that increased annual rainfall and increased number of extreme events in 2011 resulted in greater sediment yield rates than the other years of the study. When considering the results together the cause of sediment yield can be attributed to the extreme events and not just average annual rainfall.

These results correlate with the observations on the SPOT 5 images where the 2007 image looked drier with more bare soil exposed and the 2012 image showed more vegetation. The 2007 SPOT image was taken in February, which is during the summer rainfall season. However, it was a drier than average year and thus vegetation cover would have been less than average. The 2012 SPOT image was acquired in April, which is heading into the dry season, however, it was an El Nino year and March 2012 was a wetter than average month and the vegetation cover could have been good in April. This is further discussed in Section 6.1.2 with the use of NDVI.

It is clear that the majority of the sediment is generated in January and February with less in May and June slowly increasing then into October and December. This trend is reflected in the average monthly rainfall for the period with the exception of October and December. The increase in rainfall between October and December is not as pronounced in the sediment yield results, which shows that sediment yield has a slower response to rainfall initially.

6.1.2. Results of OBIA

Results of the basic accuracy assessment show a good overall accuracy, however, a poor user and producer's accuracy, which can be attributed to a number of reasons. As mentioned by Yale's Centre for Earth Observation (2003), the accuracy assessment relies on the accuracy of the reference data which in this case was the manually digitised gullies. Human error and bias are inherent in all tasks such as manually digitising, and as shown in Figure 5.10 of the results section, the data set used in this study had some errors. Another cause for the low user's and producer's accuracy can be due to the eCognition gullies having a more distinct border around the gullies whereas the manually digitised gullies were rougher and included vegetated areas. Figure 5.9 of the results section highlights this. eCognition itself did make errors (see Figure 5.11) and falsely classified some rock outcrops, sedimented areas of the river and tilled land, which was most likely the largest contribution to the low user and producer accuracies. The study aimed to create a ruleset which was transferable to the entire catchment and with some adjustments would be transferable to other images in order to conduct a time series analysis and even other catchments. It was, thus important that the ruleset was not

location dependent. It was difficult to separate rock outcrops from the gully classes as they have similar spectral properties. A similar problem was encountered with the tilled land. An up to date land cover map can help correct these errors. Rivers in the catchment of this study were badly silted during most parts of the year. Some parts of the river, especially around the river bends, contain so much sediment the MNDWI index was unable to identify these areas as water. As the speed of the water slows down along the inside of a bend it will not have enough energy to carry the suspended sediment load, which would then settle out creating areas of the river with high sediment deposition (Skinner *et al.*, 2004). eCognition falsely classified these areas as gullies. eCognition also classified some smaller channels with severe bank erosion as gullies. This highlights how it is difficult to distinguish between river channels and gullies particularly when the river channel has severe bank erosion. Sediment from these channels will, however, ultimately contribute to the sediment generated in the catchment and so it is not of great concern.

Large differences in the producer's accuracy between the two years can be explained when looking at the SPOT images and the dates they were acquired (Figure 6.1). In 2012 it appeared there was more vegetation cover than in 2007 which had more visible bare soil. This was most likely due to the changes in the weather between the two years. The 2007 SPOT image was taken in February, which is during the summer rainfall season. However, it was a drier than average year and thus vegetation cover would have been less than average. The 2012 SPOT 5 image was acquired in April, which is heading into the dry season, however, it was an El Nino year and March 2012 was a wetter than average month and the vegetation cover could have been more dense in April. In order to determine if the vegetation cover overall was less in 2012 NDVI for both images were calculated. ArcMap automatically calculates the average pixel value for each image. For 2012 the average NDVI pixel value was 0.16 while for 2007 it was 0.24. Higher NDVI values indicate greater vegetation cover, thus there was on average a greater vegetation cover in 2007 than 2012. This could result in more sheet erosion in 2012 or more vegetation on the gully sidewalls and base in 2007 leading to a lower accuracy in 2012. These factors most likely contributed to the large difference in the producer's accuracy between 2007 and 2012.

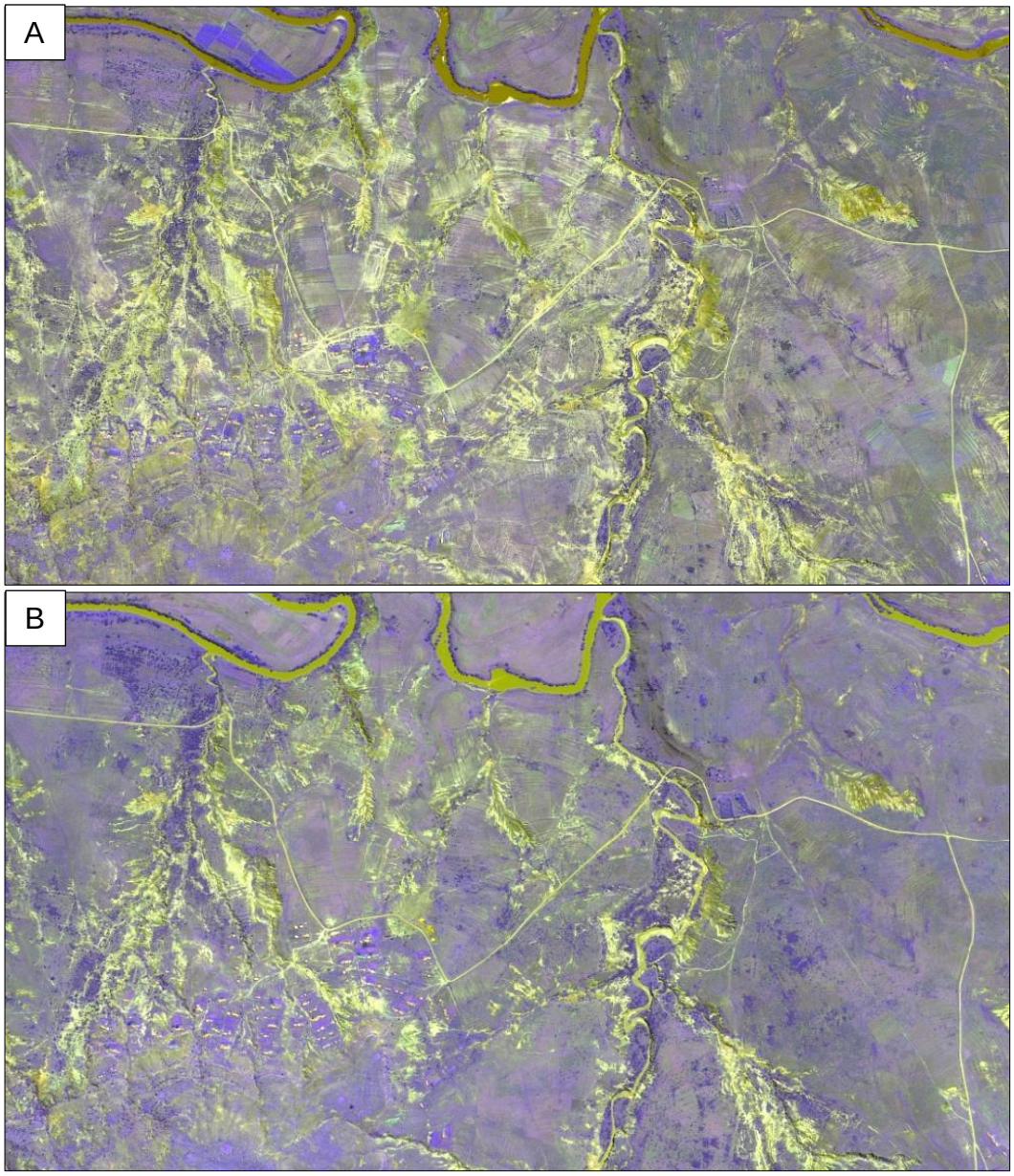

Figure 6.1: A section of the pan-sharpened SPOT images of the upper Tsitsa Catchment, Eastern Cape, South Africa, for 2007(A) and 2012(B). There appears to be more bare soil in the 2007 image.

Results of the Euclidean distance showed 52% of the gullies extracted in eCognition fell with a 40 m range of the gullies digitised manually. Although quite low, this is still a satisfactory accuracy as Murtaza and Romshoo (2014) cited an accuracy of 48% as satisfactory for their study. The reason for the low accuracy is due to the boundaries of the OBIA gullies "hugging" the boundaries more closely, the differences in the weather for each image and the method used to pan-sharpen the images. In both 2007 and 2012 eCognition

underestimated the number of gullies in the catchment when compared to the manually digitised gully map.

Results of the basic accuracy assessment compared with the results of the study conducted by d'Oleire-Oltmanns *et al.* (2014) which obtained 38% and 16% for the producer's and user's accuracy respectively. They concluded that the resolution of the image, as well as the diversity of the gullies over their study area, were the causes for the low user's and producer's accuracy overall yet they were satisfied with their results.

The object comparison accuracy assessment showed a 48% agreement when the OBIA extracted gullies were compared with the manually digitised gullies and 16% agreement when the equation was reversed. This can be attributed to various reasons, the borders of the manually digitised gullies did not hug the boundaries of the gully as closely as those created through OBIA this added a greater area around the gullies which increases the area available for successful overlap. Another cause could be due to the mis-classification of rock outcrops and tilled land by OBIA. The large variation in the results show that this accuracy assessment method must be used as a two-fold process: comparing the resulted map with the reference map and vice versa in order to get a better understanding of the accuracy and where the errors lie.

According to the results of the manually digitised gullies, erosion increased by 5.6 km^2 over the catchment in the 5-year period. OBIA found a 4 km^2 increase in gully erosion over the catchment. This indicates that OBIA underestimated gully erosion by 28%. It was further calculated that sediment yield from gully erosion was between 7 t/ha/yr and 14 t/ha/yr for the OBIA gullies. Le Roux *et al.* (2015) calculated the sediment yield from gully erosion to be 22.4 t/ha/yr in the upper Tsitsa Catchment, which is roughly 30% more than OBIA but when accounting for the under-estimation of gully surface area these results are similar. Overall increase in gully erosion was expected as gully erosion intensifies unless remediation actions are taken.

It is important to note that the actual erosion is greater than the sediment yield at the catchment outlet due to the deposition of sediment. Various SDRs have been used and suggested in literature as numerous studies have indicated that not all eroded sediments that leave the gully end up in the river (Ndoma *et al.*, 2009; Hughes & Prosser, 2012; Le Roux *et al.*, 2015). In a study

conducted by Ndomba *et al.* (2009) a SDR of 50% was used for sediment yield predictions from gully erosion in a basin in Tanzania. After estimating the gully erosion rates (13 600 t/yr), Ndomba *et al.* (2009) then applied a constant delivery ratio of 50% in order to obtain 6 800 t/yr as the sediment yield contribution from gully erosion at the catchment outlet. Le Roux *et al.* (2015) found the average SDR for the larger Mzimvubu River Catchment to be nearly 70%. SDR in the study ranged from 0% for disconnected gullies, to 40% for potentially connected gullies to 60% for partially connected gullies, to 100% for fully connected gullies. Le Roux *et al.* (2015) estimated that an overall SDR of 70% was most likely too high, however, the study modelled the sediment yield from gullies up until the sediment reaches a perennial river of which there are many in the catchment. From there not all sediment will settle in the dam as some may settle out along the channel bars, banks and islands. Therefore, Le Roux *et al.* (2015) theorised that the model gave more of a potential sediment yield estimate than an actual yield estimate.

In this study a delivery ratio of 50% was used following the study of Ndoma *et al.* (2009) and field observations that 50% of gullies were connected and 58% were continuous. With a delivery ratio of 50%, it was estimated that gully erosion contributes between 70 000- 140 000 t/yr to the sediment yield in the upper Tsitsa Catchment. Using a constant SDR of 50% did simplify the results and future studies should consider the use of variable SDR rates for gully erosion to better model reality. The resulting OBIA map created in this study can be further be used to classify gully systems and assign SDRs to gully classes.

Sediment yield from the sheet and rill erosion was calculated to be 3600 t/. This was added to the sediment yield contribution from gully erosion calculated using OBIA, which was found to be between 140 000 and 280 000 t/yr. After using a delivery ratio of 50% for gully erosion, it was found that between 73 600 t/yr and 143 600 t/yr or 3.68 t/ha/yr – 7.18 t/ha/yr of sediment was generated in the upper Tsitsa Catchment. According to Garde (2006), low sediment yield catchments are in the order of 0.01 t/ha/yr whereas high yielding catchments can be up to 100 t/ha/yr, however, these are mainly in the very large river catchments of Asia.

Most of the gullies are concentrated in the lower regions of the catchment with fewer gullies occurring on higher and steeper slopes and none on the steep slopes of the Drakensberg basalt. These results reflect those found by Le Roux & Sumner (2012) who also conducted a study on gullies in the larger T35 catchment, which the upper Tsitsa Catchment forms part of. Kakembo *et al.* (2009) also observed that gullies in the Eastern Cape Province occur predominantly on more gentle slopes. The study concluded that the critical drainage area on more gentle slopes is higher thus leading to gully initiation. Poesen *et al.* (2003) hypothesised that fewer gullies occur on steeper slopes because the critical drainage area needed for gully initiation decreases as the slope steepens. Tamene *et al.* (2006) in a study conducted in Ethiopia also found that gully erosion is less prevalent on steeper slopes. They hypothesised that the reason for the observation was due to steep areas being less accessible and thus less exposed to human and livestock influences. Furthermore, human disturbance was hypothesised to have led to gully formation in the Sneeuberg area of the Great Karoo (Boardman *et al.*, 2003). Boardman *et al.* (2003) suggested that depth to bedrock and thus soil thickness played a major role in limiting gullies. As it was found that major gully systems frequently erode through the soil to the bedrock. In the case of the hillslopes the incision was limited to 1 to 2 m whereas in the case of valley-bottom gullies, the gully incision was limited to 8 m (Boardman *et al.*, 2003). All the aforementioned hypotheses are plausible in the upper Tsitsa Catchment.

It is important to note that perspectives on sediment yield contribution from gully erosion have typically been obtained from field scale ($<10^{-1}$ km^2) and are confined to local conditions (Grellier *et al.*, 2012; Manjoro *et al.*, 2012; Slimane *et al.*, 2015). Few studies model the sediment yield contribution from gully erosion at a regional scale.

6.2. Limitations of the study

6.2.1. SWAT Limitations

The SWAT model was chosen for this study as it has been tested in many studies in South Africa and across the world in catchments of various sizes and land uses and found to be suitable at modelling sediment yield (Le Roux, 2009). SWAT is also easily available and can be used in a GIS interface. Furthermore, Le Roux *et al.* (2015) successfully used the SWAT model in the larger Mzimvubu Catchment.

However, it has been noted that the SWAT model may overestimate soil losses particularly in a catchment in the Eastern Cape (Laker, 2004). SWAT is based on the MUSLE equation which may overestimate soil loss in some South African catchments (Jackson *et al.*, 1986; Laker, 2004). Laker (2004) explains that this is due to the model using slope as the dominant factor, whereas in South Africa, other factors such as inherent erodibility of the soil and parent material may be more dominant. De Vente *et al.* (2013) also stated that the SWAT model only represents a portion of erosion and transport processes which occur in a catchment. Thus the model produces the most reliable results when the considered processes are in actual fact dominant factors. SWAT also fails to model the behavior of duplex soils correctly, where the unstable subsoil becomes a major factor, in soil erosion. In the upper Tsitsa Catchment, the underlying geology of the Elliot formation gives rise to unstable duplex soils, which SWAT could not model correctly and thus most likely underestimated erosion rates from these soils.

It was shown by Haarhoff *et al.* (1994) that the RUSLE model which, like the MUSLE model, is based on the USLE model was able to adequately predict soil erosion in soils derived from Drakensberg basalts due to the slope factor been dominant (Laker, 2004). Finally, the SWAT model 'breaks down' in areas where gully erosion is prevalent as it only estimates sheet and rill erosion. RUSLE has proven to be more effective in modelling soil loss in South African catchments (Laker, 2004). However, the results from studies conducted in the Mkabela catchment, Kwa-Zulu Natal, showed that SWAT was able to predict with good accuracy most of the peak flow events that occurred during the study year, it did over-predict the peak flow rates and under-predicted low flow

periods. For the sediment prediction in the Mkabela catchment SWAT overestimated small measured values and underestimated large measured values (Le Roux *et al.*, 2013). Soil erosion models tend to over-predict sediment delivery for small measured values, and under-predict sediment delivery for larger measured values. (Le Roux *et al.*, 2013). RUSLE differs from the MUSLE model because the rainfall energy factor in the RUSLE was replaced with a runoff energy factor for the MUSLE equation. MUSLE also considers the runoff volume and peak run of rate (Jackson *et al.*, 1986).

SWAT is still considered one of the most appropriate models for predicting the long-term impacts of land use on sediment yield in large complex watersheds with varying soils, land use, and management conditions (Ullrich & Volk, 2009; Mottes *et al.*, 2014).

6.2.2. OBIA Limitations

An interesting predicament arises through this study and other similar studies. Shruthi *et al.* (2012) and d'Oleire-Oltmanns *et al.* (2014) were able to extract gullies with good accuracy on a small scale which was not tested on the larger catchment. However, it always proves problematic to upscale the process to larger catchments. This is where the main errors arise. In larger catchments, there are more variables which could create noise such as housing, road lines, rock outcrops, deforested areas. Slope angle and incident solar radiation also change throughout a catchment changing the brightness values or shadows of the gullies. Attempting to write a workflow which can identify gullies at such a large scale will not be a simple procedure. Yet, this is where the power of OBIA is truly beneficial. OBIA was designed in order to reduce the processing time of the human interpreter. Manually mapping of gullies over large areas is extremely time consuming and the intention of OBIA is to reduce this task by creating rulesets applicable to large catchments and even images from earlier time periods in order to conduct change detection analysis. The problem is where OBIA has greatest accuracy is on small catchment scales where the time needed to manually digitise the gullies will be minimal. Where OBIA is really needed, to process large areas, the accuracy is greatly reduced. This highlights the need for better classification techniques or data. Such can be higher resolution bands covering a wider range of wavelengths or the use of

technologies mapping 3D features such as LiDAR technology, which will help bring in more aspects or properties of the classification feature in order for them to be more accurately defined. Using of texture in classification greatly helped with OBIA as features with similar colour or shape could be distinguished based on texture, which in this study allowed for the separation of tilled land from gullies.

A limitation of the ruleset developed in this study which needs to be considered is its failure to classify gullies. The ruleset was created in order to identify and map the gullies but it did not go as far as to classify whether the identified gullies were connected, disconnected, partially or potentially connected. This was outside the scope of the study and would have required more time and experimental work to incorporate into the ruleset. The study accounted for the lack of classification by applying a constant sediment delivery ratio. The ruleset also removed densely vegetated gullies in the first step by using NDVI to remove all vegetation. While this did streamline the classification process it may lead to inaccurate results as it has been noted that certain densely vegetated gullies may become active during extreme rainfall events.

In some areas of the catchment, manual digitising produced similar errors to that of eCognition, for example where digitisers were unable to distinguish certain rock outcrops from gullies. It was also noted that the operators digitised gullies which were densely vegetated. eCognition was unable to distinguish these from normal grasslands. However, this is not necessarily a problem since highly vegetated gullies are considered inactive or contribute negligible sediment to the catchment outlet as vegetation cover inhibits the dislodging and movement of sediment through the catchment (Casanovas & Zaragova, 1996).

The availability of a manually digitised gully map allowed for an accuracy assessment using not only GCP's but also the gully location map, which allowed for some degree of comparison between techniques. Using various accuracy assessment methods including those taking into account the spatial correctness of the digitised gullies also allowed for a comparison of accuracy assessment methods, which could help in decision making on types of assessments to be done in further studies of this type. The Euclidean distance accuracy assessment accounted for errors of pan-sharpening and shift and

showed a 52% accuracy. It showed an increased accuracy from that of the basic accuracy assessment's user's and producer's accuracy which averaged 32%. It also gave an indication of the spatial error in the data set as 52% of the OBIA gullies fell within a 40 m radius of a manually digitised gully. The other accuracy assessments do not give an indication of spatial accuracy. The total area of overlap assessment gave an indication of the types of errors encountered in the OBIA results. The main causes of error in the OBIA maps were the underestimation of gullies in the catchment. This was caused by errors in the manual interpretation to which the OBIA map was compared and the failure of OBIA to identify densely vegetated gullies.

Casanovas and Zaragova (1996) concluded that vegetated gullies are inactive and thus do not contribute to the sediment yield in the catchment. eCognition did not identify vegetated gullies, due to their elimination using NDVI, however, the manual interpreter did identify them which may cause an over-estimation in gully derived sediment yield. eCognition also struggled to identify smaller disconnected gullies and was better able to identify larger gully networks, which may not be such a serious problem if the gully class system used by Le Roux *et al.* (2015) is applied to the classified gullies. Le Roux *et al.* (2015) stated that small discontinuous gullies contribute negligible amounts of sediment to the catchment outlet because they are not directly connected to the river network system. Sediment produced from them will undergo more complex processes of deposition and entrapment before reaching the river. It was highlighted by Le Roux *et al.* (2015) that the most important gullies in terms of sediment output were active gullies connected to the perennial river system. Thus the results of the eCognition classification may be more accurate in terms of gully activity and which gullies are contributing to the overall sediment output.

6.3. Improvements

6.3.1. Improvements to the SWAT model

SWAT has proven to overestimate soil erosion from sheet and rill in South African catchments by up to 1000% (Laker, 2004). Thus using a different model, one which has been developed for South Africa such as SLEMSA or the ACRU model may give more accurate results.

When modelling the tillage operations in the upper Tsitsa Catchment it was assumed that either all agricultural areas were under tillage or none were under tillage. In reality, various farmers use different methods and if tilling they use different operations on different farms or crops so by assuming a constant tillage operation across the catchment the exact influence of tillage on the sediment yield from sheet and rill erosion is exaggerated. However, the modelling that was used gives a relative idea of how tillage operations affect the sediment yield from sheet and rill erosion in the catchment and can facilitate decision makers as whether to allow tilling in the catchment once the dam has been built.

When modelling the effects of climate change on the soil erosion the study did not account for how climate change will affect land use or management strategies. It simply calculated the relative change in sediment yield from sheet and rill erosion from purely climate scenarios. It has been proven that land use and management practices have the most drastic effect on soil erosion and sediment yield from sheet and rill erosion (Mullan *et al.,* 2012). Future studies should model how land use and management may change and what the influences of these changes will be on the sediment generated in the catchment.

The Satellite Radar Topography Mission (SRTM) DEM with a resolution of 30 m was used as the topography input in SWAT. Stellenbosch University has developed a DEM specific for South Africa with a 5 m resolution (Stellenbosch University, 2013). This finer resolution DEM may allow for better portioning of the catchment in HRU's and thus more accurate sediment yield models.

The upper Tsitsa catchment is a rural catchment and although there have been other studies conducted in the catchment the data area still limited. Weather data, for example, are generated from one station. Weather in the catchment varies greatly from the high escarpment to the lower plains at the catchment

outlet (Agrometeorology Staff, 1984-2008). Thus more weather stations throughout the catchment can give a better model of the amount, intensity and frequency of rainfall and how it varies spatially as this is a dominating factor in soil erosion, erosivity and erosion spatial variability (Nel & Sumner, 2007).

Soil data are also limited and there are no values on the bulk density of the soils in the catchment thus it was assumed that the soils had a uniform bulk density of 1.6. Limited field samples showed an average bulk density of 1.4 which is slightly lower than that used in the model. This generalisation is a downfall of the SWAT model set up for this study as bulk density is an important factor when calculation the sediment yield. SWAT is also very sensitive to the accuracy of soil and land use input data and better data will result in more accurate results (Romanowicz *et al.*, 2005) Bulk density is also extremely variable not just across soil types but also land use and management types. SWAT uses bulk density to determine the mass of sediment that will be eroded (Nietsch *et al.*, 2011), using a single bulk density value for the catchment will thus affect the results as it, is not a proper representation of reality (Alletto & Coquet, 2009).

6.3.2. Improvements for OBIA

SPOT 5 images have a medium spatial resolution, which allows for the classification of gullies down to 2.5 m which was extremely useful. However, the SPOT 5 image is restricted to four bands. This limited the band combinations which could be made. Indices exist for the classification of features such as vegetation, water and bare soil. Although SPOT 5 has the bands required for water and vegetation indices it lacks a blue band which is required by the bare soil index (BI) (Equation 6.1). Another soil index called the Normalized Difference Soil Index (NDSI) created for Landsat is shown in Equation 6.2. QuickBird satellite imagery will ultimately be the best images to use to extract gullies using OBIA as QuickBird has a panchromatic resolution of 61 cm and a multispectral resolution of 2.4 m for the blue, green, red, NIR and SWIR bands (Satellite Imaging Corporation, 2014). Thus a bare soil index could be created from QuickBird images, which may facilitate the classification of gullies. It may help in distinguishing between rock outcrops and bare soil. The NDSI is, unfortunately, unique to Landsat Thematic Mapper

Equation 6.1. $$BI = \frac{(SWIR+RED)-(NIR+BLUE)}{(SWIR+RED)+(NIR+BLUE)}$$

Equation 6.2. $$NDSI = \frac{Band\ 5 - Band\ 4}{Band\ 5 + Band\ 4}$$

Landsat was not considered as feasible to extract gullies as the data has a resolution of 30 m, which is relatively poor when compared with that of SPOT 5. It should be noted that there has been some success of identifying road networks using Landsat data. This is significant as roads are longer than 30 m but not usually wider than 30 m (Boggess, 1993), which means it may be possible to extract larger gully networks using Landsat data. NDVI and MNDWI indices gave immense value to the classification particularly NDVI. This allows for this method to be repeated on other satellite images such as Geo-eye, Ikonos or SPOT 6 and 7 with much higher resolution than SPOT 5, which may give results that are more accurate.

LiDAR techniques have been used quite extensively and with good accuracy in numerous studies (Chen *et al.*, 2009; Eustace *et al.*, 2009; Johansen *et al.*, 2010; Höfle *et al.*, 2013). LiDAR uses light in the form of a pulsed laser to measure variable distances to the Earth. These light pulses, combined with other data recorded by the airborne system, generate precise, three-dimensional information about the shape of the Earth and its surface characteristics (National Ocean and Atmospheric Administration, 2015). LiDAR is able to measure gully depths and volumes this will be useful in a study such as this one when trying to determine sediment volume from gullies in a catchment. As gullies are usually defined by their depth, LiDAR data will greatly facilitate in the distinction between gullies and other forms of erosion such as sheet and rill. It may also help facilitate the separation of roads from gullies, as roads are a surface feature as well as rocks from gullies as rocks are more convex structures whiles gullies display concavity.

The assumption that gullies will erode down to bedrock before expanding laterally was used to calculate gully volumes and the resultant sediment yield. It is noted that this assumption disregards other gully forming mechanisms

such as piping this is shortcoming of the sediment yield calculations. Possible methods to improve this assumption would be to use 3D data such as LiDAR to determine actual gully depths and volumes in the catchment.

6.4. Results of the future scenario models

6.4.1. Land use impacts on soil erosion

DAFF has identified several crops which can be cultivated in the upper Tsitsa Catchment. Tillage operations may also be introduced in the future. When studying the effects of land use change or land use management change the effects of tillage operations are noticeable. Tillage resulted in more sediment yield from sheet and rill erosion for all land uses. Increases ranged from 3% per annum for sweet potato to 19% per annum for the generic agriculture land use. While the land use with the least effects on sediment yield from sheet and rill erosion is sugarcane and avocado orchards. Tilled corn and generic agriculture fields produced the highest sediment yields rates.

Tillage operations redistribute plant residue, nutrients, pesticides and bacteria through the soil profile. They make the soils more prone to erosion due to the destruction of the soil structure and the removal of organic matter, which helps consolidate the soil and give it structure (Nietsch *et al.*, 2005). No-till agriculture limits the amount of soil disturbance to only necessary activities such as the application of nutrients, the conditioning of crop residue and planting crops. By not tilling the fields there is an improvement in soil organic matter content, which contributes to enhanced soil structure and resilience to erosion. It also reduces the CO_2 and particulate losses in the soil. No-till activities have proven to reduce sheet and rill erosion from water as well as wind erosion (Waidler *et al.*, 2011).

Le Roux (2005) also determined that soil erosion under sugarcane crops is less than under other vegetables such as cabbage. Reasons for the observation was that soils under sugarcane are not disturbed during harvest and the root system is left intact, which helps bind the soil making it less prone to disaggregation. Sugarcane crops are not tilled regularly this results in less erosion as the soil is undisturbed and plant residues are left intact, which also

helps in binding the soil. The second factor was that sugarcane grows faster and within two months of planting it provides a dense plant cover, which protects the soil from rain splash erosion (Le Roux, 2005).

Cabbage has the worst effect on sediment generation from sheet and rill erosion in the catchment under current conditions of no-till. This is because cabbage plants are small and do not provide good canopy cover to protect the soil from soil erosion. Also when harvesting cabbages, the entire plant is removed for the next growing season, which does not allow for the root system to provide adequate support in the soil. Corn crops also lead to increased soil erosion compared to some other crops because the corn crop takes long once planted to grow to an adequate size to protect the soil from erosion (Mullan *et al.*, 2012). Other causes of increased rates of soil erosion from corn crops can be attributed to dripping water from the tips of corn leaves, which often results in concentrated flow paths. Post-harvest over winter leaves the soil bare and exposed to the first rains of spring. Finally, corn crops provide less than 80% surface cover even at maturity, exposing the soil to rain splash (Cooke & Mancini, 2015). Corn cultivation in the upper Tsitsa Catchment can lead to adverse soil erosion rates and will thus need adequate planning and erosion control measures.

Avocado orchards also showed less sediment runoff from sheet and rill erosion than other crops such as sweet potato and cabbage. This can be attributed to three factors. First, the good plant cover supplied by the tree leaves. Second, the good surface cover provided by plant residue. Finally, orchards do not need tilling and the plants remained undisturbed for many years which allows the soils to become stable. However, it is important to note that tree canopy cover does not always protect soils from erosion and there is a certain critical height (> 3 m) after which the rain droplets falling will have a higher velocity than non-intercepted rain droplets (Wieschmeier & Smith, 1978). SWAT does not account for this and assumes tree canopy will provide good soil protection.

It was expected that tillage operations would negatively affect the sediment generation from sheet and rill erosion. For all the crops tested the sediment yield increased when tillage operations were implemented, this was similar to the results found by Ullrich and Volk (2009). Tillage operations disturb the soil and often break down the soil structure, which leaves it susceptible to erosion.

According to Ullrich and Volk (2009) the reduction of soil tillage intensity positively affects other soil properties, such as aggregate stability, macro-porosity and saturated hydraulic conductivity; and consequently increases infiltration rates, which reduce surface runoff, nutrient loss and soil erosion. It is important to take till operations and their effects into consideration as some crops respond differently to tillage, for example, corn and generic agriculture showed a much larger increase in sediment runoff with the introduction of tillage whereas the effects of tillage on sweet potato and cabbage were less pronounced. It is, however, clear that conventional tillage practices need to be replaced by less intensive tillage practices in order to minimize soil erosion and sediment yield (Ullrich & Volk, 2009).

Possible land use change in the upper Tsitsa catchment with regards to the selected crops under no-till will not have a particularly negative effect on sediment yield from sheet and rill erosion. The most influential effect on sediment yield from sheet and rill erosion would be to convert the current land use to tilled generic agriculture or corn, which will result in an increased sediment yield of up to 26.7%. If no-till management practices are exercised, then the most significant increase in sediment yield will come from planting cabbage, which will cause a 6.7% increase annually. Converting the agriculture in the catchment to sugarcane or orchards will have a positive effect on sediment yield decreasing the annual amount by 6.7%.

Alternative land management practices such as conservation or no-till, contour farming, terraces, and buffer strips are increasingly used to reduce nonpoint source and water pollution resulting from agricultural activities. Models are useful tools to investigate effects of such management practice alternatives on the watershed level. In Germany, the implementation of alternative tillage systems is increasingly supported by agro-environmental programs. In the German State of Saxony, for instance, conservation tillage and mulch seeding on arable land have increased from <1% to about 27% during 1994–2004 with support from the Saxonian Program for Environmental Agriculture (Ullrich & Volk, 2009). The ARC-ISCW is running numerous projects in the Tsitsa Catchment focusing on the use of conservation agriculture.

6.4.2. Climate impacts on soil erosion

The average of the six climate models showed similar trends, with sediment yield and erosivity decreasing in the medium term and then increasing from the mid to long term. Rainfall showed an increase in the medium term with a decrease going into the long term. The number of 10 mm and 15 mm events predicted by the models were shown to increase throughout the century, the erosivity also increases. Higher sediment yield rates towards 2100 can be explained that although less rainfall is predicted, the intensity of the events will increase causing more runoff. This finding is supported by Engelbrecht *et al.* (2011) who found that rainfall intensities will increase with predicted climate change. Engelbrecht *et al.* (2012) found that closed-low weather systems which are responsible for much of South Africa's rainfall are predicted to decrease with projected climate change. This will bring about a decline in average annual rainfall over much of South Africa. A decrease in closed-low systems can also bring about a reduction in extreme rainfall events. However, regardless of the general decrease in projected closed-low systems, the associated extreme events are in general projected to increase over large parts of southern Africa. An increase in intense convective rainfall events as well as more frequent formations of tropical-temperate cloud bands over southern Africa was cited as the main causes of increased extreme rainfall events going into 2100 (Engelbrecht *et al.*, 2009; Engelbrecht *et al.*, 2012).

Not one scenario fits all, the various models showed different changes in sediment yield from sheet and rill erosion through the century. Most noteworthy is the prediction made by the UKMO model, which shows a large drop in sediment yield between the middle and end of the century. These results, however, are similar to the average annual rainfall for the UKMO model for that period. When looking at the number of extreme events the UKMO model showed a marked decrease in 5 mm rainfall events during up until 2065 when it increases again slightly. The decrease in rainfall events could be the main reason for the sudden decrease in sediment yield with a slight increase towards 2100. SWAT does not simulate single events so it is hard to incorporate these processes, particularly since the catchment is characterised by thunderstorms where a large amount rain falls in a short period of time.

Variations between the different GCMs was expected since climate models are not perfect and the theoretical understanding of climate processes are still incomplete (Reichler & Kim, 2008). The objective of this study was to determine the impacts of climate change on soil erosion in the upper Tsitsa Catchment and assessing the variations between the six GCMs was outside the scope of the study. Often when developing climate models assumptions are made and it is up to the institute constructing them to decide which climate parametres have greater weightings. The assumptions introduce biases into the simulations, which are often difficult to correct (Reichler & Kim, 2008). Causes of variation between models are due to three broad uncertainties namely model uncertainty, prediction uncertainty and scenario uncertainty. Model internal variability, which show a large range in this quantity, is another major cause of discrepancy between the various GCMs. Hawkins *et al.* (2009) found that internal variability and model uncertainty is the dominant contribution to variability for predictions of a few decades (not more than 40 years) such as in the case of the 2015-2035 projections used in this study. The internal variability becomes increasingly important at shorter time and spatial scales, however, for decadal time scales and regional spatial scales, model uncertainty becomes of greater importance than internal variability. For predictions of more than 40 years in advance, such as in the medium and long term projections of this study, model uncertainty is the dominant contribution and can account for up to 70% of the total variance. Finally, for predictions, of 90 years and more ahead, scenario uncertainty becomes the dominant factor (Hawkins *et al.,* 2009).

Crosbie *et al.* (2011) stated that it is important to use multiple GCMs in a study involving the effects of climate change. The use of multiple models helps account for the large potential uncertainties in future estimates of soil erosion and sediment yield. This study used six GCMs which gave a major advantage over the use of a single GCM in terms of being able to quantify the uncertainty in soil erosion projections under a future climate. The six different models produced a range of estimates which can better facilitate policy and management strategies. Variations between the six GCMs highlight the importance of flexible management responses in order to account for the uncertainty in sediment yield forecasts (Crosbie *et al.,* 2012).

Seasonal or monthly sediment yield from sheet and rill erosion did not change throughout the modelled period 2015-2100. Sediment yield in January - February remained the highest with lowest falling in the winter months May-August. However, there was a shift in the timing of the erosive rainfall. Erosive rainfall shifts approximately one month earlier, from September to August, towards the end of the century; the rainfall also follows this shift. The intensity of erosive rainfall also increases throughout the contrary. This can be attributed to the increase in 10 mm and 15 mm events predicted from 2105-2100. Engelbrecht *et al.* (2011) also found an increase in rainfall intensity throughout the century. Such a result is useful to land and dam managers as well as farmers as their practices may need to change to accommodate such shifts in rainfall and sediment yield. If the dam managers plan to apply techniques such as annual sluicing to control sediment yield in the potential dam, it is important for them to account for shifts in runoff in order to keep the sluicing methods effective as the climate changes.

GFDL, MPI and CSIRO all show similar trends where sediment yield decreases until 2064 and then increases towards 2100. These models trends follow the trends of the average rainfall graph. The trends are also reflected in the number of extreme events for the CSIRO and MPI models yet the trend is not so closely related in the GFDL model. GFDL 2 and MIROC models produced the most unexpected results. GFDL 2 shows a gradual decrease in sediment yield from sheet and rill erosion from 2015-2100 yet the average annual rainfall increases during this period. It also shows an increase in 5 mm, 10 mm and 15 mm events. MIROC is similarly surprising, the sediment yield from sheet and rill erosion decreases slightly to 2065 and then increases slightly to 2100. Rainfall predicted by this model during this period shows a decrease in average annual rainfall.

The main conclusion which can be drawn is that sediment yield from sheet and rill erosion will most likely increase from 2065 onwards. Five of the six models show an increase in sediment yield from 2065. It is only the GFDL 2 model which predicts a decrease in sediment yield. This increase can be most likely be attributed to an increase in extreme events. According to some models an increase in rainfall may also be the cause for increased sediment yield. In the GFDL simulation, the sediment yield decreases while average annual rainfall increases this could be explained when looking at the effects of rainfall on

biomass. In the GFDL, as with the other scenarios, the increased rainfall and carbon dioxide concentrations in the atmosphere will result in better biomass cover and denser vegetation canopies; this will minimise or prevent the effects of increased rainfall on sediment yield (Mullan *et al.*, 2012). Unlike the other scenarios, the GFDL 2 scenario may not have enough rainfall to counteract the beneficial effects of increased vegetation on soil erosion.

One of the reasons for the decrease in sediment yield from sheet and rill erosion observed in some of the models could be due to the increased canopy cover. With higher carbon dioxide concentrations as well as more rainfall and higher temperatures the plants may have better growing conditions and for longer periods during the year. This will result in greater canopy cover and protect the soil.

It is acknowledged that this study is a simplification of projected climate change. Land use, land cover change and land management patterns are shaped by the interaction of economic, environmental, social, political, and technological forces on both the local and global scale, with the most important driver of land use change been the policies (Mullan *et al.*, 2012). However, this study aimed to determine the isolated impacts of climate on soil erosion and did not include land management changes in the model. Effects of changing climate and land use on gully erosion and sediment yield derived therefrom was also not calculated in this study. This was due to SWAT being unable to model gully erosion and the lack of available models able to model gully erosion. Developing a hydrological model which can model gully erosion was outside the scope of this thesis and is highly recommended for future research. Impacts of land use change, as well as climate change on sheet and rill erosion in the catchment, was highlighted in this study. Trends showed an increase in sheet and rill erosion between 2015 and 2100 for the upper Tsitsa Catchment which is concerning. It is thus recommended that further studies be conducted on other important water resource areas in South Africa in order to effectively plan for future climate change.

6.5. Soil erosion in the catchment

The upper Tsitsa River catchment is highly susceptible to soil erosion. Studies conducted by van Tol *et al.* (2014) and Le Roux *et al.* (2015) have shown accelerated rates of soil erosion in the catchment, attributed to the soils and steep slopes higher up in the catchment. The primary contribution to sediment yield in the catchment is from gully erosion. Over 2200 gullies were mapped in the catchment, which cover a total surface area of 17 km^2. Gully erosion produced between 7 and 14 tons of sediment a year for the duration of this study. This is roughly 70 times more sediment than that produced through sheet and rill erosion. The study showed similar results to previous studies by van Tol *et al.* (2014) and Le Roux *et al.* (2015) with increased soil erosion rates, particularly from gully erosion. Current land use in the catchment was found to be one of the most optimal land uses to minimize soil erosion from sheet and rill erosion. However, the use of the majority of the land for unmanaged grazing accelerates gully erosion, which is the primary cause of sediment yield. Thus changing the land use to more commercial farming particularly sugarcane or avocado orchards may be the best land use in order to minimize future gully erosion and sediment yield. Changing the crop types to corn or cabbage will also increase sediment yield and negativity impact any dam or water resource development.

Effects of climate change in the catchment are extremely variable with some models showing a steep increase in sediment yield and other models showing a decrease in sediment yield. The land management practices which will be implemented due to a changing climate will most likely affect sediment yield to a much larger extent than the effects of climate change itself (Mullan *et al.,* 2012). This is mainly because the Tsitsa Catchment falls within the coastal belt zone of South Africa, wedged between the coast and the Drakensberg, where the impacts of climate change are buffered so there are minimal changes in climate compared to other areas of South Africa (Engelbrecht *et al.*, 2015). CEPF Ecosystem Profile showed that the Mzimvubu Corridor was an area with greater resilience to climate change than other regions in South Africa (Environmental and Rural Solutions, 2011). As average annual rainfall and temperatures are not predicted to increase by as large amounts as predicted in other regions of South Africa such as the Northern Cape and Limpopo (Figure

6.2 and Figure 6.3). A study such as this one conducted in another catchment in the North or interior of South Africa would most likely show changes that are more significant for soil erosion.

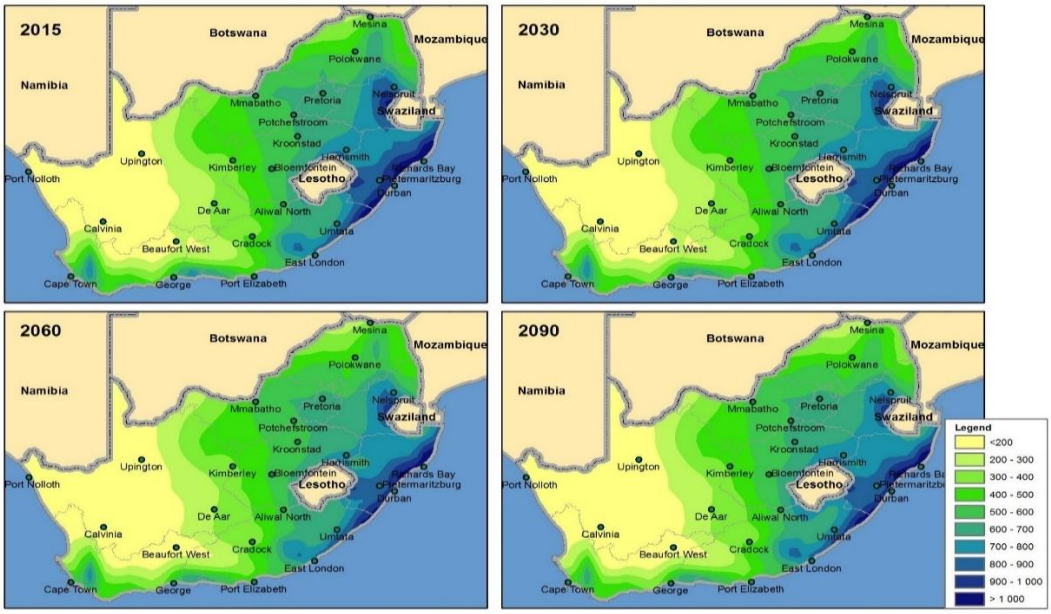

Figure 6.2: The average annual rainfall over South Africa as a median of the six GCM projections for 2015, 2030, 2060 and 2090 (reproduced with permission from Weepener *et al*., 2014).

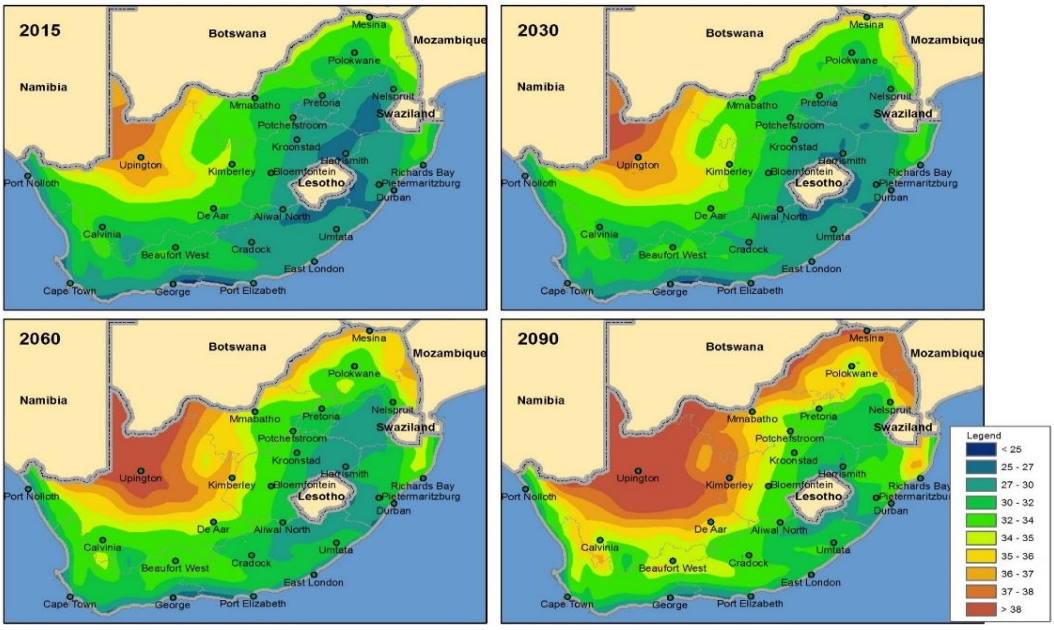

Figure 6.3: The average maximum temperature over South Africa as a median of the six GCM projections for 2015, 2030, 2060 and 2090 (reproduced with permission from Weepener *et al*., 2014).

In the upper Tsitsa catchment, the dominant type of soil erosion is that caused by water erosion and not wind erosion. However, sediment deposited by wind may still be a significant contributor to the overall sediment yield in the catchment. This study did not account for wind erosion and it may be a limitation to understanding the overall dynamics of soil erosion and sediment yield in the upper Tsitsa River Catchment.

7. Conclusion

7.1. Conclusion

Results of both the gully monitoring and sheet and rill erosion showed high sediment yield rates in the upper Tsitsa Catchment ranging between 140 000 t/yr and 280 000 t/yr. The majority of the sediment is derived from gully erosion, with approximately 70 times more sediment been produced by gullies than sheet and rill erosion. Sheet and rill erosion produced 0.18 t/ha/yr of sediment while gully erosion resulted in 7 to 14 t/ha/yr. It was found that gully erosion increased by 4 km^2 during the five-year modelling period. These results are similar to those found by Le Roux *et al.*, (2015) who found a 5.6 km^2 increase in gully surface area. The main cause of gully erosion can be attributed to inadequate land management with free grazing of livestock, poor soils in the catchment and the presence of steep slopes in the higher reaches of the catchment creating a critical drainage area leading to gullying (Poesen *et al.*, 2003; van Tol *et al.*, 2014).

In order to map the gullies, a ruleset was developed in eCognition to facilitate OBIA. The ruleset was based on SPOT 5 images from 2007 and 2012 in order to determine lateral gully extent. Spectral, textural and geographical properties were used to distinguish gullies in the images. The accuracy of the ruleset was then calculated using several accuracy assessment techniques and a manually digitised gully location map. It was found that the accuracy ranged from 16% to 99%. Reasons for the variation in accuracies can be attributed to the technique used to test the accuracy, the boundaries drawn by each technique and false classification (Yale's Centre for Earth Observation, 2003; Lilliesand *et al.*, 2004; d'Oleire-Oltmanns *et al.,* 2014). It was found that OBIA falsely classified some rock outcrops, sediment in the river and tilled land as gullies. However, OBIA was able to distinguish and map gullies faster and more objectively than manual digitising.

Results of the OBIA-created gully map and the methodology used in this study, will be beneficial for the improved assessment of gully-derived sediment yield. These maps will be especially useful for modelling gully derived sediment yield under changing climate change and land use scenarios. By creating a methodology through which an accurate and objective gully location or gully

expansion map can be created, sediment yield results derived therefrom can be estimated with acceptable accuracy and used for planning and monitoring of important catchments.

The use of SWAT to conduct scenario analysis on the catchment proved to be very useful and effortless once the model had been set up. This allowed for multiple scenarios to be tested without much alteration in the model. The model was able to determine sediment yield using climate predictions from six climate models as well as predicted land use change.

Results from the scenario analysis conducted in SWAT showed that the current land use scenario was one of the best scenarios along with sugarcane and avocado orchards for minimal sheet and rill erosion. Most other agricultural developments will cause increased soil erosion unless measures are taken to mitigate the causes. The most soil erosion will be caused from cultivating maize under either till or no-till management in the catchment. Mullan *et al.*, (2012) found similar results as maize takes a while to grow big enough to provide adequate soil cover and protection. Cabbage also produced high amounts of sediment yield under no-till management. It is recommended that conservation agriculture techniques are used in the catchment as tillage will increase soil erosion and sediment yield. These results compare favourably with those found by Ullrich and Volk (2009).

These results will facilitate both DAFF and DWS in decision making and catchment management particularly with regards to increasing agriculture in the upper Tsitsa Catchment. Results showed that if a dam is to be built the DWS will need to rehabilitate the exsisting gullies in the catchment which will increase the expenses of the construction budget. Furthermore, continuous monitoring of the catchment and the dam will need to be under taken by the DWS to ensure the dam is not silting up too rapidly. The results also showed that certain crops will have a greater impact on siltation which can help DAFF decide the best crops to be cultivated if they wish to reduce sediment yield as well as develop agriculture.

The impact of climate change had variable effects on sediment yield from sheet and rill erosion, however, the majority of the models predicted an overall increase in sediment yield while one model showed a slight decrease from 2015-2100. This was attributed to two main causes, first due to an increase in

rainfall and second, an increase in extreme rainfall events (Engelbrecht & van Garderen, 2013). Erosivity of rainfall events also increased during the period 2015-2100. These results are important for any long term plans in the upper Tsitsa Catchment as plans should account for and mitigate against increased soil erosion. If sediment yield increases throughout the century the dam's lifespan will be reduced unless mitigation measures are put in place.

Future studies should determine the land use or land management changes which may be brought about by climate change and how this will affect sediment yield in the catchment. The study also brought up an interesting question of how predicted climate change will affect catchments in South Africa and this should be explored in more detail on other catchments which may be more susceptible to climate change impacts. Wind patterns are also predicted to change with changing climate although wind erosion currently accounts for minimal sediment yield this may not be the case going into 2100, thus future studies should determine the effects of wind on sediment yield and how it may affect future water resource developments or conservation efforts. The effect of changing climate and land use on gully erosion and sediment yield derived therefrom was also not calculated in this study. This was due SWAT been unable to model gully erosion and the lack of available models able to model gully erosion. Soil erosion under a changing climate is a large research gap, especially for gully erosion. In order to estimate the effects of climate and land use change on gully erosion, one will need a gully erosion model that is coupled with a hydrological component, applicable at a large catchment scale. Such a model does not exist. Thus modelling the effects of climate and land use change on gully erosion was outside the scope of this study and it is recommended for future research.

Future studies should look at the potential use of the OBIA methodology developed in this study on other catchments in South Africa or to create a gully monitoring algorithm which can be used to determine how gullies are changing over the short term. Furthermore, the ruleset can be further developed to allow for the classification of gullies. It has been noted that some vegetated gullies may become active during extreme rainfall events and future research can aim to incorporate vegetated gully systems in an identification and classification ruleset. It will also be interesting to study the use of LiDAR technology to improve the results of OBIA as well as the use of other satellite data for a

greater spectral resolution. Another recommendation for future studies is the effects of conservation agriculture on sediment yield and its feasibility in the catchment as well as the better land management practices to determine grazing rotations and how to lower sediment yield.

It is recommended that soil erosion prevention methods are put in place in the upper Tsitsa catchment. The methods most suitable to the catchment will be terracing along the hillslopes, intercropping or the use of vegetative strips along the river courses and grazing management practices. However, due to the extreme soil erosion in the catchment, it is also recommended that the potential dam has sediment traps or smaller dams upstream to collect and drain sediment in order to optimise the dam's lifespan.

This study highlighted the importance of incorporating sediment yield from gullies in erosion studies. In the upper Tsitsa Catchment gullies contribute 70 times more sediment than sheet and rill. Thus using hydrological models which do not account for gully erosion can severely underestimate soil erosion. This study also highlighted the impacts of land use change as well as climate change on sheet and rill erosion in the catchment.

The primary aim of this study was to determine the sediment yield in the upper Tsitsa River Catchment, South Africa under current and future scenarios. There were two main themes throughout the thesis the one focusing on the identification and classification of gully erosion and the other focusing on sheet and rill aspects of erosion under the current conditions as well as changing climate and land use. The two themes coincided as both aimed to determine the sediment yield which would be generated in the catchment under current conditions. Conducting scenario analysis helped in understanding how land use and climate change may affect the sheet and rill aspects of erosion, which could be useful when planning future developments in the upper Tsitsa Catchment. Perspectives on sediment yield contribution from gully erosion have typically been obtained from field scale ($<10^{-1}$ km^2) and are confined to local conditions. Few studies model the sediment yield contribution from gully erosion at a regional scale. Furthermore, the use of eCognition for gully classification had been rarely explored in the past and this study used the opportunity to determine whether OBIA was able to identify gullies at the catchment scale and the accuracy of its results.

The upper Tsitsa River Catchment is highly susceptible to soil erosion in particular gully erosion, which is worsening every year. It is imperative that better land management practices are adopted or soil erosion mediation measures are taken before any water resource project is pursued in the catchment. Extreme rates of sediment yield in the catchment will result in any dam project becoming economically unfeasible within a few years of operation under current land use conditions.

7.2. Recommendations for dam management

Results obtained in this study can assist dam designers and dam management projects. Due to the high rates of soil erosion in the catchment, it is imperative that the dam is able to withstand large amounts of sediment runoff while maintaining adequate storage capacity. Dam management strategies are also very important in order to minimise the effect of sediment runoff on the dam lifespan. Common dam management strategies allow dams to fill with sediment slowly, which means that the benefits of storage are only felt over a limited period of time (Plamieri *et al.*, 2001). In the case of a dam in the upper Tsitsa catchment this type of management will be disastrous as the sediment yield generated in the catchment is extremely high. The limited period of time will be short lived and the economic benefits of the dam may not be felt before it has become unfeasible.

Dam construction considerations include the building of sediment traps or settling facilities or the construction of an underwater dike or massive tunnels, which allow for annual sluicing. Sediment traps and settling facilities were tested in South Africa and recommended by Ferreira and Waygood (2009). These measures, however, are expensive and their benefits should be weighed against the cost of implementing them (Plamieri *et al.*, 2001).

Although the dam design can have a considerable effect on the lifespan of the dam, preventing upstream soil erosion has a substantial benefit on the lifespan of a dam (Plamieri *et al.*, 2001; Prosdocimi *et al.*, 2016; Vogel *et al.,* 2016). Such practices can include field margins or the use of vegetation for mixed and inter-cropping (Vogel *et al.*, 2016). There are also mechanical techniques such as terracing and parcelling which can be used to limit soil erosion (Hudson, 1993).

In the upper Tsitsa Catchment, the best method to increase the lifespan of a dam would be to prevent soil erosion upstream. Using of conservation farming techniques as well as field margins or inter-cropping with sugarcane will help reduce soil erosion. It is also important to introduce better land management practices such as rotational grazing or limiting stock sizes to the carrying capacity of the land.

8. References

Abalu, G. & Hassan, R. 1998. Agricultural productivity and natural resource use in southern Africa. *Food Policy*, *23*, 477-290.

Agrometeorology Staff. (1984-2008). *ARC-ISCW Agrometeorology weather station network data for South Africa. Unpublished*. ARC-Institute for Soil, Climate and Water: Pretoria.

Alletto, L. & Coquet, Y. (2009). Temporal and spatial variability of soil bulk density and near-saturated hydraulic conductivity under two contrasted tillage management systems. *Geoderma*, *152*, 85-94.

Anders, N. S., Seijmonsbergen, A. C. & Bouten, W. (2011). Segmentation optimization and stratified object-based analysis for semi-automated geomorphological mapping. *Remote Sensing of the Environment*, *115*, 2976-2985.

Arnaez, J., Lasanta, T., Ruiz-Flaño, P. & Ortigosa, L. (2007). Factors affecting runoff and erosion under simulated rainfall in Mediterranean vineyards. *Soil and Tillage Research, 93,* 324-334.

Asres, M. T. & Awulachew, S. B. (2010). SWAT based runoff and sediment yield modelling: a case study of the Gumera watershed in the Blue Nile basin. *Ecohydrology and Hydrology, 10*, 191-200.

Baker, T. J. & Miller, S. N. (2013). Using the Soil and Water Assessment Tool (SWAT) to assess land use impact on water resources in an East African watershed. *Journal of Hydrology*, *486*, 100-111.

Bäse, F., Helmschrot, J., Müller Schmied, H. & Flugel, W. A. (2006). The impact of land use change on the hydrological dynamic of the semi-arid Tsitsa Catchment in South Africa. *Proceedings of the 2nd Göttingen GIS and Remote Sensing*, Göttingen. 257-268.

Bates, B. C., Kundzewicz, Z. W., Wu, S. & Palutikof, J. P. (2008). *Climate change and water. IPCC Technical Report VI.* IPCC: Geneva.

Beckedahl, H. R., Bowyer-bower, T. A., Dardis, G. F. & Hanvey, P. M. (1988). Geomorphic effects on soil erosion. *Geomorphology of Southern Africa,* 249-276. Southern Book Publishers: Johannesburg.

Breetzke, G. D., Koomen, E. & Critchley, W. R. S. (2013). GIS-assisted modelling of soil erosion in a South African catchment: evaluating the USLE and SLEMSA approach. *Water Resources Planning, Development and Management,* 53-71.

Blaschke, T. (2010). Object-based image analysis for remote sensing. *Journal of Photogrammetry and Remote Sensing, 65*, 2-16.

Boardman, J., Parsons, A. J., Holland, R., Holmes, P. J., & Washington, R. (2003). Development of badlands and gullies in the Sneeuberg, Great Karoo, South Africa. *Catena*, *50*, 165-184.

Boggess, J. E. (1993). *Identification of roads in satellite imagery using artificial neural networks: a conceptual approach.* Scientific Services Program: Mississippi.

Boix-Fayos, C., Martinez-Mena, M., Arnau-Rosalen, E., Calvo-Cases, A., Castillo, V. & Albaladejo, J. (2006). Measuring soil erosion by field plots: understanding the sources of variation. *Earth-Science Reviews, 78*, 267-285.

Bordy, E. M., Hancox, P. J. & Rubidge, B. S. (2005). The contact of the Molteno and Elliot formations through the main Karoo Basin, South Africa: a second-order sequence boundary. *South African Journal of Geology, 108*, 351-364.

Bossa, A. Y., Diekkrüger, B., Igué, A. M., & Gaiser, T. (2012). Analysing the effects of different soil databases on modelling of hydrological processes and sediment yield in Benin (West Africa). *Geoderma*, *173*, 61-74.

Botha, G. A. & Singh, R. (2012). *Geology, geohydrology and development potential zonation of the uThukela district municipality; specialist contribution towards the environmental management framework.* Council for Geo-Science: Pietermaritzburg.

Bruland, G. (2015). *USLE and other models .* Retrieved 10/14/2015, from www.ctahr.hawaii.edu/brulandg/teaching/46109%20USLE.pdf.

Buhmann, C., Rapp, I. & Laker, M. C. (1996). Differences in mineral ratios between disaggregated and original clay fractions in some South African soils as affected by amendments. *Soil Research*, *34*, 909-923.

Casanovas, J. A. & Zaragova, T. C. 1996. Gully erosion mapping by remote sensing techniques: a case study in the Anoia, Penedes region, Spain. *Sitges,* 29-31*.* Barcelona.

Cardei, P. (2010). The dimensional analysis of the USLE- MUSLE soil erosion model. *Proceedings of the Romanian Academy, 3*, 249-253.

Chen, D. & Stow, D. (2002). The effect of training strategies on supervised classification at different spatial resolutions. *Photogrammetric Engineering & Remote Sensing, 68*, 1155-1161.

Chen, E. & Mackay, D. S. (2004). Effects of distribution-based parameter aggregation on a spatially distributed agricultural non-point source pollution model. *Journal of Hydrology, 295*, 211-224.

Chen, Y., Su, W., Li, J. & Sun, Z. (2009). Hierarchical object-oriented classification using very high-resolution imagery and LiDAR data over urban areas. *Advances in Space Research, 43*, 1101-1110.

Chmielewski, F. M., Müller, A. & Bruns, E. (2004). Climate changes and trends in phenology of fruit trees and field crops in Germany, 1961–2000. *Agricultural and Forest Meteorology*, *121*, 69-78.

Cooke, A. & Mancini A. (2015). *Erosion in Maize*. Retrieved 26/1/2016, from http://www.thedirtdoctors.com/erosion-in-maize/.

Council for Geoscience. (2008). *Vector geological data derived from the 1:250 000 geological map series for South Africa.* Council for Geoscience: Pretoria.

Crosbie, R. S., Dawes, W. R., Charles, S. P., Mpelasoka, F. S., Aryal, S., Barron, O. & Summerell, G. K. (2011). Differences in future recharge estimates due to GCMs, downscaling methods and hydrological models. *Geophysical Research Letters, 38,* L11406

Crosbie, R. S., McCallum, J. L., Walker, G. R. & Chiew, F. H. (2012). Episodic recharge and climate change in the Murray-Darling Basin, Australia. *Hydrogeology Journal*, 20, 245-261.

d'Oleire-Oltmanns, S., Marzolff, I., Tiede, D. & Blaschke, T. (2014). Detection of gully-affected areas by applying object-based image analysis (OBIA) in the region of Taroudannt, Morocco. *Remote Sensing*, *6*, 8288-8309.

Das, M. M. & Saikia, M. D. (2013). *Watershed Management* (First ed.). PHI Learning, Private Limited: New Delhi.

Dechmi, F., Burguete, J. & Skhiri, S. (2012). SWAT application in intensive irrigation systems: model modification, calibration and validation. *Journal of Hydrology*, *471*, 227-238.

de Vente, J., Poesen, J., Verstraeten, G., Govers, G., Vanmaercke, M., Van Rompaey, A. & Boix-Fayos, C. (2013). Predicting soil erosion and sediment yield at regional scales: Where do we stand? *Earth-Science Reviews, 127*, 16-29.

Devia, G. K., Ganasri, B. P. & Dwarakish, G. S. (2015). A review on hydrological models. *Aquatic Procedia*, *4,* 1001-1007.

Department of Water and Sanitation, South Africa. (2014). *Environmental impact assessment for the Mzimvubu: environmental impact assessment report.* Pretoria.

Department of Water and Sanitation. (2015). *Caledon/modder transfer scheme*. Retrieved 2/23/2016, from https://www.dwa.gov.za/orange/mid_orange/calmod.htm.

Dezso, B., Fekete, I., Gera, D. A., Giachetta, R. & László, I. (2012). Object-based image analysis in remote sensing applications using various segmentation techniques. *Annales Universitatis Scientiarum Budapestinensis de Rolando Eotvos Nominatae Sectio Computatorica*, *37*, 103-120.

Drăguţ, L. & Eisank, C. (2012). Automated object-based classification of topography from SRTM data. *Geomorphology*, *141*, 21-33.

Duda, T. & Canty, M. (2002). Unsupervised classification of satellite imagery: choosing a good algorithm. *International Journal of Remote Sensing, 23*, 2193-2212.

Duncan, N., van Veelen, M. & Calmeyer, T. (2015). *Integrated water use licence for the Mzimvubu water project: technical report.* Department of Water and Sanitation: Pretoria

Encyclopedia Brittanica. (2015). *Encyclopedia Britannica*. Retrieved 9/4/2015, from www.global.britannica.com/science/sheet-erosion.

Engelbrecht, C. J., Engelbrecht, F. A. & Dyson, L. L. (2013). High-resolution model-projected changes in mid-tropospheric closed-lows and extreme

rainfall events over southern Africa. *International Journal of Climatology*, *33*, 173-187.

Engelbrecht, F. A., McGregor, J. L., & Engelbrecht, C. J. (2009). Dynamics of the Conformal-Cubic Atmospheric Model projected climate-change signal over southern Africa. *International Journal of Climatology, 29*, 1013-1033.

Engelbrecht, F., Adegoke, J., Bopape, M. J., Naidoo, M., Garland, R., Thatcher, M. & Gatebe, C. (2015). Projections of rapidly rising surface temperatures over Africa under low mitigation. *Environmental Research Letters*, *10*, 1-16.

Engelbrecht, F. & van Garderen, E. A. (2013). *The global change challenge: a regional perspective*. CSIR: Pretoria.

Engelbrecht, F.A., Landman, W.A., Engelbrecht, C.J., Bopape, M.M., Roux, B., McGregor, J.L. & Thatcher, M. (2011). Multi-scale climate modelling over Southern Africa using a variable-resolution global model. *Water SA, 37*, 647-658.

Environmental and Rural Solutions. (2011). *Umzimvubu catchment overview.* Retrieved 2/29/2016, from https://umzimvubu.files.wordpress.com/2014/09/umzimvubu-summary-report-dec-2011.pdf.

Esprey, L. J. (1997). *Hillslope experiments in the north-east cape region to measure and model subsurface flow processes.* Masters Thesis*.* University of Natal: Pietermaritzburg.

Eustace, A., Pringle, M. & Witte, C. (2009). Give me the dirt: detection of gully extent and volume using high-resolution LiDAR. *Innovations in Remote Sensing and Photogrammetry*, *8*, 255-269.

Evans, R. (2002). An alternative way to assess water erosion of cultivated land – field-based measurements: and analysis of some results. *Applied Geography, 22*, 187-207.

Ferreira, S. & Waygood, C. (2009). A South African case study on sediment control measures with the use of silt traps in the coal mining industry. *Abstracts of the International Mine Water Conference,* 497-506*.* Document Transformation Technologies cc: Pretoria.

Ferro, V. & Minacapilli, M. (1995). Sediment delivery processes at basin scale. *Hydrological Sciences Journal*, *40*, 703-717.

Fielding, A. H. & Bell, J. F. (1997). A review of methods for the assessment of prediction errors in conservation presence/absence models. *Environmental Conservation, 24*, 38-49.

Flanagan, D. C., Ascough, J. C., Nearing, M. A. & Laflen, J. M. (2001). Chapter 7: Water erosion prediction project (WEPP) model. In *Landscape Erosion and Evolution Modelling*, 145-199. Springer: New York.

Flanders, D., Hall-Beyer, M. & Pereverzoff, J. (2003). Preliminary evaluation of eCognition object-based software for cut block delineation and feature extraction. *Canadian Journal of Remote Sensing*, *29*, 441-452.

Flugel, W. A., Marker, M., Moretti, S., Rodolfi, G. & Sidrochuk, A. (2003). Integrating geographical information systems, remote sensing, ground truthing and modelling approaches for regional erosion classification of semi-arid catchments in South Africa. *Hydrological Processes, 17*, 929-942.

Franks, P. J., Adams, M. A., Amthor, J. S., Barbour, M. M., Berry, J. A., Ellsworth, D. S. & Norby, R. J. (2013). Sensitivity of plants to changing atmospheric CO_2 concentration: from the geological past to the next century. *New Phytologist, 197*, 1077-1094.

Fraser, A. I., Harrod, T. R. & Haygarth, P. M. (1999). The effect of rainfall intensity on soil erosion and particulate phosphorus transfer from arable soils. *Water and Science Technology, 39*, 41-45.

Freese, C., Lorentz, S., le Roux, P., van Tol, J. & Vermeulen, D. (2010). *A description and quantification of hillslope hydrological processes in the necf, Weatherley Catchment.* Retrieved 12/6/2014, from www. ru. ac. za/static/institutes/iwr/SANCIAHS/2011/the. pdffiles/C_Freese_Paper. pdf.

Food and Agriculture Organization. (1978). *Soil erosion by water: some measures for its control on cultivated lands* (Second ed.). Food and Agriculture Organization of the United Nations: Rome.

Food and Agriculture Organization: Natural Resource Management and Environment Department. (1996). Land husbandry- components and strategy. Food and Agricultural Organisation of the United Nations. Retrieved 10/14/2015, from www.fao.org/docrep/t1765e/t1765e0e.htm

Gao, B. C. (1996). NDWI: A normalized difference water index for remote sensing of vegetation liquid water from space. *Remote Sensing of the Environment, 96*, 257-266.

Garde, A. (2006). *River Morphology* (First ed.). New Age International Publishers: New Delhi.

Gassman, P. W., Reyes, M. R., Green, C. H. & Arnold, J. G. (2007). The soil and water assessment tool: historical development, applications, and future research directions. *Transactions of the American Society of Agricultural and Biological Engineers, 50*, 1211-1250.

Gebejes, A. & Huertas, R. (2013). Texture characterization based on grey-level co-occurrence matrix. *Proceedings of Conference of Informatics and Management Sciences.* Slovakia.

Gilau, A. N. P. (2015). *The use of erosion models to predict the influence of land use changes on urban impoundments.* Doctoral dissertation, Faculty of Engineering and the Built Environment, University of the Witwatersrand: Johannesburg.

Gillan, J. K., Karl, J. W., Barger, N. N., Elaksher, A. & Duniway, M. C. (2016). Spatially explicit rangeland erosion monitoring using high-resolution digital aerial imagery. *Rangeland Ecology & Management*, *69*, 95-107.

Govaerts, B. & Verhulst, N. (2010). *The normalized difference vegetation index (NDVI) GreenSeekerTM handheld sensor: Toward the integrated evaluation of crop management.* International Maize and Wheat Improvement Centre: Mexico

Government of Alberta. (2011). *Erosion control manual: section 12 - guidelines for the design of sediment containment*. Retrieved 3/16/2016, from http://www.transportation.alberta.ca/Content/docType372/Production/12GuidelinesDsgnSediCntnment.pdf

Grellier, S., Kemp, J., Janeau, J. L., Florsch, N., Ward, D., Barot, S. & Valentin, C. (2012). The indirect impact of encroaching trees on gully extension: a 64-year study in a sub-humid grassland of South Africa. *Catena, 98*, 110-119.

Haarhoff, D., Smith, H.J., Beytell, J.F. & Schoeman, J.L. (1994). *The testing of techniques for the determination of the erosion potential of areas in South*

Africa. ISCW Report GW/A/94/6. ARC-Institute for Soil, Climate and Water: Pretoria.

Haralick, R. M., Shanmugam, K. & Dinstein, I. (1973). Textural features for image classification. *IEEE Transactions on Systems Management and Cybernetics, 3*, 610-621.

Hawkins, E. & Sutton, R. (2009). The potential to narrow uncertainty in regional climate predictions. *Bulletin of the American Meteorological Society, 90,* 1095.

Höfle, B., Griesbaum, L. & Forbriger, M. (2013). GIS-Based detection of gullies in terrestrial LiDAR data of the Cerro Llamoca Peatland (Peru). *Remote Sensing, 5*, 5851-5870.

Hooke, J. (2003). Coarse sediment connectivity in river channel systems: a conceptual framework and methodology. *Geomorphology, 56*, 79-94.

Huang, Y. F., Chen, X., Huang, G. H., Chen, B., Zeng, G. M., Li, J. B. & Xia, J. (2003). GIS-based distributed model for simulating runoff and sediment load in the Malian River basin. *Hydrobiologica, 494*, 127-134.

Hudson, C. A. (1987). *A Regional Application of the SLEMSA in the Cathedral Peak Area of the Drakensberg.* Doctoral dissertation, University of Cape Town: Cape Town.

Hudson, N. W. (1993). *Food and Agricultural Organisation: Field measurements of soil erosion and runoff*. Retrieved 10/5/2015, from www.fao.org/docrep/t0848e00.HTM.

Hughes, A. O. & Prosser, I. P. (2012). Gully erosion prediction across a large region: Murray–Darling Basin, Australia. *Soil Research, 50*, 267-277.

Igue, A. M. (2002). The qualitative assessment of water erosion risk in the moist savanna of Benin. *12th International Soil Conservation Organization Conference.* Beijing.

Intergovernmental Panel on Climate Change. (2000). *Special Report on Emissions Scenarios.* Cambridge: Cambridge University Press.

Ivanciuc, O. (2005). *SVM - Support vector machines*. Retrieved 10/8/2015, from http://www.support-vector-machines.org/.

Jackson, W. L., Gebhardt, K. & van Haveren, B. P. (1986). Use of the modified universal soil loss equation for average annual sediment yield estimates

on small rangeland drainage basins. *International Association of Hydrological Sciences Publication, 159,* 413-423.

Jain, M. K., Kothyari, U. C. & Ranga-Raju, K. G. (2005). GIS-based distributed model for soil erosion and rate of sediment outflow from catchments. *Journal of Hydraulic Engineering, 131*, 755-769.

Japanese Association of Remote Sensing. (2012). *Japanese Association of Remote Sensing.* Retrieved 10/8/2015, from http://www.jars1974.net/pdf/12_Chapter11.pdf.

Jetten, V., Shruthi, B.V.R. & Kerle, N. (2011). Object-based gully feature extraction using high spatial resolution imagery. *Geophysical Research Abstracts*, *3*, 260-268.

Jewitt, G. P. & Schulze, R. E. (1999). Verification of the ACRU model for forest hydrology applications. *Water SA, 25*, 483-490.

Ji, L., Zhang, L. & Wylie, B. (2009). Analysis of dynamic thresholds for the normalized difference water index. *Photogrammetric Engineering & Remote Sensing, 75*, 1307-1317.

Johansen, K., Arroyo, L. A., Armston, J., Phinn, S. & Witte, C. (2010). Mapping riparian condition indicators in a sub-tropical savanna environment from discrete return LiDAR data using object-based image analysis. *Ecological Indicators, 10*, 796-807.

Jones, B. & Thompson, D. (2007). Workshop on common criteria for risk area identification in the soil framework directive.: European Commission- Joint Research Centre: Hannover.

Kakembo, V., Xanga, W. W. & Rowntree, K. (2009). Topographic thresholds in gully development on the hillslopes of communal areas in Ngqushwa Local Municipality, Eastern Cape, South Africa. *Geomorphology, 110*, 188-194.

Kannan, N., White, S. M., Worrall, F. & Whelan, M. J. (2007). Hydrological modelling of a small catchment using SWAT-2000 – Ensuring correct flow partitioning for contaminant modelling. *Journal of Hydrology, 334*, 64-72.

Knight, J., Spencer, J., Brooks, A. & Phinn, S. (2007). Large-area, high-resolution remote sensing based mapping of alluvial gully erosion in Australia's tropical rivers. *Proceedings of the 5th Australian Stream Management Conference,* 199-204. Charles Sturt University.

Laflen, J. M., Elliot, W. J., Flanagan, D. C., Meyer, C. R. & Nearing, M. A. (1997). WEPP-predicting water erosion using a process based model. *Journal of Soil and Water Conservation, 52*, 96-102.

Laker, M. C. (2004). Advances in soil erosion, soil conservation, land suitability evaluation and land use planning research in South Africa, 1978-2003. *South African Journal of Plant Science, 21*, 345-368.

Land Type Survey Staff. (1972 – 2006). *Land Types of South Africa: Digital map (1:250 000 scale) and soil inventory databases*. ARC-Institute for Soil, Climate and Water: Pretoria.

Le Roux, J. J. (2005). *Soil erosion prediction under changing land use on Mauritius.* Masters Thesis, University of Pretoria, Department of Geography, Geoinformatics and Meteorology: Pretoria.

Le Roux, J. J., Newby, T. S. & Sumner, P. D. (2007). Monitoring soil erosion in South Africa at a regional scale: review and recommendations. *South African Journal of Science, 103*, 329-335.

Le Roux, J. J., Morgenthal, T. L., Malherbe, J., Pretorius, D. J. & Sumner, P. D. (2008). Water erosion prediction at a national scale for South Africa. *Water SA*, *34*, 305-314.

Le Roux, J. J. (2009). *Guidelines for the use of SWAT for the evaluation of economic tradeoffs of NPS pollution control measures.* WRC Report *K5/1516.* Water Research Commission: Pretoria.

Le Roux, J. J. & Sumner, P. D. (2012). Factors controlling gully development: comparing continuous and discontinuous gullies. *Land Degradation and Development, 23*, 440-449.

Le Roux, J. J., Sumner, P. D., Lorentz, S. A. & Germishuyse, T. (2013). Connectivity aspects in sediment migration modelling using the Soil and Water Assessment Tool. *Geosciences, 3*, 1-12.

Le Roux, J. J. & van den Berg, E. (2014). *Sediment yield modelling in the uMzimvubu River Catchment: progress report.* Water Research Commission: Pretoria.

Le Roux, J. J., Barker, C. H., Weepener, H. L., van den Berg, E. C. & Pretorius, S. N. (2015). *Sediment yield modelling in the Mzimvubu River Catchment.* WRC Report 2243/1/15. Water Research Commission: Pretoria.

Lilliesand, T. M., Kiefer, R. W. & Chipman, J. W. (2004). *Remote sensing and image interpretation.* (First ed.). John Wiley & Sons Ltd: Chichester.

Lillesand, T. M., Kiefer, R. W. & Chipman, J. W. (2008). Digital image interpretation and analysis. *Remote Sensing and Image Interpretation*, *6*, 545-81.

Lindemann, H. J. & Pretorius, D. J. (2005). *Towards a soil protection strategy and policy for South Africa.* Directorate Land Use and Soil Management, National Department of Agriculture. *Unpublished*: Pretoria.

Lu, D., Li, G., Morana, E., Freitas, C. C., Dutra, L. & Sant'Anna, S. J. (2012). A comparison of maximum likelihood classifier and object-based method based on multiple sensor data sets for land-use/cover classification in the Brazilian amazon. *Proceedings of the 4th Geographic Object-based Image Analysis.* Rio de Janerio.

Manjoro, M., Rowntree, K., Kakembo, V. & Foster, I. D. (2012). Gully fan morphodynamics in a small catchment in the Eastern Cape, South Africa. *Land Degradation and Development, 23*, 569–576.

Manyatsi, A. M. & Ntshangase, N. (2008). Mapping of soil erosion using remotely sensed data in Zombodze South, Swaziland. *Physics and Chemistry of the Earth, 33*, 800-806.

Mararakanye, N. & Le Roux, J. J. (2012). Gully location mapping at a national scale for South Africa. *South African Geographical Journal, 94*, 208-218.

Mararakanye, N. & Nethengwe, N. S. (2012). Gully features extraction using remote sensing techniques. *South African Journal of Geomatics*, *1*, 109-118.

Martha, T. R., Kerle, N., Jetten, V., van Westen, C. J., & Kumar, K. V. (2010). Characterising spectral, spatial and morphometric properties of landslides for semi-automatic detection using object-oriented methods. *Geomorphology*, *116*, 24-36.

Martínez-Casasnovas, J. A., Antón-Fernández, C. & Ramos, M. C. (2003). Sediment production in large gullies of the Mediterranean area (NE Spain) from high-resolution digital elevation models and geographical information systems analysis. *Earth Surface Processes and Landforms*, *28*, 443-456.

McCarthey, T. & Rubidge, B. (2005). *The story of earth and life. a Southern African perspective on a 4.6-billion-year journey.* Struik Nature: South Africa

McFeeters, S. K. (1996). The use of the Normalized Difference Water Index (NDWI) in the delineation of open water features. *International Journal of Remote Sensing*, *17*, 1425-1432.

Metternicht, G. I. & Zinck, J. A. (1998). Evaluating the information content of JERS-1 SAR and Landsat TM data for discrimination of soil erosion features. ISPRS *Journal of Photogrammetry and Remote Sensing*, 53, 143-153.

Mhangara, P., Kakembo, V. & Lim, K. J. (2012). Soil erosion risk assessment of the Keiskamma catchment, South Africa using GIS and remote sensing. *Environmental Earth Sciences, 65*, 2087-2102.

Mohamadi, M. A. & Kavian, A. (2015). Effects of rainfall patterns on runoff and soil erosion in field plots. *International Soil and Water Conservation Research, 3*, 273-281.

Mokonyane, N. (2015). The status of drought across South Africa 2015. *Televised Interview*. 1/11/2015. South Africa.

Mottes, C., Lesueur-Jannoyer, M., Le Bail, M. & Malézieux, E. (2014). Pesticide transfer models in crop and watershed systems: a review. *Agronomy for Sustainable Development, 34*, 229-250.

Msadala, V., Gibson, L., Le Roux, J. J., Rooseboom, A. & Basson, G. R. (2010). *Sediment yield prediction for South Africa.* WRC Report 1765/1/10. Water Research Commission: Pretoria.

Mucina, L. & Rutherford, M. C. (2009). *National vegetation map of South Africa.* Biodiversity GIS: Cape Town.

Mullan, D., Favis-Mortlock, D. & Fealy, R. (2012). Addressing key limitations associated with modelling soil erosion under the impacts of future climate change. *Agricultural and Forest Meteorology,156*, 18-30.

Murtaza, K. O. & Romshoo, S. A. (2014). Determining the suitability and accuracy of various statistical algorithms for satellite data classification. *International Journal of Geomatics and Geosciences*, *4*, 585.

National Oceanic and Atmospheric Administration. (2004). *Muskingum Routing.* Retrieved 10/14/2015, from www.nws.noaa.gov/oh/hrl/nwsrfs/user's_manual/part2/_pdf/24muskrout.pdf.

National Ocean and Atmospheric Administration. (2015). *What is LiDAR?* Retrieved 30/3/2015, from http://oceanservice.noaa.gov/facts/lidar.html.

Nearing, M. A., Lane, L. J. & Lopes, V. L. (1994). Modeling soil erosion. *Soil Erosion Research Methods*, 2, 127-156.

Nearing, M. A. (2000). Evaluating soil erosion models using measured plot data: accounting for variability in the data. *Earth Surface Processes and Landforms*, 25, 1035-1043.

Nel, W. & Sumner, P. D. (2007). Intensity, energy and erosivity attributes of rainstorms in the KwaZulu-Natal Drakensberg, South Africa. *South African Journal of Science*, 103, 398-402.

Ndomba, P. M., Mtalo, F. & Killingtveit, A. (2009). Estimating gully erosion contribution to large catchment sediment yield rate in Tanzania. *Physics and Chemistry of the Earth, 34*, 241-248.

Nietsch, S. L., Arnold, J. G., Kiniry, J. R. & Williams, J. R. (2005). *Soil and Water Assessment Tool: theoretical documentation. Version 2005.* Blackland Research Centre: Texas.

Nietsch, S. L., Arnold, J. G., Kiniry, J. R. & Williams, J. R. (2011). *Soil and Water Assessment Tool: theoretical documentation 2009.* Texas Water Resources Institute: Texas.

Plamieri, A., Shah, F. & Dinar, A. (2001). Economics of resevoir sedimentation and sustainable management of dams. *Journal of Environmental Management, 61*, 149-163.

Poesen, J., Nachtergaele, J., Verstraeten, G. & Valentin, C. (2003). Gully erosion and environmental change: importance and research needs. *Catena, 50*, 91-133.

Prosdocimi, M., Jordán, A., Tarolli, P., Keesstra, S., Novara, A. & Cerdà, A. (2016). The immediate effectiveness of barley straw mulch in reducing soil erodibility and surface runoff generation in Mediterranean vineyards. *Science of the Total Environment*, *547*, 323-330.

Qiu, L. J., Zheng, F. L. & Yin, R. S. (2012). SWAT-based runoff and sediment simulation in a small watershed, the loessial hilly-gullied region of China: capabilities and challenges. *International Journal of Sediment Research*, *27*, 226-234.

Rademacher, F. E. (1991). *Using the SOTER database for soil erosion assessment.* International Soil Reference and Information Centre: Wageningen.

Reichler, T. & Kim, J. (2008). How well do coupled models simulate today's climate?. *Bulletin of the American Meteorological Society, 89*, 303.

Romanowicz, A. A., Vanclooster, M., Rounsevell, M. & La Junesse, I. (2005). Sensitivity of the SWAT model to the soil and land use data parametrisation: a case study in the Thyle catchment, Belgium. *Ecological Modelling*, *187*, 27-39.

Routschek, A., Schmidt, J. & Kreienkamp, F. (2014). Impact of climate change on soil erosion- A high-resolution projection on catchment scale until 2100 in Saxony/Germany. *Catena, 121*, 99-109.

Rowntree, K. M. & Wadeson, R. A. (1999). *A Hierarchical Geomorphological Model for the Classification of Selected South African Rivers: Final Report to the Water Research Commission*: Pretoria.

Russow, F., & Garland, G. (2000). Factors accounting for the rapid siltation of Hazelmere Dam, KwaZulu-Natal. *South African Geographical Journal*, *82*, 182-188.

Rust, B. & Williams, J. D. (n.d.). *How tillage affects soil erosion and runoff.* USDA/ARS Columbia Plateau Conservation Research Centre: Pendleton, Oregon

Satellite Imaging Corporation. (2014). *QuickBird satellite sensor*. Retrieved 3/30/2015, from http://www.satimagingcorp.com/satellite-sensors/quickbird/.

Schulze, R. E. (1979). Soil loss in the key areas of the Drakensburg-a regional application of the soil loss estimation model for southern Africa (SLEMSA). In Hydrology and Water Resources of the Drakensburg (149-167). Natal Town and Regional Planning Commission: Pietermartizburg.

Schulze, R. E. (2012). *Mapping hydrological soil groups over South Africa for use with the SCS –SA design hydrograph technique: methodology and results.* University of KwaZulu-Natal: Pietermaritzburg.

Shakesby, R. A., Blake, W. H., Doerr, S. H., Humphreys, G. S., Wallbrink, P. J. & Chafer, C. J. (2006). Hillslope soil erosion and bioturbation after the Christmas 2001 forest fires near Sydney, Australia. In *Soil Erosion and*

Sediment Redistribution in River Catchments: Measurement, Modelling and Management in the 21st Century (51-61). *Eds PN Owens, AJ Collins.*

Shen, Z. Y., Gong, Y. W., Li, Y. H., Hong, Q., Xu, L. & Liu, R. M. (2009). A comparison of WEPP and SWAT for modelling soil erosion of the Zhangjiachong Watershed in the Three Gorges Reservoir Area. *Agricultural Water Management, 96*, 1435-1442.

Shruthi, R. B., Kerle, N. & Jetten, V. (2011). Object-based gully feature extraction using high spatial resolution imagery. *Geomorphology, 134*, 260-268.

Shruthi, R. V., Kerle, N. & Jetten, V. (2012). Extracting gully features and its dynamics from high spatial resolution imagery using object-based image analysis. *Proceedings of the 4th Geographic Object-based Image Analysis*, 7-12. Rio de Janeiro.

Shruthi, R. B., Kerle, N., Jetten, V., Abdellah, L. & Machmach, I. (2015). Quantifying temporal changes in gully erosion areas with object-based classification. *Catena, 128*, 262-277.

Sidorchuk, A., Marker , M., Moretti, S. & Rodolfi, G. (2003). Gully erosion modelling and landscape response in the Mbuluzi River catchment of Swaziland. *Catena, 50*, 507-525.

Simonneaux, V., Cheggour, A., Deschamps, C., Mouillot, F., Cerdan , O. & Le Bissonnais, Y. (2015). Land use and climate change effects on soil erosion in a semi-arid mountainous watershed (High Atlas, Morocco). *Journal of Arid Environments, 122*, 64-75.

Skinner, B. J., Porter, S. C. & Park, J. (2004). *Dynamic Earth* (Fifth ed.). John Wiley and Sons: United States of America.

Slimane, A. B., Raclot, D., Evrard, O., Sanaa, M., Lefevre, I. & Le Bissonnais, Y. (2015). Relative contribution of rill/interill and gully/channel erosion to small reservoir siltation in Mediterranean environments. *Land Degradation and Development, DOI, 10.*

Smith, H. J. (1999). Application of empirical soil loss models in southern Africa: A review. S*outh African Journal of Plant and Soil, 16*, 158-163.

Smith, H. J., Van Zyl, A. J., Claassens, A. S., Schoeman, J. L. & Laker, M. C. (2000). Soil loss modelling in the Lesotho Highlands Water Project catchment areas. *South African Geographical Journal, 82*, 64-69.

Smithers, J., Schulze, R. & Kienzle, S. (1997). Design Flood estimation using a modelling approach: a case study using the ACRU model. *Sustainability of water resources under increasing uncertainty.* LAHS Publishing: Rabat.

Sonneveld, B. G. & Dent, D. L. (2009). How good is GLASOD?. *Journal of Environmental Management*, *90*, 274-283.

Soto, J. & Navas, A. (2008). A simple model of Cs-137 profile to estimate soil redistribution in cultivated stony soils. *Radiation Measurements, 43*, 1285-1293.

Statsoft Incorporated. (2015). *Statsoft*. Retrieved 10/8/2015, from http://www.statsoft.com/Textbook/Support-Vector-Machines.

Stehman, S. V. (1996). Estimating the kappa coefficient and its variance under stratified random sampling. *Photogrammetric Engineering and Remote Sensing, 62*, 401-407.

Stellenbosch University. (2013). *Stellenbosch University Digital Elevation Model (SUDEM)*. Retrieved 1/24/2016, from http://www.innovus.co.za/pages/english/technology/our-technologies-and-spin-out-companies/physical-sciences/stellenbosch-university-digital-elevation-model-28sudem29.php.

Stocking, M., Chakela, Q. & Elwell, H. (1988). An improved methodology for erosion hazard mapping part I: the technique. *Geografiska Annaler. Series A. Physical Geography*, *1*, 169-180.

Stroosnijder, L. (2005). Measurement of erosion: is it possible? *Catena, 64*, 162-173.

Symeonakis, E. & Drake, N. 2010. 10-Daily soil erosion modelling over sub-Saharan Africa. *Environmental Monitoring and Assessment, 1, 369-387.*

Tamene, L., Park, S. J., Dikau, R. & Vlek, P. L. (2006). Analysis of factors determining sediment yield variability in the highlands of northern Ethiopia. *Geomorphology, 76*, 76-91.

Taruvinga, K. (2008). *Gully mapping using remote sensing: a case study in KwaZulu-Natal, South Africa. Masters Thesis.* University of Waterloo: Waterloo.

Tibebe, D. & Bewket, W. (2011). Surface runoff and soil erosion estimation using the SWAT model in the Keleta watershed, Ethiopia. *Land Degradation & Development*, *22*, 551-564.

Tiwari, A. K., Risse, L. M. & Nearing, M. A. (2000). Evaluation of WEPP and its comparison with USLE and RUSLE. *Transactions of the American Society of Agricultural Engineers, 43,* 1129-1135.

Tombus, F. E., Yuksel, M., Sahin, M., Ozulu, I. M. & Cosar, M. (2012). Assessment of soil erosion based on the method USLE: Corum Province example. *FIG Working Week: Knowing to manage the territory, protect the environment, evaluate the cultural heritage.* Technical Aspects of Spatial Information: Rome.

Trimble Navigation Limited. (2014). *eCognition*. Retrieved 10/3/2015, from http://www.ecognition.com/.

Ullrich, A. & Volk, M. (2009). Application of the Soil and Water Assessment Tool (SWAT) to predict the impact of alternative management practices on water quality and quantity. *Agricultural Water Management, 96*, 1207-1217.

USDA-ARS National Soil Erosion Research Laboratory. (2015). *USDA-ARS National Soil Erosion Research Laboratory*. Retrieved 9/4/2015, from http://milford.nserl.purdue.edu/weppdocs/overview/rill.html.

van den Berg, H. M. & Weepener, H. L. (2009). *Development of spatial modelling methodologies for semi-detailed soil mapping, primarily in support of curbing soil degradation and the zoning of high potential land.* Department of Agriculture: Pretoria.

van Huyssteen, C. W., Hensley, M., Le Roux, P. A., Zere, T. B. & Du Preez, C. C. (2005). *The relationship between soil water regime and soil profile morphology in the Weatherly Catchment, an afforestation area in the Eastern Cape.* WRC Report 1317/1/05. Water Research Commission: Pretoria.

van Tol, J. J., Le Roux, P. A. L., Hensley, M. & Lorentz, S. A. (2010). Soil as indicator of hillslope hydrological behaviour in the Weatherley Catchment, Eastern Cape, South Africa. *Water SA*, *36*, 513-520.

van Tol, J., Akpan, W., Kanuka, G., Ngesi, S. & Lange, D. (2014). Soil erosion and dam dividends: science facts and rural fiction around the upper Tsitsa dam, Eastern Cape, South Africa. *South African Geographical Journal*, *98*, 1-3.

van Zijl, G. M. (2010). *An investigation of the soil properties controlling gully erosion in a sub-catchment in Maphutseng, Lesotho.* Masters Thesis. Stellenbosch University: Stellenbosch.

van Zyl, A. J. (2007). A knowledge gap analysis on multi-scale predictive ability for agriculturally derived sediments under South African conditions. *Water Science and Technology, 55*, 107-114.

van Zyl, A. & Lorentz, S. A. (2004). *Predicting the Impact of Farming Systems on Sediment Yield in the Context of Integrated Catchment Management*, WRC Report 1059/1/03. Water Research Commission: Pretoria.

Vogel, E., Deumlich, D. & Kaupenjohann, M. (2016). Bioenergy maize and soil erosion- risk assessment and erosion control concepts. *Geoderma, 261*, 80-92.

Vrieling, A. (2005). Satellite remote sensing for water erosion assessment: a review. *Catena, 2*, 3-13.

Vrieling, A., Rodrigues, S. C., Bartholomeus, H. & Sterk, G. (2007). Automatic identification of erosion gullies with ASTER imagery in the Brazilian Cerrados. *International Journal of Remote Sensing*, *28*, 2723-2738.

Waidler, D., White, M., Steghlich, E., Wang, S., Williams, J., Jones, C. A. & Srinivasan, R. (2011). *Conservation practice modelling guide for SWAT and APEX.* Technical Report No. 399. Texas Water Resources Institute: Texas.

Walling, D. E. (1983). The sediment delivery problem. *Journal of Hydrology, 65*, 209-237.

Walling, D. E. & Quine, T. A. (1992). The use of caesium-137 measurements in soil erosion surveys. *Erosion and Sediment Transport Monitoring Programmes in River Basins*, 143-152. IAHS Publishing: Oslo.

Wang, Z. & Hu, C. (2009). Strategies for managing reservoir sedimentation. *International Journal of Sediment Research, 24*, 369-384.

Wang, T., He, F., Zhang, A., Gu, L., Wen, Y., Jiang, W. & Shao, H. (2014). A Quantitative Study of gully erosion based on object-oriented analysis techniques: a case study in Beiyanzikou Catchment of Qixia, Shandong, China. *The Scientific World Journal*, *2014*.

Warburton, M. L., Schulze, R. E. & Jewitt, G. P. (2010). Confirmation of ACRU model results for applications in land use and climate change studies. *Hydrological Earth System Science, 7*, 4591-4634.

Weepener, H.L., van den Berg H.M., Metz, M. & Hamandawana, H. (2012). *The development of a hydrologically improved Digital Elevation Model and derived products for South Africa based on the SRTM DEM*. WRC Report 1908/1/11. Water Research Commission: Pretoria.

Weepener, H. L., Engelbrecht, C. J. & Carstens, J. P. (2014). *Sensitivity of crop suitability in South Africa to climate change.* GW/A/2015/29. ARC-ISCW: Pretoria.

Weepener, H. L., Le Roux, J. J., van den Berg, E. C. & Tswai, D. R. (2014). *A methodology to create a South African river network with hydraulic intelligence.* WRC Report K5/2164. Water Research Commission: Pretoria.

Weepener, H.L., Engelbrecht, C.J., Carstens, J.P., Malherbe, J., Newby, T.S. & Beukes, P.J. (2015). *Climate Change and Water Scarcity mega forces: Is the Land Bank prepared? Unpublished. ARC-ISCW: Pretoria.*

Wieschmeier, W. H. & Smith, D. D. (1978). P*redicting rainfall erosion losses: a guide to conservation planning.* United Sates Department of Agriculture.

Winchell, M., Srinivasan, R., Di Luzio, M. & Arnold, J. (2013). *ArcSWAT interface for SWAT 2012 user's guide.* Texas.

Wuest, S. B., Williams, J. D., Gollany, H. T., Siemens, M. C., & Long, D. S. (2009). Comparison of runoff and soil erosion from no-till and inversion tillage production systems. *Journal of Soil and Water Conservation, 64*, 74-85.

Xu, H. (2006). Modification of normalised difference water index (NDWI) to enhance open water features in remotely sensed imagery. *International Journal of Remote Sensing, 27*, 3025-3033.

Yale's Centre for Earth Observation. (2003). *www.yale.edu.* Retrieved 19/3/2015, from http://www.yale.edu/ceo/OEFS/Accuracy_Assessment.pdf.

Yan, G. (2003). *Pixel based and object oriented image analysis for coal fire research.* Masters Thesis: University of Twente: Enschede.

Yang, Q., Meng, F.R., Zhao, Z., Chow, T.L., Benoy, G., Rees, H.W. & Bourque, C.P. (2009). Assessing the impacts of flow diversion terraces on stream water and sediment yields at a watershed level using SWAT model. *Agriculture, Ecosystems & Environment, 132,* 23-31.

Yesuf, H. M., Assen, M., Alamirew, T. & Melesse, A. M. (2015). Modeling of sediment yield in Maybar gauged watershed using SWAT, northeast Ethiopia. *Catena, 127*, 191-205.

Yu, B., & Rosewell, C. J. (1996). An assessment of a daily rainfall erosivity model for New South Wales. *Soil Research*, *34,* 139-152.

Zhang, Y., Degroote, J., Wolter, C. & Sugumaran, R. (2009). Integration of MUSLE into a GIS framework to access soil erosion risk. *Faculty Publications, 37*, 1-21.

Zhou, F., Xu , Y., Chen, Y., Xu, C. Y., Gao, Y. & Du, J. (2013). Hydrological response to urbanization at different spatiotemporal scales simulated by coupling of CLUE-S and the SWAT model in the Yangtze River Delta Region. *Journal of Hydrology, 485*, 113-125.

Zivotic, L., Perovic, V., Jaramaz, D., Dordevic, A., Petrovic, R. & Todorovic, M. (2012). Application of USLE, GIS and remote sensing in the assessment of soil erosion rates in southeastern Serbia. *Polish Journal of Environmental Studies, 21*, 1929-1935.

Appendices

Appendix 1.

Field observation data captured in June 2014 for gully erosion classification and verification.

#	Photo [1]	Scale[2]	Active[3]	Contin-uity[4]	Depth [5]	Veg-cover [6]	Connectivity [7]
1	28	Hillslope	Yes	c	d	<30 / >60	c
2	31	Catchm.	Yes	c	vd	30-60 / >60	c
3		Catchm.	Yes	c	vd	<30 / >60	c
4	33	Hillslope	Yes	c	vd	<30 / >60	p
5		Hillslope	Yes	d	d	>60 / >60	c
6	34	Hillslope	Yes	c	vd/d	<30 / >60	p
7	35	Hillslope	Yes	d	vd	30-60 / >60	p
8	36	Hillslope	Yes	d	vd	<30 / >60	p
9	37	Hillslope	Yes	d	d	30-60 / >60	d
10	38	Hillslope	Yes	c	vd	30-60 / >60	c
11	43	Hillslope	Yes	d	S	<30 / >60	d
12	44	Hillslope	Yes	c	d	<30 / >60	p
13	45	Hillslope	Yes	c	d	30-60 / >60	c

14	46	Hillslope	Yes	c	vd	30-60 / >60	c
15	48	Hillslope	Yes	c	d	30-60 / >60	p
16	49	Catchm.	Yes	c	vd	<30 / >60	c
17	50	Hillslope	Yes	c	d	30-60 / >60	c
18	51	Hillslope	Yes	d	d	<30 / >60	d
19	52	Catchm.	Yes	c	d	<30 / >60	d
20	53	Hillslope	Yes	d	s	<30 / >60	d
21	54	Hillslope	Yes	d	s	<30 / >60	c
22	55	Hillslope	Yes	d	s	30-60 / >60	c
23	56	Hillslope	Yes	c	d	>60 / >60	c
24	57	Hillslope	Yes	d	d	30-60 / >60	p

1. Photo numbers of photos that were taken (GPS camera; and second camera) in the field but not shown here.
2. Hillslope scale typically extends from upslope/crest areas to a stream channel with varying topography, soil and land management (van Zyl, 2007); whereas a catchment (catchm.) is a land surface which contributes water and sediment to any given stream network (Rowntree and Wadeson, 1999), including smaller (sub)catchments (<10 km^2) to a very large catchment (>10 km^2).
3. Active gullies contribute to or deliver sediments in a catchment, whereas non-active stable gullies have no none.

4. c = continuous gullies have a branching network that discharges into a stream/river at the base of a slope; and d = small discontinuous fade out into a depositional zone.
5. s = shallow (< 1.5 m); d = deep (1.5 to 3 m); and vd = very deep (>3 m).
6. Vegetation cover in percentage inside of gully and externally i.e. between gully and river.
7. c = connected (coarse sediment transfer during 'normal' flood events); p = partially connected (transfer only in extreme flood events) or potentially connected (competence to transport but lack of supply); d = disconnected (transfer is obstructed) (Hooke, 2003).

Appendix 2

The ruleset in eCognition was based on a "top-down" approach where the smallest level is pixel-based and the largest level is the "entire scene", creating three levels of differing segment sizes from large to small. The first step was to segment the image at a coarse scale using multi-resolution segmentation. Creating level 1 with segments size 150 and shape 0.3 and compactness 0.8. On this first level classes were assigned to the largest features such as dense grass and rivers using the following rules:

- Assign class, "vegetation", at level 1, with Hue (R= layer 1, G= layer 2, B= layer 3) >= 0.6 and mean layer 5 > 0. Layer 5 is the NDVI index layer so using values less than 0 account for high vegetation areas.
- Assign class, "river", at level 1 with Hue (R= layer 1, G= layer 2, B= layer 3) <= 0.25 and Hue (R= layer 1, G= layer 2, B= layer 3)>=0.19 The hue of the river pixels all fall within this range.
- Merge region, "river", at level 1 with Hue (R= layer 1, G= layer 2, B= layer 3) <= 0.25 and Hue (R= layer 1, G= layer 2, B= layer 3)>=0.19 in order to create a long river network.

The second step was to segment the image at a finer scale using multi-resolution segmentation creating a second level with segments size 50 and shape and compactness 0.3 and 0.8 respectively.

- Assign class at level 2, "shadow", brightness <60 removing shadows limits the objects still needing classification.
- Assign class, "dense vegetation" with Mean Layer 5 <= -0.16 using the NDVI layer to classify the areas of dense vegetation.

Finally, the image was segmented at a finer scale using multi-resolution segmentation creating level 3 with segments 10 and shape and compactness 0.2 and 0.6 respectively.

- Assign class, "gullies", with Hue (R= layer 1, G= layer 2, B= layer 3)>= 0.25 and Hue (R= layer 1, G= layer 2, B= layer 3) <= 0.32.
- Assign class, "gullies", with border to "gullies" > 5 this includes areas of shadow created by gully walls.

- Assign class, “houses”, to class “gullies”, with area<= 80 pixels this is to remove the houses which have been incorrectly classified as gullies.

Assign class, “gullies” to the area enclosed by class “gullies” this also allows the classification of shadows created by gully walls.

The final step used texture after Haralick to separate the rock outcrops and tilled land from the gully class.

Appendix 3

Bulk Density samples collected in the upper Tsitsa Catchment in January 2015.

Sample Number	GPS Position of Sample (Decimal Degrees)	Weigh t (g)	Volume (cm^3)	Bulk Density (g/cm^3)
1	28.30 -31.05	347,21	293,11	1,18
2	28.22 -30.99	448,06	293,11	1,53
2	28.22 -30.99	503,66	293,11	1,72
3	28.28 -31.04	420,26	293,11	1,43
4	28.26 -30.98	383,16	293,11	1,31
5	28.27 -30.98	444,71	293,11	1,52
6	28.30 -31.05	301,21	293,11	1,03
7	28.31 -31.06	356,51	293,11	1,22
8	28.31 -31.06	369,66	293,11	1,26
9	28.32 -31.06	417,46	293,11	1,42
10	28.45 -31.09	464,61	293,11	1,59
10	28.45 -31.09	386,61	293,11	1,32
11	28.47 -31.10	488,91	293,11	1,67
12	28.47 -31.10	436,91	293,11	1,49
Average Bulk Density				**1,41**